U. S. DEPARTMENT OF THE INTERIOR
U. S. GEOLOGICAL SURVEY

High-Temperature Permeability Studies --- I. Permeability of Granite and Novaculite at 300° to 500°C

by

D. E. Moore, L.-Q. Liu, D. A. Lockner, R. Summers, and J. D. Byerlee[1]

Open-File Report 95-28

[1]345 Middlefield Road, Menlo Park, CA 94025

Abstract

This report presents the data collected during initial investigations of the permeability of rock and gouge materials at elevated temperatures, conducted to test the hypothesis that impermeable mineral seals can form in fault zones in the intervals between earthquakes. The work was focused on granite and granite gouge, but some early experiments used novaculite and/or quartz gouge. The novaculite exhibited creep under the applied effective pressure at elevated temperatures, reducing its suitability for the investigation of permeability change by mineral sealing reactions. The permeability of intact granite decreased over time at temperatures between 300°C and 500°C at a constant effective pressure, and the rate of change increased overall with increasing temperature but with some reversals. The permeability reductions in the granite were caused by solution transfer and metamorphic reactions. The flow rate was initially high for a granite sample with a through-going fracture, but it eventually dropped to the level of intact granite as the fracture surface became sealed with mineral deposits. The rate of permeability decrease at a given temperature was higher for samples containing granite gouge than for intact granite samples, because of the enhanced reactivity of the very fine-grained materials in the gouge. Application of a differential stress to a gouge-bearing sample led to an increase in permeability, however, because flow of the gouge caused tensile cracks to form in the adjoining rock.

The higher temperature results are consistent with the rapid development of impermeable barriers at the base of the seismogenic zone. The lower temperature data provide less conclusive support for rapid sealing at shallower depths, because of conflicting rates at 300° and 350°C. This uncertainty precludes extrapolation of the rates to temperatures below 300°C. The results suggest, however, that the generation of fault gouge should enhance the initial sealing rates at any depth. In addition, the relatively high permeability of fractures may also be readily reduced by mineral deposition.

Introduction

The 21 experiments presented in this report represent the initiation of a long-term investigation of permeability at elevated temperatures and pressures. The ultimate goal of the research is to provide data on high-temperature permeability under static and stressed conditions, for application to the analysis of fault-zone behavior. Recent studies of active and exhumed faults have demonstrated the importance of fluids and fluid-rock interactions to fault-zone processes at depth (Sibson, 1981; Knipe, 1992; Chester and others, 1993). Mineral sealing processes, in particular, may have an important effect on fluid pressures in fault zones, and some recent models of the earthquake cycle call for the development of mineral seals within faults in the intervals between earthquakes (Byerlee, 1993; Chester and others, 1993). High-temperature permeability investigations on rock and gouge materials will help determine whether or not the implied rapid sealing rates of these models are reasonable.

The main purpose of this report is to provide a data repository for experiments that are discussed elsewhere in the literature (Moore and others, 1994, and in preparation). The results of some early reconnaissance experiments are also included, because they provide a useful background for the direction of subsequent experiments. This report also documents the evolution of the experimental design and the possible impact of design changes on the permeability measurements.

Previous Studies

Most of the early investigations of permeability at elevated temperatures and pressures were conducted to test the feasibility of hot dry rock geothermal energy systems (for example, Balagna and Charles, 1975; Potter, 1978; Summers and others, 1978) and the disposal by burial of high-level nuclear waste (for example, Morrow and others, 1981, 1984, 1985;

Moore and others, 1983, 1986). Many of these studies focused on granitic rock types, because granitic bodies were to provide the source of heat for the hot dry rock systems and they were also favored burial sites for nuclear waste in Canada and Europe.

Summers and others (1978) measured the permeability of Westerly granite at temperatures of 100° to 400°C, in the presence of a large pore-pressure drop of 27.4 MPa. The permeability rose immediately upon heating but then dropped dramatically over the first one-half day. At 400°C, flow essentially ceased after a few days. The marked permeability reductions were attributed to solution of minerals near the pore-pressure inlet and their redeposition at the outlet, in response to the pressure gradient.

Morrow and others (1981) and Moore and others (1983) investigated the effect of fluid flow down a temperature gradient on the permeability of Westerly and Barrre granite. These experiments simulated the thermal regime around buried canisters of nuclear waste. Similar to the results of Summers and others (1978), permeability decreased markedly over time, with the most rapid decreases occurring in the first few days. The rate of initial decrease was greater for the experiments with the highest maximum temperatures. A sample in which water flowed along a throughgoing fracture had similar permeability decreases. The fracture surfaces showed evidence of mineral dissolution on the high-temperature side and deposition on the low-temperature side.

Morrow and others (1985) extended the measurements of permeability in a temperature gradient to other crystalline rock types such as quartzite, anorthosite, and gabbro. Morrow and others (1984) and Moore and others (1986) conducted similar experiments on tuffaceous rocks from the Nevada Test Site, which is also under consideration for the underground disposal of nuclear waste. The pore fluid for the crystalline rock experiments was deionized water, whereas a groundwater collected at the Nevada Test Site was used for the tuff experiments. The permeability of all the crystalline rock types decreased over time, and the rate and amount of decrease were directly correlated with the percentage of quartz in the rock.

The quartzite sample became almost completely sealed in an experiment at 250°C maximum temperature. On the other hand, the tuffs were very porous and vuggy, resulting in high permeabilities that did not change with time.

Balagna and Charles (1975) and Potter (1978) conducted permeability studies on granitic core samples obtained from the Los Alamos Scientific Laboratory experimental geothermal borehole. Balagna and Charles described the anisotropy relative to permeability of a foliated monzo-granite gneiss. Potter found that the permeability of two quartz monzonite core samples first decreased and then increased with increasing temperature to 200°C. The permeability minimum of the 9522'-sample was near 140°C whereas the minimum for the 8580'-sample occurred at about 130°C. Potter proposed that the permeability minima reflect the temperatures at which the pore/crack systems in the samples last equilibrated. Potter also tested Westerly granite, whose behavior differed in that permeability decreased only slightly with increasing temperature to about 100°C and then increased exponentially above 100°C. According to Potter, the results for Westerly granite may reflect the unroofing of the pluton to surface weathering conditions. The permeability of the quartz monzonite increased during long-term flow experiments at 200°C, perhaps as a result of quartz dissolution that widened cracks. Flow in these experiments was in one direction only, and the initial pore fluid was distilled, deaerated water.

Aruna (1976) investigated the permeability of nearly pure quartz sandstone and unconsolidated sands. Permeability measured using water decreased by a factor of two as temperature was increased, but no permeability changes were found with other pore fluids. Aruna therefore attributed the permeability decreases to reactions between quartz and water. Scholz and others (in review) measured the permeability of granular mixtures of quartz and labradorite at temperatures to 350°C, using deionized water. The aggregates compacted upon heating, with accompanying rapid decreases in permeability; thereafter, permeability decreased more slowly. Permeability change was an irregular function of temperature, with

more pronounced decreases occurring at 200°C than at 250°C. Scholz and others ascribed the permeability reductions to compaction combined with some mineral precipitation in low-stress regions such as the throats of pores.

The objective of our current research is to obtain permeability data under nearly uniform pressure-temperature conditions, avoiding the large temperature and/or fluid-pressure gradients of many previous studies that would generate strong driving forces for mineral precipitation. Recent improvements in the experimental design, described in the next section, allow us to run experiments of several weeks' duration, thereby providing a more solid basis for extrapolation to the time scale of earthquake-recurrence intervals. With the triaxial deformation apparatus used in these experiments we can apply a differential stress to the sample, although thus far this capability has only been utilized in preliminary tests. Nevertheless, plans for future studies include sliding experiments using fault gouge.

Procedures

Most of the experiments in this study were conducted on Westerly granite (Table 1), a granodiorite consisting principally of plagioclase (~40%), quartz (~25%), K-feldspar (~25%), and biotite (~5%) (Moore, 1993). Samples of Arkansas novaculite, which is a fine-grained, porous metachert (Keller and others, 1977), were used in a few early experiments (Table 1). Four experiments employed one of two gouge materials. The one gouge consisted of Westerly granite, which was crushed and the fraction less than 90 μm in size ground in a ball mill to produce a rock flour. The second gouge was a finely ground (5μm) quartz powder obtained from U. S. Silica, Mill Creek, Oklahoma.

Most of the samples were intact cylinders of rock 21.9 mm long and 19.1 mm in diameter. One granite sample consisted of a cylinder that was fractured in tension parallel to the axis (Fig. 1), to simulate the fractured country rock adjacent to a fault zone. The gouge-

Table 1. Summary of Experiments

All experiments were conducted at 150 MPa confining pressure and 100 MPa fluid pressure.

Experiment Number	Ms Number*	Sample Configuration	Temp. (°C)	# Days heated	k - room T ($m^2 \times 10^{-21}$)	k - heated ($m^2 \times 10^{-21}$) initial	k - heated ($m^2 \times 10^{-21}$) final
HTQP01	- -	intact novaculite	400	1.9	6856	12693	4146
HTQP02	- -	qtz gouge, novaculite end pieces	400	4.2	10817	13920	4368
HTQP03	- -	quartz gouge, granite end pieces	400	14.1	144	38.4	66.8
HTQP04	- -	granite gouge, granite end pieces	500	9.9	82	514.4	42.0
HTQP05	500i-1	intact granite	500	10.0	102	326.8	19.4
HTQP06	500i-2	intact granite	500	9.8	609	465.4	0.4
HTQP07	400i-1	intact granite	400	45.8	193	137.6	18.3
HTQP08	400s	granite gouge, granite end pieces	400	23.7	876	1230.9	171.8
HTQP09	- -	intact granite	450	0.3	309	211.6	179.2
HTQP10	450i-1	intact granite	450	19.5	1240	364.5	129.9
HTQP11	300i-1	intact granite	300	19.5	413	166.1	59.1
HTQP12	350i-1	intact granite	350	13.6	473	171.5	92.0
HTQP13	300i-2	intact granite	300	17.6	104	99.6	56.5
HTQP14	400f	tensile fracture in granite	400	27.8	- -	- -	(31.4)
HTQP15	350i-3	intact granite	350	12.9	63	213.1	122.4
HTQP16	350i-2	intact granite	350	19.1	103	170.0	91.5
HTQP17	- -	intact granite	450	0.1	489	326.4	273.3
HTQP18	450i-2	intact granite	450	20.0	466	404.0	121.4
HTQP19	- -	intact granite	400	9.9	348	234.1	136.4
HTQP20	- -	intact granite	400	5.9	99	197.6	136.8
HTQP21	- -	intact granite	400	31.9	71	139.6	38.6

* Sample numbers used in Moore and others (1994)

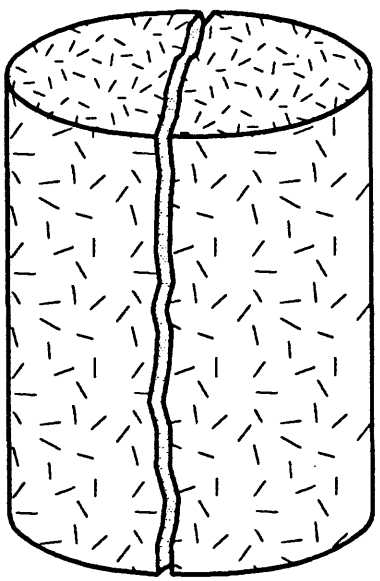

Tensile Fracture

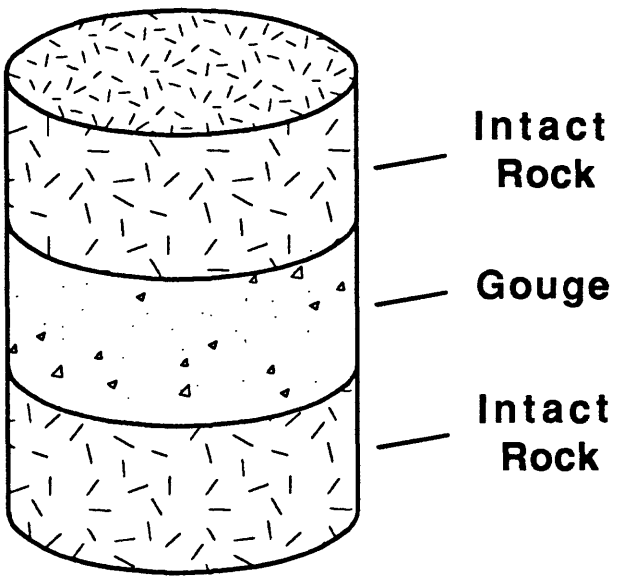

Sandwich

Figure 1. Sample configurations used in some experiments. The remaining samples were cylinders of intact rock.

bearing samples had a sandwich form (Fig. 1), consisting of a layer of gouge held in place between end pieces of intact rock. The three parts of the sandwich samples were initially the same length, but the gouge layer shortened under compaction when the confining pressure was applied.

The experimental assembly is shown schematically in Figure 2. The sample was placed between titanium carbide end plugs and Lucalox (aluminum oxide) insulating pieces in a copper jacket. Beginning with experiment HTQP06, a stainless steel screen was added to each end of the rock sample, to ensure that water reached the entire cross-sectional area of the cylinder. The jacketed sample was put inside a cylindrical furnace in a triaxial deformation apparatus. The jacket has a double seal (Fig. 3) to isolate the sample from the confining pressure medium. The space between the two O-ring seals is vented to air, such that a leak past one O-ring would be discharged from the sample assembly. The double seals greatly reduce the possibility of a jacket leak, thereby increasing the potential for long-term experiments.

All of the experiments in this group were conducted at a confining pressure of 150 MPa and a pore pressure of 100 MPa; the pore fluid was deionized water. The confining pressure corresponds to a depth of about 5 km in a fault zone. In recent earthquake models, fluid pressure within a fault is considered to vary between hydrostatic values immediately after an earthquake to nearly lithostatic levels in some seal-bounded compartments (for example, Byerlee, 1993; Byerlee and Lockner, 1994). The selected fluid pressure for the experiments is intermediate between the two end-member cases. The confining and pore pressures were held constant by a computer-controlled servo-mechanism. The fluid pressure at each end of the sample was maintained by a separate pump (Fig. 2). During an experiment, the pumps were set to maintain the pore pressure on one side of the sample at a fixed value up to 2.0 MPa above the pressure on the other side, to produce steady-state flow through the sample. The high- and low-pore-pressure sides were reversed periodically during each experiment to measure permeability in both directions; the flow rate stabilized within a few minutes of a given

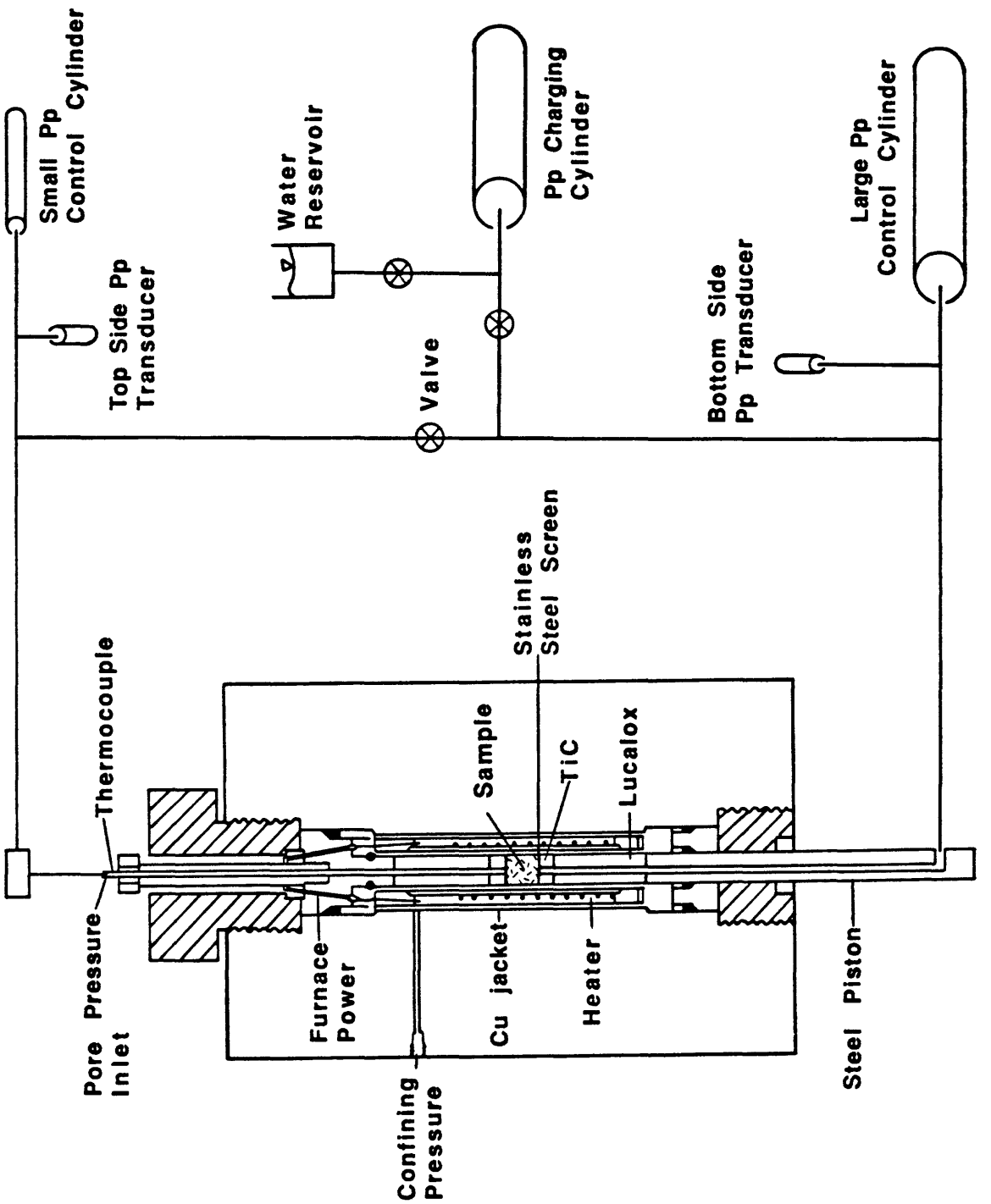

Figure 2. Schematic diagram of the triaxial deformation apparatus. The stainless-steel screens separating the sample from the TiC end plugs were added beginning with experiment HTQP06.

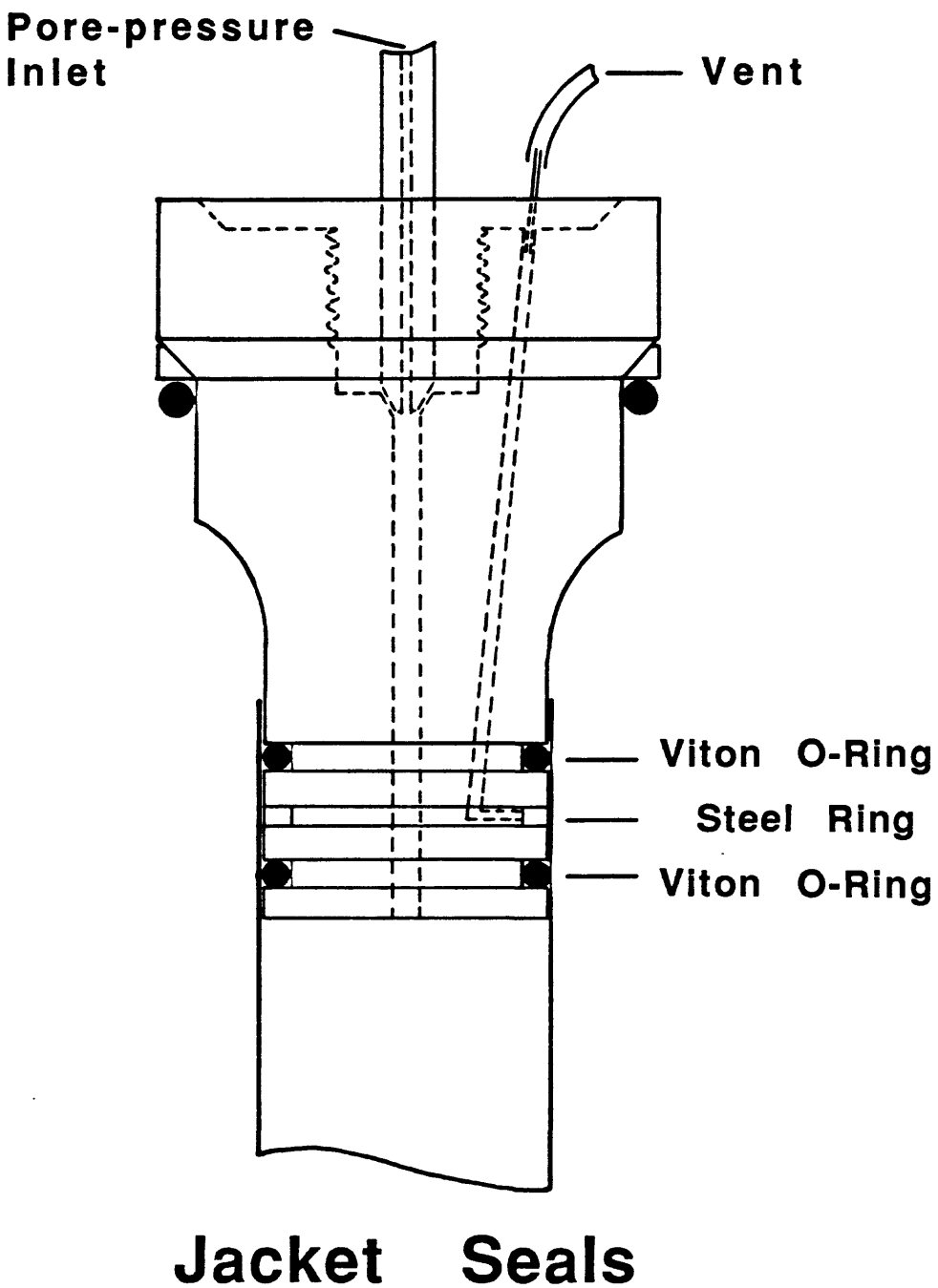

Figure 3. Close-up view of double jacket seals for separation of the confining- and pore-pressure media. The steel ring, situated between the two O-ring seals, contains a vent to air. A leak past one O-ring would be discharged from the sample assembly along the vent.

reversal. During experiments HTQP01-HTQP05, a given flow measurement lasted a maximum of 1 hour, and up to 5 measurements at different pore-pressure drops and flow directions were made each day. In subsequent experiments, flow was reversed by means of a computer command file at intervals of 2×10^4, 4×10^4, or 9×10^4 s, depending on the flow rate. The capacity of the smaller pore-pressure pump is about 0.28 cm^3, and in most cases the entire fluid volume moved through the sample before the direction of flow was reversed. As a result, periods of flow alternated with periods without flow during all of the experiments. The same small volume of fluid was continually pushed back and forth through the sample. In this way, although the initial fluid is deionized water, it should rapidly become charged with ions upon heating, making its composition more akin to natural groundwaters. The small amount of fluid utilized combined with the two-way flow system should minimize the effects of leaching caused by the use of deionized water (see, for example, Potter, 1978).

Confining pressure was applied first to the sample, followed by pore pressure. After the pressures had equilibrated, one or more room-temperature measurements of permeability were made. The sample was then heated to a temperature in the range 300° to 500°C. All the temperatures tested are high for the fault depth represented by the confining pressure; they were chosen to accelerate mineral reactions. Heating took place over a period of 15 to 30 minutes, depending on the amount of temperature increase. Temperature was monitored by a thermocouple inserted along the upper pore-pressure inlet. For experiments HTQP01-HTQP20, the thermocouple and the midpoint of the sample cylinder were positioned at the temperature maximum of the furnace. Temperature decreased by 2% between the middle and ends of the sample in these experiments; for example, during an experiment at 400°C the middle of the cylinder would be at 400°C and the ends at 392°C. A new furnace with a smaller temperature gradient was used in experiment HTQP21. With this furnace, the top of the sample and the thermocouple were placed at the temperature maximum, and temperature decreased by less than 2% across the entire length of the cylinder.

Permeability of the intact and sandwich samples was determined by measuring the fluid flux at intervals over a constant pore-pressure gradient, according to Darcy's law:

$$(q/A) = (k/\mu)\ (\Delta P_p/\Delta l) \qquad (1)$$

where q is flow rate; A is the circular cross-sectional area of the cylinder; k is permeability (units of m^2); μ is the dynamic viscosity of water at the temperature and pressure of the experiment; ΔP_p is the pore-pressure drop along the cylinder; and Δl is the length of the cylinder. Rearranging terms to solve for k gives:

$$k = \mu\ (q/A)\ (\Delta l/\Delta P_p) \qquad (2)$$

The flow rate of water through the cylinder was determined by measuring the change with time of fluid volume in the pore fluid reservoir, giving $q_{25°C}$. The flow rate through a sample heated to temperature T was then calculated by:

$$q_T = q_{25°C}\ (v_T/v_{25°C}) \qquad (3)$$

where v is the specific volume of water. Data for the specific volume of water at the temperatures and pressures of the tests come from Table 1 of Burnham and others (1969); dynamic viscosities were obtained from Table IX of Tödheide (1972). The accuracy of the calculated permeability values is estimated to be within ±5% over most of the range of measurements. The error increases for k less than 1×10^{-21} m^2, which is at the lower measuring limits of the experimental apparatus.

In the case of the fractured sample, flow was initially concentrated in the break rather than distributed through the cylinder. Morrow and others (1981) demonstrated that the

parallel plate model analogy to Darcy's law (Gale, 1975) is appropriate for an irregular fracture surface. Here, the cross-sectional area A = wd in equation (1), where w is the fracture width (equal to the diameter of the cylinder) and d is the separation between the fracture walls. Because d is not known, it is combined with k to produce a new parameter λ (Morrow and others, 1981):

$$\lambda = \mu\ (q/w)\ (\Delta l/\Delta P_p) \qquad (4)$$

Both k and λ relate flow in a crack to the pore-pressure gradient, but λ has units of m^3 instead of m^2 and is not strictly a crack permeability.

Permeability Measurements

The data collected during the 21 experiments of this study are presented in Table 2. A time of 0 days is the time that the sample reached the selected temperature of the experiment. The time listed for a given measurement is the midpoint of the measuring interval, which will be longer for the lower-permeability samples. The columns of pore-pressure drop (ΔP_p), flow rate (q), and length are presented in the units that yield k in terms of m^2. The reported values of ΔP_p are somewhat variable, because (1) the actual pore-pressure drop was generally slightly lower than the set point, and (2) the zero position of ΔP_p tended to drift during an experiment, due to drift of the transducer and preamplifier in response to room temperature variations. For convenience, the set-point value is used in the text. Columns of length are included for experiments in which sample length changed as a result of compaction (gouge-bearing samples) or creep (novaculite samples). The one exception is gouge experiment HTQP08, in which the final sample length was used for all calculations of k. This results in a maximum error of 0.3% for the initial determinations of k. The last column presents k in units

Table 2. Permeability measurements made during experiments HTQP01 through HTQP21.

HTQP01

File #	Time (days)	Temp. (°C)	Length (cm)	ΔPp (bars)	q x 10^{-6} (cm^3/s)	k x 10^{-18} (m^2)	k (nDa)
HTQP01-01	-0.09	25	2.380	9.50	87.63	6.856	6946
HTQP01-02	-0.04	200	2.380	2.00	166.84	12.693	12861
	-0.03	200	2.380	-2.70	-165.53	9.328	9451
HTQP01-03	0.02	400	2.380	3.12	165.66	5.769	5845
HTQP01-04	0.06	400	2.380	4.29	166.18	4.209	4265
	0.08	400	2.380	-4.54	-165.92	3.971	4023
HTQP01-05	0.83	400	2.375	3.86	166.32	4.672	4734
HTQP01-06	1.07	400	2.371	4.04	166.58	4.463	4522
HTQP01-07	1.80	400	2.368	4.36	167.24	4.146	4201

HTQP02

File #	Time (days)	Temp. (°C)	Length (cm)	ΔPp (bars)	q x 10^{-6} (cm^3/s)	k x 10^{-18} (m^2)	k (nDa)
HTQP02-01	-0.02	25	2.3850	9.450	137.24	10.817	10960
HTQP02-02	0.02	400	2.3850	0.938	164.08	19.045	19296
	0.04	400	2.3850	-1.810	-164.47	9.893	10024
	0.06	400	2.3850	1.080	164.61	16.594	16813
	0.07	400	2.3850	-1.990	-165.79	9.071	9191
	0.09	400	2.3850	0.938	166.05	19.274	19528
	0.11	400	2.3850	-2.360	-164.87	7.606	7706
	0.13	400	2.3850	0.800	165.13	22.473	22770
	0.14	400	2.3850	-2.450	-166.58	7.403	7501
HTQP02-03	0.29	400	2.3138	1.750	167.90	10.134	10268
	0.30	400	2.3138	-1.130	-168.29	12.078	16008
HTQP02-04	0.98	400	2.2994	2.460	167.11	7.131	7225
	0.99	400	2.2994	-2.460	-166.05	7.085	7179
HTQP02-05	1.27	400	2.2968	2.140	165.53	8.110	8217
	1.28	400	2.2968	-2.110	-168.95	8.395	8506
HTQP02-06	3.06	400	2.2867	3.600	166.97	4.842	4906
	3.08	400	2.2867	-3.550	-168.82	4.964	5030
HTQP02-07	3.99	400	2.2842	3.840	165.74	4.501	4560
	4.01	400	2.2842	-4.140	-166.45	4.192	4247
HTQP02-08	4.22	400	2.2835	3.700	166.45	4.339	4751
	4.23	400	2.2835	-4.000	-168.68	4.396	4454

HTQP03

File #	Time (days)	Temp. (°C)	Length (cm)	ΔPp (bars)	q x 10^{-6} (cm^3/s)	k x 10^{-20} (m^2)	k (nDa)
HTQP03-01	-1.03	25	2.4855	10.00	1.86	14.41	146.0
HTQP03-03	0.09	400	2.4293	-20.00	-5.79	3.21	32.5
	0.13	400	2.4293	-10.00	-3.13	3.47	35.2
	0.17	400	2.4293	0.00	0.02		
	0.21	400	2.4293	10.00	3.87	4.29	43.5
	0.26	400	2.4293	19.64	7.75	4.38	44.4
HTQP03-05	1.11	400	2.4202	-20.00	-7.49	4.14	41.9
	1.15	400	2.4202	-10.00	-3.99	4.41	44.7
	1.19	400	2.4202	0.00	0.29		
	1.22	400	2.4202	10.00	4.22	4.66	47.2
	1.28	400	2.4202	19.69	7.54	4.23	42.9
HTQP03-07	3.14	400	2.4178	-20.00	-8.67	4.78	48.4
	3.18	400	2.4178	-10.00	-3.77	4.16	42.1
	3.22	400	2.4178	0.00	0.03		
	3.26	400	2.4178	10.00	3.51	3.87	39.2
	3.30	400	2.4178	19.67	6.51	3.65	37.0
HTQP03-09	4.13	400	2.4166	-20.00	-6.15	3.39	34.4
	4.17	400	2.4166	-10.00	-2.79	3.08	31.2
	4.21	400	2.4166	0.00	0.52		
	4.26	400	2.4166	10.00	2.33	2.57	26.0
	4.30	400	2.4166	20.00	4.39	2.42	24.5
HTQP03-11	5.14	400	2.4154	-20.00	-8.66	4.77	48.3
	5.18	400	2.4154	-10.00	-4.68	5.16	52.3
	5.23	400	2.4154	0.00	0.76		
	5.27	400	2.4154	10.00	4.86	5.36	54.3
	5.31	400	2.4154	20.00	4.64	2.56	25.9
HTQP03-13	6.12	400	2.4142	-20.00	-6.20	3.42	34.7
	6.17	400	2.4142	-10.00	-2.66	2.93	29.7
	6.21	400	2.4142	0.00	0.16		
	6.25	400	2.4142	10.00	3.01	3.32	33.6
	6.29	400	2.4142	20.00	4.39	2.42	24.5
HTQP03-15	7.13	400	2.3780	-20.00	-5.86	3.18	32.2
	7.17	400	2.3780	-10.00	-3.78	4.10	41.5
HTQP03-17	8.11	400	2.2485	-20.00	-5.29	2.71	27.5
	8.15	400	2.2485	-10.00	-2.82	2.89	29.3
	8.19	400	2.2485	0.00	-0.38		
	8.23	400	2.2485	10.00	1.91	1.96	19.9
	8.27	400	2.2485	20.00	3.66	1.88	19.0
HTQP03-19	11.13	400	2.2349	19.75	7.21	3.72	37.7
	11.18	400	2.2349	10.00	3.16	3.22	32.6
	11.22	400	2.2349	0.00	0.77		
	11.26	400	2.2349	-9.90	-6.46	6.66	67.5
	11.30	400	2.2349	-19.64	-15.55	8.08	81.9
HTQP03-21	12.10	400	2.2280	19.59	10.88	5.65	57.2
	12.14	400	2.2280	9.69	5.41	5.68	57.5
	12.18	400	2.2280	0.00	0.14		
	12.22	400	2.2280	-9.88	-5.76	5.93	60.1
	12.26	400	2.2280	-19.67	-11.61	6.00	60.9
HTQP03-23	13.11	400	2.2213	19.61	11.03	5.70	57.8

File #	Time (days)	Temp. (°C)	Length (cm)	ΔPp (bars)	q x 10^{-6} (cm^3/s)	k x 10^{-20} (m^2)	k (nDa)
	13.15	400	2.2213	9.74	5.20	5.41	54.8
	13.19	400	2.2213	0.00	0.40		
	13.23	400	2.2213	-9.90	-5.36	5.49	55.6
	13.27	400	2.2213	-19.66	-11.93	6.15	62.3
HTQP03-25	14.08	400	2.2000	20.00	13.30	6.68	67.7

HTQP04

File #	Time (days)	Temp. (°C)	Length (cm)	ΔPp (bars)	q x 10^{-6} (cm^3/s)	k x 10^{-20} (m^2)	k (nDa)
HTQP04-01	-0.07	25	2.2665	19.99	2.32	8.21	83.2
HTQP04-02	0.02	500	2.2964	-19.70	-94.87	50.98	516.5
	0.05	500	2.2964	-9.67	-45.66	49.99	506.5
	0.07	500	2.2964	9.44	46.05	51.64	523.2
	0.09	500	2.2964	19.40	97.37	53.13	538.3
HTQP04-04	2.94	500	2.2883	19.50	29.08	15.73	159.4
	2.96	500	2.2883	9.44	14.08	15.73	159.4
	2.98	500	2.2883	-9.78	-18.09	19.51	197.7
	3.00	500	2.2883	-19.70	-37.76	20.22	204.9
HTQP04-06	3.88	500	2.2879	19.50	26.71	14.45	146.4
	3.90	500	2.2879	9.44	13.29	14.85	150.5
	3.92	500	2.2879	-9.78	-12.57	13.56	137.4
	3.95	500	2.2879	-19.70	-26.62	14.25	144.4
HTQP04-08	4.86	500	2.2875	19.50	22.57	12.21	123.7
	4.88	500	2.2875	9.44	10.59	11.83	119.9
	4.91	500	2.2875	-10.00	-11.25	11.86	120.2
	4.93	500	2.2875	-19.70	-22.37	11.97	121.3
HTQP04-10	5.86	500	2.2872	19.50	15.92	8.61	87.2
	5.88	500	2.2872	9.55	7.83	8.64	87.5
	5.91	500	2.2872	-10.10	-9.09	8.45	85.6
	5.93	500	2.2872	-19.70	-16.58	8.87	89.9
HTQP04-12	6.85	500	2.2868	19.60	14.77	7.94	80.4
	6.88	500	2.2868	9.55	7.01	7.74	78.4
	6.90	500	2.2868	-10.10	-5.56	5.80	58.8
	6.92	500	2.2868	-19.70	-13.55	7.25	73.5
HTQP04-14	9.85	500	2.2857	19.60	8.75	4.70	47.6
	9.87	500	2.2857	9.78	4.01	4.30	43.6
	9.90	500	2.2857	-10.10	-2.95	3.08	31.2
	9.92	500	2.2857	-20.10	-9.00	4.72	47.8

HTQP05

File #	Time (days)	Temp. (°C)	ΔPp (bars)	q x 10^{-6} (cm^3/s)	q/ΔP x 10^{-6}	k x 10^{-21} (m^2)	k (nDa)
HTQP05-01	-0.08	25	19.99	3.00	0.1501	102.4	103.8
HTQP05-03	0.04	500	19.56	62.37	3.1887	321.7	325.9
	0.08	500	-19.60	-64.47	3.2893	331.9	336.3
HTQP05-05	1.23	500	19.60	38.36	1.9571	197.5	200.1
HTQP05-07	1.96	500	19.50	30.86	1.5826	159.7	161.8
	2.00	500	-19.70	-32.43	1.6462	166.1	168.3
HTQP05-09	2.98	500	-19.74	-26.25	1.3298	134.2	136.0
	3.03	500	19.51	27.89	1.4295	144.2	146.1
HTQP05-11	3.99	500	-19.74	-22.76	1.1530	116.3	117.8
	4.04	500	19.51	23.82	1.2209	123.2	124.8
HTQP05-13	4.98	500	-20.08	-0.70	0.0349	3.5	3.5
	5.02	500	19.50	7.83	0.4015	40.5	41.0
HTQP05-14	5.08	500	-20.08	-3.45	0.1718	17.3	17.5
	5.12	500	19.50	6.91	0.3544	35.8	36.3
HTQP05-16	5.98	500	-20.00	0.40	0.0200	2.0	2.0
	6.02	500	20.00	0.40	0.0200	2.0	2.0
HTQP05-18	6.97	500	-20.08	-6.25	0.3113	31.4	31.8
	7.01	500	19.96	3.60	0.1804	18.2	18.4
HTQP05-21	9.90	500	19.50	5.78	0.2964	29.9	30.3
	9.97	500	-20.08	-1.76	0.0876	8.8	8.9
HTQP05-22	10.13	25	19.50	9.34	0.4790	326.7	331.0
	10.18	25	-20.08	-10.66	0.5309	362.1	366.9
HTQP05-24	10.95	25	19.50	11.65	0.5974	407.5	412.9
	11.00	25	-20.08	-9.28	0.4622	315.3	319.5

HTQP06

File #	Time (days)	Temp. (°C)	ΔPp (bars)	q x 10^{-6} (cm^3/s)	q/ΔPp x 10^{-6}	k x 10^{-21} (m^2)	k (nDa)
HTQP06-01	0.00	25	19.60	17.5	0.8929	609.0	617.0
HTQP06-02	0.05	500	19.12	88.2	4.6130	465.4	471.5
	0.28	500	-20.01	-77.8	3.8881	392.3	397.5
	0.51	500	19.60	74.0	3.7755	380.9	385.9
	0.74	500	-19.47	-71.9	3.6929	372.6	377.5
	0.97	500	19.60	71.5	3.6480	368.1	373.0
	1.20	500	-19.63	-71.4	3.6373	367.0	371.8
	1.44	500	19.79	72.3	3.6534	368.6	373.5
	1.67	500	-19.25	-68.0	3.5325	356.4	361.1
	1.90	500	19.67	69.1	3.5130	354.5	359.2
	2.13	500	-19.54	-67.7	3.4647	349.6	354.2
	2.36	500	19.73	67.6	3.4263	345.7	350.3
	2.59	500	-19.21	-64.6	3.3628	339.3	343.8
HTQP06-03	2.82	500	20.20	66.2	3.2772	330.7	335.1

File #	Time (days)	Temp. (°C)	ΔPp (bars)	q x 10^{-6} (cm^3/s)	q/ΔPp x 10^{-6}	k x 10^{-21} (m^2)	k (nDa)
	3.06	500	-19.20	-63.3	3.2969	332.6	337.0
	3.29	500	19.64	62.4	3.1772	320.6	324.8
	3.52	500	-19.77	-61.3	3.1007	312.9	317.0
	3.75	500	19.59	60.0	3.0628	309.0	313.1
HTQP06-04	3.99	500	-19.62	-58.3	2.9715	299.8	303.8
	4.22	500	19.57	55.0	2.8104	283.6	287.3
	4.45	500	-19.65	-54.9	2.7939	281.9	285.6
	4.68	500	19.87	56.4	2.8384	286.4	290.2
HTQP06-05	4.91	500	-18.89	-50.9	2.6945	271.9	275.5
	5.25	500	19.56	50.8	2.5971	262.1	265.6
	5.38	500	-19.65	-46.8	2.3817	240.3	243.5
	5.62	500	19.64	40.0	2.0367	205.5	208.2
HTQP06-06	6.39	500	19.95	0.3	0.0135	1.4	1.4
HTQP06-07	8.28	500	-20.00	-0.0	0.0040	0.4	0.4
HTQP06-08	10.09	25	19.56	13.9	0.7106	484.7	491.1
	10.32	25	-19.74	-11.8	0.5978	407.7	413.1
	10.55	25	19.62	7.6	0.3874	264.2	267.7

HTQP07

File #	Time (days)	Temp. (°C)	ΔPp (bars)	q x 10^{-6} (cm^3/s)	q/ΔPp x 10^{-6}	k x 10^{-20} (m^2)	k (nDa)
HTQP07-01	-0.52	25	19.65	7.80	0.3969	27.07	274.3
	-0.29	25	-19.90	-5.59	0.2809	19.16	194.1
	-0.10	25	19.61	5.59	0.2851	19.45	197.1
HTQP07-02	0.08	400	19.90	27.47	1.3804	13.76	139.4
	0.32	400	-19.93	-27.17	1.3633	13.59	137.7
	0.56	400	18.96	23.39	1.2336	12.30	124.6
	0.78	400	-20.22	-25.56	1.2641	12.60	127.7
HTQP07-03	1.01	400	20.09	25.10	1.2494	12.46	126.2
	1.24	400	-19.26	-24.74	1.2845	12.81	129.8
	1.47	400	19.50	23.95	1.2282	12.25	124.1
	1.71	400	-19.38	-24.44	1.2611	12.57	127.4
	1.94	400	19.18	23.42	1.2211	12.17	123.3
	2.17	400	-20.22	-25.36	1.2542	12.50	126.6
	2.40	400	19.73	23.42	1.187	11.83	119.9
	2.63	400	-19.45	-24.28	1.2483	12.45	126.1
	2.86	400	18.78	22.76	1.2119	12.08	122.4
	3.09	400	-20.51	-24.57	1.1980	11.94	121.0
	3.33	400	19.13	22.93	1.1986	11.95	121.1
	3.56	400	-19.59	-23.52	1.2006	11.97	121.3
	3.79	400	19.59	22.76	1.1618	11.58	117.3
HTQP07-04	4.03	400	-18.52	-21.45	1.1582	11.55	117.0
	4.26	400	18.94	20.72	1.0940	10.91	110.5
	4.49	400	-20.00	-22.76	1.1380	11.35	115.0

File #	Time (days)	Temp. (°C)	ΔPp (bars)	q x 10^{-6} (cm^3/s)	q/ΔPp x 10^{-6}	k x 10^{-20} (m^2)	k (nDa)
	4.73	400	19.62	21.48	1.0948	10.92	110.6
HTQP07-05	4.96	400	-18.84	-20.62	1.0945	10.91	110.5
	5.20	400	18.81	21.64	1.1505	11.47	116.2
	5.43	400	-19.97	-21.56	1.0796	10.76	109.0
	5.66	400	19.52	20.00	1.0246	10.22	103.5
	5.89	400	-18.85	-19.41	1.0297	10.27	104.1
HTQP07-06	6.13	400	20.40	20.95	1.0270	10.24	103.8
	6.36	400	-20.17	-20.76	1.0293	10.26	104.0
	6.59	400	19.35	19.31	0.9979	9.95	100.8
	6.82	400	-18.89	-18.72	0.9910	9.88	100.1
HTQP07-07	7.28	400	19.06	17.86	0.9370	9.34	94.6
	7.52	400	-19.87	-19.05	0.9587	9.56	96.9
	7.75	400	19.59	18.42	0.9403	9.37	94.9
HTQP07-08	7.98	400	-19.62	-17.14	0.8736	8.71	88.2
	8.21	400	19.57	18.32	0.9337	9.31	94.3
	8.44	400	-19.62	-18.29	0.9322	9.29	94.1
	8.67	400	19.58	17.80	0.9091	9.06	91.8
	8.90	400	-19.63	-17.73	0.9032	9.00	91.2
	9.14	400	19.59	15.99	0.8162	8.14	82.5
	9.37	400	-19.63	-17.10	0.8711	8.68	87.9
	9.60	400	19.60	16.38	0.8357	8.33	84.4
	9.83	400	-19.64	-16.61	0.8457	8.43	85.4
	10.06	400	19.60	15.26	0.7786	7.76	78.6
	10.29	400	-19.64	-16.18	0.8238	8.21	83.2
	10.52	400	19.61	15.63	0.7970	7.95	80.5
	10.76	400	-19.65	-15.26	0.7766	7.74	78.4
HTQP07-09	11.00	400	19.57	16.38	0.8370	8.34	84.5
	11.24	400	-19.74	-14.74	0.7467	7.44	75.4
	11.47	400	19.58	14.55	0.7431	7.41	75.1
	11.71	400	-19.77	-14.70	0.7436	7.41	75.1
	11.94	400	19.59	15.59	0.7958	7.93	80.3
HTQP07-10	12.19	400	-19.67	-13.59	0.6909	6.89	69.8
	12.42	400	19.59	13.85	0.7070	7.05	71.4
	12.65	400	-19.67	-14.11	0.7173	7.15	72.4
	12.88	400	19.65	14.93	0.7598	7.58	76.8
HTQP07-11	13.11	400	-19.67	-12.87	0.6543	6.52	66.1
	13.34	400	19.65	12.70	0.6463	6.44	65.3
	13.57	400	-19.67	-13.76	0.6995	6.97	70.6
	13.81	400	19.65	13.63	0.6936	6.92	70.1
HTQP07-12	14.03	400	-19.75	-11.71	0.5929	5.91	59.9
	14.26	400	19.59	12.66	0.6462	6.44	65.3
	14.49	400	-19.90	-13.18	0.6623	6.60	66.9
	14.72	400	19.61	12.50	0.6374	6.36	64.4
	14.95	400	-19.90	-12.13	0.6095	6.08	61.6
HTQP07-13	15.18	400	19.61	13.22	0.6741	6.72	68.1
	15.41	400	-19.97	-12.61	0.6314	6.30	63.8
	15.64	400	19.61	11.74	0.5987	5.97	60.5
	15.87	400	-19.96	-11.51	0.5767	5.75	58.3
	16.10	400	19.62	11.48	0.5851	5.83	59.1
	16.34	400	-19.94	-11.30	0.5667	5.65	57.2
	16.57	400	19.62	11.41	0.5815	5.80	58.8

File #	Time (days)	Temp. (°C)	ΔPp (bars)	q x 10^{-6} (cm^3/s)	q/ΔPp x 10^{-6}	k x 10^{-20} (m^2)	k (nDa)
	16.80	400	-19.92	-11.12	0.5582	5.57	56.4
	17.03	400	19.62	10.95	0.5581	5.56	56.3
	17.26	400	-19.95	-11.05	0.5539	5.52	55.9
	17.49	400	19.57	10.60	0.5416	5.40	54.7
	17.72	400	-19.94	-10.50	0.5266	5.25	53.2
	17.96	400	19.57	10.04	0.5130	5.11	51.8
	18.19	400	-19.93	-10.10	0.5068	5.05	51.2
	18.42	400	19.57	10.30	0.5263	5.25	53.2
	18.65	400	-19.92	-10.00	0.5020	5.01	50.8
	18.88	400	19.57	10.00	0.5110	5.09	51.6
HTQP07-14	19.11	400	-20.00	-9.61	0.4805	4.79	48.5
HTQP07-15	19.34	400	19.57	9.47	0.4839	4.82	48.8
	19.58	400	-19.95	-9.76	0.4892	4.88	49.4
	19.81	400	19.61	10.08	0.5140	5.12	51.9
HTQP07-16	20.04	400	-19.97	-8.36	0.4186	4.17	42.2
	20.27	400	19.61	9.20	0.4691	4.68	47.4
	20.50	400	-19.97	-9.45	0.4732	4.72	47.8
	20.73	400	19.61	9.33	0.4758	4.74	48.0
	20.96	400	-19.97	-8.09	0.4051	4.04	40.9
HTQP07-17	21.20	400	19.61	9.87	0.5033	5.02	50.9
	21.43	400	-19.97	-9.08	0.4547	4.53	45.9
	21.66	400	19.61	8.86	0.4518	4.50	45.6
	21.89	400	-19.97	-8.38	0.4196	4.18	42.4
HTQP07-18	22.12	400	19.59	9.33	0.4763	4.75	48.1
	22.35	400	-19.97	-8.68	0.4347	4.33	43.9
	22.59	400	19.59	8.95	0.4569	4.55	46.1
	22.82	400	-19.97	-7.62	0.3816	3.80	38.5
	23.05	400	19.60	8.25	0.4209	4.20	42.6
	23.28	400	-19.97	-7.62	0.3816	3.80	38.5
	23.51	400	19.60	8.66	0.4418	4.40	44.6
	23.74	400	-19.97	-7.50	0.3756	3.74	37.9
	23.97	400	19.60	7.61	0.3883	3.87	39.2
	24.20	400	-19.97	-7.66	0.3836	3.82	38.7
	24.44	400	19.61	8.29	0.4227	4.21	42.7
	24.67	400	-19.97	-7.26	0.3635	3.62	36.7
	24.90	400	19.61	7.99	0.4074	4.06	41.1
HTQP07-19	25.13	400	-19.97	-6.45	0.3230	3.22	32.6
	25.36	400	19.61	7.05	0.3595	3.58	36.3
	25.59	400	-19.97	-7.46	0.3736	3.72	37.7
	25.83	400	19.61	8.45	0.4309	4.30	43.6
HTQP07-20	26.06	400	-19.97	-6.29	0.3150	3.14	31.8
	26.29	400	19.64	7.59	0.3865	3.85	39.0
	26.52	400	-19.97	-7.13	0.3570	3.56	36.1
	26.75	400	19.59	8.08	0.4125	4.11	41.6
HTQP07-21	26.98	400	-19.97	-5.99	0.2999	2.99	30.3
	27.21	400	19.59	8.37	0.4273	4.26	43.2
	27.45	400	-19.97	-7.59	0.3801	3.79	38.4
	27.68	400	19.61	7.57	0.3860	3.85	39.0
	27.91	400	-19.97	-6.38	0.3195	3.19	32.3
HTQP07-22	28.14	400	19.62	6.32	0.3221	3.21	32.5
	28.37	400	-19.97	-6.83	0.3420	3.41	34.6

File #	Time (days)	Temp. (°C)	ΔPp (bars)	q x 10^{-6} (cm^3/s)	q/ΔPp x 10^{-6}	k x 10^{-20} (m^2)	k (nDa)
	28.60	400	19.59	6.97	0.3558	3.55	36.0
	28.83	400	-19.97	-6.32	0.3165	3.16	32.0
HTQP07-23	29.07	400	20.33	7.17	0.3527	3.52	35.7
	29.88	400	-19.97	-6.71	0.3360	3.35	33.9
	30.34	400	19.65	6.97	0.3547	3.54	35.9
	30.80	400	-19.97	-6.09	0.3050	3.04	30.8
	31.26	400	19.66	6.57	0.3342	3.33	33.7
	31.73	400	-19.97	-5.61	0.2809	2.80	28.4
	32.19	400	19.63	6.63	0.3377	3.37	34.1
	32.65	400	-19.97	-5.61	0.2809	2.80	28.4
	33.12	400	19.64	6.63	0.3376	3.37	34.1
	33.58	400	-19.97	-5.29	0.2649	2.64	26.7
	34.04	400	19.65	6.24	0.3176	3.17	32.1
	34.51	400	-19.97	-5.47	0.2739	2.73	27.7
	34.97	400	19.62	6.26	0.3191	3.18	32.2
	35.43	400	-19.97	-5.07	0.2539	2.53	25.6
	35.89	400	21.67	6.05	0.2792	2.78	28.2
HTQP07-24	36.60	400	-20.00	-4.89	0.2445	2.44	24.7
	37.06	400	19.93	4.66	0.2338	2.33	23.6
	37.52	400	-20.00	-4.69	0.2345	2.34	23.7
	37.99	400	19.93	4.62	0.2318	2.31	23.4
	38.45	400	-20.00	-4.54	0.2270	2.26	22.9
	38.91	400	20.31	5.69	0.2802	2.79	28.3
	39.38	400	-19.36	-4.80	0.2479	2.47	25.0
	39.84	400	20.41	5.10	0.2499	2.49	25.2
	40.30	400	-19.36	-4.49	0.2319	2.31	23.4
	40.76	400	21.25	4.97	0.2339	2.33	23.6
HTQP07-25	41.23	400	-18.70	-4.41	0.2358	2.35	23.8
	41.69	400	21.25	4.55	0.2141	2.13	21.6
HTQP07-26	42.15	400	-18.20	-3.61	0.1984	1.98	20.1
	42.62	400	21.80	4.57	0.2106	2.10	21.3
	43.08	400	-18.20	-3.38	0.1857	1.85	18.7
	43.54	400	21.80	4.52	0.2073	2.07	21.0
	44.00	400	-18.20	-3.75	0.2060	2.05	20.8
	44.47	400	21.80	4.54	0.2083	2.07	21.0
	44.93	400	-18.20	-3.53	0.1940	1.93	19.6
	45.39	400	21.80	4.39	0.2014	2.01	20.4
	45.80	400	-18.20	-3.34	0.1835	1.83	18.5

HTQP08

File #	Time (days)	Temp. (°C)	ΔPp (bars)	q x 10^{-6} (cm^3/s)	q/ΔPp x 10^{-6}	k x 10^{-19} (m^2)	k (nDa)
HTQP08-01	-0.05	25	19.60	25.92	1.3224	8.758	887.4
HTQP08-02	0.03	400	13.60	172.90	12.7132	12.309	1247.1
	0.26	400	-19.18	-170.00	8.8634	8.582	869.5
	0.49	400	19.67	152.90	7.7733	7.526	762.5
	0.72	400	-18.96	-140.00	7.3840	7.149	724.3
	0.95	400	20.02	138.42	6.9141	6.694	678.2
	1.18	400	-18.96	-127.76	6.7384	6.524	661.0
	1.41	400	20.32	132.63	6.5271	6.320	640.3
	1.65	400	-18.46	-113.82	6.1658	5.970	604.9
	1.88	400	20.52	123.68	6.0273	5.836	591.3
	2.11	400	-18.52	-107.50	5.8045	5.620	569.4
	2.34	400	20.44	115.21	5.6365	5.457	552.9
	2.57	400	-18.52	-100.00	5.3996	5.228	529.7
HTQP08-03	2.80	400	19.12	99.74	5.2165	5.051	511.8
	3.04	400	-20.28	-105.66	5.2101	5.044	511.1
	3.27	400	18.70	94.47	5.0519	4.891	495.6
	3.50	400	-20.43	-102.11	4.9980	4.839	490.3
	3.73	400	19.57	94.47	4.8273	4.674	473.6
HTQP08-04	3.96	400	-19.25	-92.63	4.8119	4.659	472.0
	4.19	400	18.99	89.34	4.7046	4.555	461.5
	4.66	400	-19.90	-89.47	4.4960	4.353	441.0
HTQP08-05	5.12	400	19.26	82.37	4.2767	4.141	419.6
	5.58	400	-20.18	-83.03	4.1145	3.984	403.7
HTQP08-06	6.04	400	19.33	78.03	4.0367	3.908	396.0
	6.51	400	-20.18	-77.11	3.8211	3.700	374.9
HTQP08-07	6.97	400	19.97	71.58	3.6335	3.518	356.4
	7.43	400	-20.13	-72.50	3.6016	3.487	353.3
	7.90	400	18.76	64.61	3.4440	3.334	337.8
	8.36	400	-20.41	-69.08	3.3846	3.277	332.0
	8.82	400	18.75	60.20	3.2107	3.109	315.0
	9.29	400	-20.56	-65.13	3.1678	3.067	310.7
	9.75	400	19.60	57.63	2.9403	2.847	288.5
	10.22	400	-20.29	-60.46	2.9798	2.885	292.3
	10.69	400	19.27	55.53	2.8817	2.790	282.7
	11.15	400	-19.84	-57.17	2.8743	2.783	282.0
	11.61	400	19.45	53.36	2.7434	2.656	269.1
	12.07	400	-19.19	-52.83	2.7254	2.639	267.4
	12.54	400	19.27	50.59	2.6253	2.542	257.6
	13.00	400	-18.82	-48.03	2.5521	2.471	250.4
	13.46	400	19.28	48.82	2.5322	2.452	248.4
HTQP08-08	13.94	400	-18.74	-46.05	2.4573	2.379	241.0
	14.40	400	19.57	48.03	2.4543	2.376	240.7
	14.86	400	-19.75	-48.55	2.4582	2.380	241.1
	15.33	400	19.33	45.00	2.3280	2.254	228.4
	15.79	400	-19.87	-46.25	2.3276	2.253	228.3
	16.25	400	19.39	43.62	2.2496	2.178	220.7
	16.72	400	-19.25	-42.17	2.1906	2.121	214.9
HTQP08-09	17.18	400	19.56	41.91	2.1426	2.074	210.1
	17.64	400	-19.35	-40.59	2.0977	2.031	205.8

File #	Time (days)	Temp. (°C)	ΔPp (bars)	q x 10^{-6} (cm^3/s)	q/ΔPp x 10^{-6}	k x 10^{-19} (m^2)	k (nDa)
HTQP08-10	18.10	400	20.20	41.64	2.0614	1.996	202.2
	18.57	400	-19.31	-40.43	2.0937	2.027	205.4
HTQP08-11	19.03	400	-19.15	-39.01	2.0371	1.972	199.8
	19.49	400	19.69	39.87	2.0249	1.961	198.7
HTQP08-12	19.96	400	-19.03	37.66	1.9790	1.916	194.1
HTQP08-13	20.42	400	19.56	37.50	1.9172	1.856	188.0
	20.88	400	-18.99	-36.32	1.9126	1.852	187.6
HTQP08-14	21.34	400	20.24	37.20	1.8379	1.779	180.2
	21.81	400	-18.98	-35.33	1.8614	1.802	182.6
	22.27	400	20.31	37.58	1.8503	1.791	181.5
	22.73	400	-18.91	-34.57	1.8281	1.770	179.3
	23.19	400	20.18	36.05	1.7873	1.730	175.3
	23.66	400	-18.70	-33.19	1.7749	1.718	174.1

HTQP09*

File #	Time (days)	Temp. (°C)	ΔPp (bars)	q x 10^{-6} (cm^3/s)	q/ΔPp x 10^{-6}	k x 10^{-19} (m^2)	k (nDa)
HTQP09-02	-0.66	25	19.62	9.00	0.4587	3.129	317.0
	-0.43	25	-19.97	-9.17	0.4592	3.132	317.3
	-0.19	25	19.69	8.70	0.4417	3.013	305.3
HTQP09-03	0.06	450	19.36	41.64	2.1508	2.116	214.4
	0.31	450	-19.76	-36.00	1.8219	1.792	181.6

*Experiment terminated because furnace failed.

HTQP10

File #	Time (days)	Temp. (°C)	ΔPp (bars)	q x 10^{-6} (cm^3/s)	q/ΔPp x 10^{-6}	k x 10^{-19} (m^2)	k (nDa)
HTQP10-01	-0.02	25	20.24	36.78	1.8172	12.395	1255.9
	0.03	450	20.24	75.00	3.7055	3.645	369.3
	0.22	450	-18.46	-50.00	2.7086	2.664	269.9
	0.45	450	21.32	54.34	2.5488	2.507	254.0
	0.68	450	-17.70	-43.09	2.4345	2.395	242.7
	0.91	450	21.26	52.17	2.4539	2.414	244.6
	1.15	450	-17.66	-42.57	2.4105	2.371	240.2
	1.38	450	21.57	51.71	2.3973	2.358	238.9
	1.61	450	-17.29	-40.00	2.3135	2.276	230.6
	1.84	450	21.57	49.93	2.3148	2.277	230.7
	2.07	450	-17.86	-41.91	2.3466	2.308	233.8

File #	Time (days)	Temp. (°C)	ΔPp (bars)	q x 10^{-6} (cm^3/s)	q/ΔPp x 10^{-6}	k x 10^{-19} (m^2)	k (nDa)
	2.30	450	21.46	49.28	2.2964	2.259	228.9
	2.53	450	-17.62	-40.13	2.2775	2.240	227.0
	2.77	450	21.57	49.05	2.2740	2.237	226.7
	3.01	450	-17.63	-39.90	2.2632	2.226	225.5
	3.24	450	21.57	48.16	2.2327	2.196	222.5
	3.47	450	-17.64	-39.31	2.2285	2.192	222.1
	3.70	450	21.57	47.60	2.2068	2.171	220.0
	3.94	450	-17.69	-38.85	2.1962	2.160	218.9
	4.17	450	21.49	46.00	2.1405	2.106	213.4
	4.40	450	-17.74	-38.16	2.1511	2.116	214.4
	4.62	450	21.57	45.59	2.1136	2.079	210.6
HTQP10-02	4.86	450	-19.57	-41.45	2.1180	2.083	211.0
	5.09	450	19.31	39.74	2.0580	2.024	205.1
	5.32	450	-19.78	-40.62	2.0536	2.020	204.7
	5.56	450	19.69	40.62	2.0630	2.029	205.6
HTQP10-03	5.79	450	-19.38	-39.15	2.0201	1.987	201.3
	6.02	450	19.74	39.21	1.9863	1.954	198.0
	6.25	450	-19.58	-39.11	1.9974	1.965	199.1
	6.48	450	20.10	39.18	1.9493	1.917	194.2
HTQP10-04	6.71	450	-19.76	-38.42	1.9443	1.913	193.8
	6.94	450	18.92	37.30	1.9715	1.939	196.5
	7.41	450	-20.05	-38.68	1.9292	1.898	192.3
HTQP10-06	8.80	450	19.15	34.67	1.8104	1.781	184.0
	9.26	450	-20.25	-37.70	1.8617	1.831	185.5
	9.72	450	19.20	35.00	1.8229	1.793	181.7
HTQP10-07	10.19	450	-19.89	-35.69	1.7944	1.765	178.8
	10.65	450	19.56	35.10	1.7945	1.765	178.8
	11.11	450	-19.30	-34.24	1.7741	1.745	176.8
	11.57	450	20.20	35.33	1.7490	1.720	174.3
HTQP10-08	12.05	450	-19.75	-33.37	1.6896	1.662	168.4
	12.51	450	19.90	33.09	1.6628	1.636	165.8
	12.97	450	-19.95	-32.96	1.6521	1.625	164.6
	13.44	450	19.61	31.33	1.5977	1.572	159.3
	13.90	450	-19.80	-32.07	1.6197	1.593	161.4
	14.36	450	19.63	30.72	1.5650	1.539	155.9
HTQP10-09	14.83	450	-19.94	-31.32	1.5707	1.545	156.5
	15.29	450	19.06	29.28	1.5362	1.511	153.1
HTQP10-10	15.75	450	-19.77	-30.58	1.5468	1.522	154.2
	16.22	450	19.10	28.32	1.4827	1.459	147.8
	16.68	450	-20.08	-29.54	1.4711	1.447	146.6
	17.14	450	19.60	28.00	1.4286	1.405	142.4
	17.60	450	-19.33	-27.84	1.4402	1.417	143.6
	18.07	450	20.00	27.43	1.3715	1.349	136.7
	18.53	450	-19.02	-26.00	1.3670	1.345	136.3
HTQP10-12	19.00	450	19.60	26.45	1.3495	1.327	134.4
	19.46	450	-19.38	-25.59	1.3204	1.299	131.6
HTQP10-13	19.79	25	19.60	13.24	0.6755	4.608	466.9

HTQP11

File #	Time (days)	Temp. (°C)	ΔPp (bars)	q x 10^{-6} (cm^3/s)	q/ΔPp x 10^{-6}	k x 10^{-20} (m^2)	k (nDa)
HTQP11-01	-0.04	25	19.60	11.86	0.6051	41.27	418.1
	0.03	300	-19.48	-30.59	1.5703	16.61	168.3
	0.20	300	20.05	20.77	1.0359	10.96	111.0
	0.44	300	-19.07	-18.45	0.9675	10.24	103.8
	0.67	300	20.18	19.22	0.9524	10.08	102.1
HTQP11-02	0.92	300	-19.02	-16.54	0.8696	9.20	93.2
	1.15	300	20.18	17.12	0.8484	8.98	91.0
	1.38	300	-18.72	-15.58	0.8323	8.81	89.3
	1.61	300	20.94	17.39	0.8307	8.79	89.1
HTQP11-03	1.84	300	-18.30	-14.75	0.8060	8.53	86.4
	2.12	300	20.91	15.87	0.7590	8.03	81.4
	2.58	300	-18.42	-13.70	0.7438	7.87	79.7
	3.05	300	21.26	16.00	0.7526	7.96	80.7
	3.51	300	-17.86	-12.41	0.6948	7.35	74.5
	3.97	300	21.61	15.77	0.7298	7.72	78.2
	4.46	300	-17.67	-12.08	0.6836	7.23	73.3
HTQP11-04	4.92	300	19.18	13.24	0.6903	7.30	74.0
	5.11	300	-19.79	-14.83	0.7494	7.93	80.3
	5.62	300	19.49	13.72	0.7040	7.45	75.5
	6.08	300	-19.83	-14.05	0.7085	7.50	76.0
	6.54	300	19.49	13.40	0.6875	7.27	73.7
	7.01	300	-19.75	-13.58	0.6876	7.27	73.7
	7.47	300	19.61	13.21	0.6736	7.13	72.2
	7.93	300	-20.31	-13.65	0.6721	7.11	72.0
	8.39	300	19.27	12.67	0.6575	6.96	70.5
	8.86	300	-19.78	-13.42	0.6785	7.18	72.7
	9.32	300	19.95	12.82	0.6426	6.80	68.9
	9.80	300	-19.41	-12.14	0.6255	6.62	67.1
	10.26	300	19.95	12.63	0.6331	6.70	67.9
	10.72	300	-19.30	-12.16	0.6301	6.67	67.6
	11.18	300	20.16	12.42	0.6161	6.52	66.1
	11.65	300	-19.97	-11.82	0.5919	6.26	63.4
HTQP11-06	12.11	300	19.07	11.63	0.6099	6.45	65.4
	12.57	300	-20.61	-12.17	0.5905	6.25	63.3
	13.04	300	18.91	11.11	0.5875	6.22	63.0
	13.50	300	-20.40	-11.80	0.5784	6.12	62.0
	13.97	300	18.64	10.95	0.5874	6.22	63.0
	14.44	300	-20.63	-11.80	0.5720	6.05	61.3
	14.90	300	18.70	10.76	0.5754	6.09	61.7
	15.36	300	-20.95	-12.05	0.5752	6.09	61.7
	15.83	300	18.91	11.05	0.5843	6.18	62.6
	16.29	300	-20.28	-11.58	0.5710	6.04	61.2
	16.75	300	19.27	10.88	0.5646	5.97	60.5
	17.21	300	-20.36	-11.43	0.5614	5.94	60.2
	17.68	300	19.25	10.88	0.5652	5.98	60.6
	18.14	300	-20.19	-11.40	0.5646	5.97	60.5
	18.60	300	19.28	10.71	0.5555	5.88	59.6
HTQP11-06'	19.07	300	-20.61	-11.58	0.5619	5.94	60.2
	19.53	300	18.98	10.60	0.5585	5.91	59.9

File #	Time (days)	Temp. (°C)	ΔPp (bars)	q x 10^{-6} (cm^3/s)	q/ΔPp x 10^{-6}	k x 10^{-20} (m^2)	k (nDa)
HTQP11-07	20.06	25	-20.00	-3.07	0.1535	10.47	106.1
	20.52	25	20.00	2.89	0.1445	9.86	99.9
HTQP11-08	20.99	25	-19.70	-2.80	0.1421	9.69	98.2
	21.45	25	20.33	2.80	0.1377	9.39	95.1

HTQP12

File #	Time (days)	Temp. (°C)	ΔPp (bars)	q x 10^{-6} (cm^3/s)	q/ΔPp x 10^{-6}	k x 10^{-20} (m^2)	k (nDa)
HTQP12-01	0.02	25	-19.44	-131.25	6.7515	460.52	4666.0
	0.05	25	19.54	108.55	5.5553	378.93	3839.3
	0.36	25	-18.50	-104.28	5.6368	384.48	3895.6
	0.59	25	21.31	82.89	3.8897	265.32	2688.2
	0.83	25	-17.77	-73.16	4.1171	280.82	2845.3
	1.06	25	21.39	77.30	3.6138	246.50	2497.5
	1.29	25	-17.59	-65.07	3.6993	252.33	2556.5
	1.52	25	21.55	77.04	3.5749	243.85	2470.7
	1.75	25	-17.58	-59.08	3.3606	229.23	2322.6
HTQP12-02	1.98	25	19.69	76.64	3.8923	265.50	2690.6
	2.21	25	-19.12	-66.78	3.4927	238.24	2413.8
	2.45	25	20.20	71.25	3.5272	240.59	2437.7
	2.68	25	-19.30	-61.21	3.1715	216.33	2191.9
	2.93	25	19.17	43.03	2.2447	153.11	1551.3
	3.20	25	-19.93	-20.39	1.0231	69.78	707.0
	3.39	25	19.62	54.01	2.7528	187.77	1902.5
	3.66	25	-19.64	-18.58	0.9460	64.53	653.8
HTQP12-03	3.86	25	18.95	34.55	1.8232	124.36	1260.0
	4.15	25	-20.25	-15.97	0.7886	53.79	545.0
	4.33	25	19.88	35.56	1.7887	122.01	1236.2
	4.62	25	-19.64	-13.62	0.6935	47.30	479.2
HTQP12-05	0.03	350	-19.60	-32.70	1.6684	17.15	173.8
	0.17	350	19.19	24.00	1.2507	12.86	130.3
	0.40	350	-20.04	-23.78	1.1866	12.20	123.6
	0.63	350	20.08	21.84	1.0876	11.18	113.3
	0.88	350	-19.20	-20.86	1.0865	11.17	113.2
HTQP12-06	1.12	350	19.20	19.87	1.0349	10.64	107.8
	1.35	350	-20.01	-21.26	1.0625	10.92	110.6
	1.58	350	19.80	19.77	0.9985	10.26	104.0
	1.81	350	-19.51	-19.15	0.9815	10.09	102.2
HTQP12-07	2.04	350	19.60	18.82	0.9602	9.87	100.0
	2.28	350	-19.62	-20.30	1.0347	10.64	107.8
	2.51	350	19.62	18.98	0.9674	9.94	100.7
	2.97	350	-19.62	-20.07	1.0229	10.52	106.6
	3.43	350	19.64	19.08	0.9715	9.99	101.2
	3.90	350	-19.45	-18.84	0.9686	9.96	100.9

File #	Time (days)	Temp. (°C)	ΔPp (bars)	q x 10^{-6} (cm^3/s)	q/ΔPp x 10^{-6}	k x 10^{-20} (m^2)	k (nDa)
	4.37	350	19.57	18.63	0.9520	9.79	99.2
	4.83	350	-19.27	-18.36	0.9528	9.79	99.2
	5.30	350	18.96	17.94	0.9462	9.73	98.6
	5.76	350	-19.65	-18.00	0.9160	9.42	95.4
HTQP12-08	6.22	350	18.85	17.54	0.9305	9.57	97.0
	6.69	350	-19.19	-18.29	0.9531	9.80	99.3
HTQP12-09	7.15	350	18.68	17.13	0.9170	9.43	95.5
	7.61	350	-19.45	-18.65	0.9589	9.86	99.9
HTQP12-10	8.07	350	19.53	17.57	0.8996	9.25	93.7
	8.54	350	-19.83	-18.91	0.9536	9.80	99.3
HTQP12-11	9.00	350	19.73	17.24	0.8738	8.98	91.0
	9.46	350	-19.92	-18.65	0.9362	9.62	97.5
	9.93	350	19.37	17.83	0.9205	9.46	95.8
	10.39	350	-19.96	-18.49	0.9264	9.52	96.5
	10.85	350	19.37	17.84	0.9210	9.47	96.0
	11.31	350	-19.57	-17.99	0.9193	9.45	95.7
	11.78	350	19.96	18.41	0.9223	9.48	96.1
HTQP12-12	12.24	350	-19.62	-17.68	0.9011	9.26	93.8
	12.70	350	19.78	18.35	0.9277	9.54	96.7
HTQP12-13	13.17	350	-19.91	-17.90	0.8990	9.24	93.6
	13.63	350	19.93	17.84	0.8951	9.20	93.2

HTQP13

File #	Time (days)	Temp. (°C)	ΔPp (bars)	q x 10^{-6} (cm^3/s)	q/ΔPp x 10^{-6}	k x 10^{-20} (m^2)	k (nDa)
HTQP13-01	-1.62	25	-18.40	-2.14	0.1165	7.95	80.5
	-1.36	25	21.60	2.86	0.1322	9.02	91.4
HTQP13-02	-0.82	25	-20.00	-3.13	0.1566	10.69	108.3
	-0.60	25	-17.91	-2.63	0.1471	10.03	101.6
	-0.27	25	22.09	3.41	0.1544	10.53	106.7
HTQP13-03	0.08	300	-19.61	-18.46	0.9414	9.96	100.9
	0.34	300	19.63	16.38	0.8344	8.83	89.5
	0.57	300	-19.61	-17.32	0.8832	9.34	94.6
	0.80	300	19.63	16.47	0.8390	8.88	90.0
	1.03	300	-19.62	-16.71	0.8517	9.01	91.3
	1.27	300	19.63	15.40	0.7845	8.30	84.1
	1.50	300	-19.63	-15.38	0.7835	8.29	84.0
	1.74	300	19.64	15.20	0.7739	8.19	83.0
	1.97	300	-19.64	-14.61	0.7439	7.87	79.7
	2.20	300	19.64	14.28	0.7271	7.69	77.9
	2.43	300	-19.65	-13.88	0.7064	7.47	75.7
	2.66	300	19.64	14.54	0.7403	7.83	79.3
	2.89	300	-19.65	-13.14	0.6687	7.07	71.6
HTQP13-04	3.19	300	19.02	12.64	0.6646	7.03	71.2

File #	Time (days)	Temp. (°C)	ΔPp (bars)	q x 10^{-6} (cm^3/s)	q/ΔPp x 10^{-6}	k x 10^{-20} (m^2)	k (nDa)
	3.66	300	-20.03	-13.72	0.6850	7.25	73.5
HTQP13-05	4.12	300	18.90	12.68	0.6709	7.10	71.9
	4.58	300	-20.09	-13.42	0.6680	7.07	71.6
HTQP13-06	5.04	300	18.82	12.22	0.6493	6.87	69.6
	5.51	300	-21.07	-13.21	0.6270	6.63	67.2
	5.97	300	19.49	11.96	0.6136	6.49	65.8
HTQP13-07	6.44	300	-20.93	-13.22	0.6316	6.68	67.7
	6.90	300	19.35	11.46	0.5922	6.27	63.5
HTQP13-08	7.36	300	-20.75	-13.16	0.6342	6.71	68.0
	7.82	300	19.00	11.70	0.6158	6.52	66.1
	8.29	300	-20.67	-12.58	0.6086	6.44	65.3
	8.75	300	19.10	11.54	0.6042	6.39	64.7
HTQP13-09	9.22	300	-20.40	-12.37	0.6064	6.42	65.0
	9.68	300	19.08	11.57	0.6064	6.42	65.0
HTQP13-10	10.14	300	-20.94	-12.08	0.5769	6.10	61.8
	10.61	300	19.08	11.03	0.5781	6.12	62.0
	11.07	300	-21.05	-12.00	0.5701	6.03	61.1
	11.53	300	20.06	11.20	0.5583	5.91	59.9
HTQP13-11	12.00	300	-19.30	-11.86	0.6145	6.50	65.9
	12.47	300	18.66	10.85	0.5815	6.15	62.3
	12.93	300	-19.35	-11.27	0.5824	6.16	62.4
	13.39	300	19.27	10.42	0.5407	5.72	58.0
	13.85	300	-19.59	-10.24	0.5227	5.53	56.0
HTQP13-12	14.32	300	19.30	10.65	0.5518	5.84	59.2
	14.79	300	-20.18	-10.79	0.5347	5.66	57.3
	15.25	300	19.59	10.83	0.5528	5.58	59.3
	15.72	300	-20.30	-10.55	0.5197	5.50	55.7
	16.18	300	19.36	10.77	0.5563	5.89	59.7
	16.64	300	-19.97	-10.51	0.5263	5.57	56.4
HTQP13-13	17.11	300	19.13	10.00	0.5227	5.53	56.0
	17.57	300	-20.25	-10.82	0.5345	5.65	57.2
HTQP13-14	18.44	25	19.97	2.81	0.1407	9.60	97.3

HTQP14

File #	Time (days)	Temp. (°C)	ΔPp (bars)	q x 10^{-6} (cm^3/s)	q/ΔPp x 10^{-6}	λ x 10^{-22} (m^3)	k x 10^{-20} (m^2)
HTQP14-01	-0.90	25	-6.67	-169.6	25.427	2594.8	
	-0.82	25	9.41	170.7	18.140	1851.2	
	-0.59	25	-6.95	-170.5	24.532	2503.5	
	-0.36	25	10.12	172.3	17.026	1737.5	
	-0.13	25	-8.18	-169.5	20.721	2114.6	
HTQP14-02	0.02	400	0.82	171.6	209.268	3122.3	
	0.09	400	-1.08	-171.6	158.889	2370.6	
	0.18	400	1.18	173.3	146.864	2191.2	

File #	Time (days)	Temp. (°C)	ΔPp (bars)	q x 10^{-6} (cm^3/s)	q/ΔPp x 10^{-6}	λ x 10^{-22} (m^3)	k x 10^{-20} (m^2)
	0.41	400	-1.33	-171.8	129.173	1927.3	
	0.65	400	1.39	174.5	125.540	1873.0	
	0.87	400	-1.41	-174.1	123.475	1842.2	
	1.11	400	1.44	177.0	122.917	1833.9	
	1.34	400	-1.36	-173.0	127.206	1897.9	
	1.57	400	1.37	176.6	128.905	1923.3	
	1.80	400	-1.35	-174.7	129.407	1930.8	
	2.03	400	1.29	175.8	136.279	2033.3	
	2.27	400	-1.27	-172.3	135.669	2024.2	
	2.50	400	1.23	175.7	142.846	2131.3	
	2.73	400	-1.22	-170.8	140.000	2088.8	
HTQP14-04	3.93	400	1.30	177.2	136.308	2033.7	
	4.12	400	-1.31	-175.8	134.198	2002.2	
	4.35	400	1.32	175.5	132.954	1983.7	
	4.58	400	-1.35	-174.8	129.482	1931.9	
	4.81	400	1.30	172.8	132.923	1983.2	
HTQP14-05	5.04	400	-1.29	-175.7	136.202	2032.1	
	5.28	400	1.32	178.4	135.152	2016.5	
	5.51	400	-1.29	-175.0	135.659	2024.0	
	5.74	400	1.29	171.3	132.791	1981.2	
HTQP14-06	5.97	400	-1.28	-171.7	134.141	2001.4	
	6.20	400	1.27	171.8	135.276	2018.3	
	6.43	400	-1.23	-173.4	140.976	2103.4	
	6.66	400	1.24	174.4	140.645	2098.4	
	6.90	400	-1.27	-173.0	136.220	2032.4	
HTQP14-07	7.13	400	1.24	173.2	139.677	2083.9	
	7.36	400	-1.26	-171.6	136.190	2032.0	
	7.59	400	1.24	174.0	140.323	2093.6	
HTQP14-08	9.94	400	-1.72	-171.4	99.651	1486.8	
	10.22	400	1.52	170.7	112.303	1675.6	
	10.69	400	-2.16	-174.6	80.833	1206.0	
HTQP14-09	11.13	400	1.67	173.3	103.772	1548.3	
	11.59	400	-3.97	-175.1	44.106	658.1	
HTQP14-10	12.06	400	1.58	170.7	108.038	1611.9	
	12.52	400	-5.30	-175.8	33.170	494.9	
HTQP14-11	12.98	400	1.58	171.4	108.481	1618.5	
	13.45	400	-1.75	-174.0	99.429	1483.5	
	13.91	400	2.39	174.2	72.887	1087.5	
HTQP14-12	14.37	400	-6.76	-175.3	25.932	3869.0	
	14.84	400	4.08	171.5	42.034	627.2	
	15.30	400	-11.66	-173.3	14.863	221.8	
	15.76	400	6.95	175.8	25.295	377.4	
	16.22	400	-16.92	-177.7	10.502	156.7	
	16.69	400	14.49	175.0	12.077	180.2	
HTQP14-13	17.20	400	-19.98	-7.9	0.395	6.0	3.94
	17.79	400	19.86	5.2	0.262	3.9	2.61
HTQP14-14	18.17	400	-19.99	-4.1	0.206	3.1	2.05
	18.75	400	19.90	3.5	0.177	2.6	1.76
HTQP14-15	19.22	400	-19.93	-5.9	0.298	4.4	2.97
	19.68	400	19.93	3.4	0.171	2.5	1.70
HTQP14-16	20.00	400	-19.98	-10.3	0.515	7.7	5.13

File #	Time (days)	Temp. (°C)	ΔPp (bars)	q x 10^{-6} (cm^3/s)	q/ΔPp x 10^{-6}	λ x 10^{-22} (m^3)	k x 10^{-20} (m^2)
	20.90	400	20.00	3.1	0.155	2.3	1.54
HTQP14-17	21.55	400	-20.00	-7.5	0.376	5.6	3.74
	22.98	400	20.00	3.1	0.156	2.3	1.56
	23.65	400	-20.00	-7.8	0.390	5.8	3.89
HTQP14-18	25.07	400	19.97	4.0	0.198	3.0	1.98
HTQP14-19	25.76	400	-20.00	-7.6	0.381	5.7	3.80
HTQP14-20	27.15	400	19.91	3.9	0.198	3.0	1.97
HTQP14-21	27.38	400	-20.00	-8.3	0.416	6.2	4.14
	27.79	400	20.00	4.3	0.215	3.2	2.14

HTQP15

File #	Time (days)	Temp. (°C)	ΔPp (bars)	q x 10^{-6} (cm^3/s)	q/ΔPp x 10^{-6}	k x 10^{-20} (m^2)	k (nDa)
HTQP15-04	-0.64	25	20.00	1.80	0.0900	6.14	62.2
	-0.41	25	-20.00	-2.00	0.1000	6.82	69.1
	-0.18	25	20.00	1.73	0.0865	6.00	60.8
HTQP15-05	0.04	350	-19.60	-40.63	2.0729	21.31	215.9
	0.18	350	19.37	29.49	1.5224	15.65	158.6
	0.42	350	-19.81	-26.36	1.3305	13.68	138.6
	0.66	350	19.93	25.01	1.2547	12.90	130.7
	0.89	350	-19.46	-23.75	1.2179	12.52	126.9
HTQP15-06	1.12	350	19.36	23.56	1.2169	12.51	126.7
	1.35	350	-19.53	-23.57	1.2069	12.41	125.7
	1.59	350	19.79	23.49	1.1871	12.20	123.6
	1.82	350	-19.47	-23.18	1.1908	12.24	124.0
	2.05	350	19.74	23.19	1.1748	12.08	122.4
	2.28	350	-19.53	-23.17	1.1861	12.19	123.5
	2.51	350	19.77	23.21	1.1741	12.07	122.3
	2.74	350	-19.48	-23.17	1.1892	12.22	123.9
	2.97	350	19.78	23.21	1.1735	12.06	122.2
	3.21	350	-19.48	-23.17	1.1892	12.22	123.9
	3.44	350	19.72	23.21	1.1770	12.10	122.6
	3.67	350	-19.48	-23.17	1.1909	12.22	123.9
	3.90	350	19.90	23.26	1.1690	12.02	121.8
HTQP15-07	4.13	350	-19.69	-23.20	1.1782	12.11	122.7
	4.36	350	19.74	22.93	1.1616	11.94	121.0
	4.59	350	-19.60	-23.33	1.1903	12.23	124.0
	4.82	350	20.14	23.44	1.1639	11.96	121.2
HTQP15-08	5.06	350	-19.99	-23.95	1.1983	12.32	124.8
	5.29	350	19.44	22.71	1.1680	12.01	121.7
	5.52	350	-19.60	-23.17	1.1819	12.15	123.1
	5.75	350	19.54	23.48	1.2016	12.35	125.2
	5.98	350	-19.72	-23.47	1.1917	12.25	124.1
HTQP15-09	6.21	350	19.31	22.41	1.1606	11.93	120.9

File #	Time (days)	Temp. (°C)	ΔPp (bars)	q x 10^{-6} (cm^3/s)	q/ΔPp x 10^{-6}	k x 10^{-20} (m^2)	k (nDa)
	6.44	350	-19.90	-23.26	1.1690	12.02	121.8
	6.68	350	19.97	22.79	1.1410	11.73	118.8
	6.91	350	-19.78	-23.23	1.1729	12.06	122.2
HTQP15-10	7.14	350	19.02	22.38	1.1766	12.10	122.5
	7.14	350	19.96	24.34	1.2197	12.54	127.0
	7.37	350	-19.55	-24.31	1.2436	12.78	129.5
	7.60	350	19.48	22.71	1.1656	11.98	121.4
	7.83	350	-19.37	-23.20	1.1976	12.31	124.7
HTQP15-11	8.06	350	19.37	22.54	1.1638	11.96	121.2
	8.30	350	-19.95	-23.53	1.1792	12.12	122.8
	8.53	350	19.34	22.61	1.1690	12.02	121.8
	8.76	350	-19.98	-23.26	1.1643	11.97	121.3
	8.99	350	19.34	22.44	1.1605	11.93	120.9
	9.22	350	-19.83	-23.43	1.1814	12.14	123.0
	9.45	350	19.63	22.67	1.1551	11.87	120.3
	9.69	350	-19.73	-23.47	1.1897	12.23	123.9
	9.92	350	19.46	22.71	1.1668	11.99	121.5
	10.15	350	-20.00	-23.57	1.1786	12.12	122.8
	10.38	350	19.34	22.64	1.1707	12.03	121.9
	10.61	350	-19.98	-23.49	1.1758	12.09	122.5
	10.84	350	19.30	22.64	1.1710	12.04	122.0
HTQP15-12	11.07	350	-20.19	-23.79	1.1782	12.11	122.7
	11.31	350	19.23	22.38	1.1637	11.96	121.2
	11.54	350	-19.98	-23.44	1.1732	12.06	122.2
	11.77	350	19.36	22.94	1.1829	12.16	123.2
HTQP15-13	12.00	350	-20.06	-24.00	1.1964	12.30	124.6
	12.23	350	19.76	23.26	1.1773	12.10	122.6
	12.46	350	-20.38	-23.72	1.1640	11.96	121.2
	12.69	350	19.32	22.41	1.1600	11.92	120.8
	12.69	350	19.42	23.39	1.2049	12.39	125.5
	12.93	350	-19.92	-23.72	1.1909	12.24	124.0

HTQP16

File #	Time (days)	Temp. (°C)	ΔPp (bars)	q x 10^{-6} (cm^3/s)	q/ΔPp x 10^{-6}	k x 10^{-20} (m^2)	k (nDa)
HTQP16-01	-0.53	25	19.93	3.60	0.1806	12.32	124.8
	-0.17	25	-19.95	-3.00	0.1504	10.26	103.9
HTQP16-02	0.03	350	19.60	32.40	1.6533	17.00	172.2
	0.20	350	-19.47	-24.97	1.2823	13.18	133.6
	0.38	350	19.78	22.27	1.1261	11.58	117.3
	0.62	350	-19.27	-20.87	1.0831	11.13	112.8
	0.85	350	20.56	21.02	1.0214	10.50	106.4
HTQP16-03	1.08	350	-19.46	-19.66	1.0102	10.39	105.2
	1.31	350	19.70	19.36	0.9830	10.10	102.4

File #	Time (days)	Temp. (°C)	ΔPp (bars)	q x 10^{-6} (cm^3/s)	q/ΔPp x 10^{-6}	k x 10^{-20} (m^2)	k (nDa)
	1.55	350	-19.48	-19.36	0.9941	10.22	103.5
	1.78	350	19.85	19.20	0.9673	9.94	100.7
	2.01	350	-19.45	-18.87	0.9703	9.97	101.1
	2.24	350	19.74	18.71	0.9478	9.74	98.7
	2.47	350	-19.46	-18.55	0.9530	9.80	99.3
	2.70	350	19.93	18.83	0.9447	9.71	98.4
	2.93	350	-19.38	-18.60	0.9596	9.86	100.0
	3.17	350	19.89	18.81	0.9456	9.72	98.5
	3.40	350	-19.32	-18.64	0.9650	9.92	100.5
	3.63	350	20.58	18.71	0.9091	9.35	94.7
	3.86	350	-18.87	-18.00	0.9539	9.81	99.4
HTQP16-04	4.10	350	19.50	18.18	0.9326	9.59	97.1
	4.33	350	-19.61	-18.71	0.9541	9.81	99.4
	4.56	350	19.77	18.51	0.9364	9.63	97.5
	4.79	350	-19.46	-18.00	0.9250	9.51	96.3
HTQP16-05	5.03	350	19.37	18.15	0.9371	9.63	97.6
	5.26	350	-19.91	-18.84	0.9463	9.73	98.6
	5.50	350	19.76	18.22	0.9219	9.48	96.0
	5.73	350	-19.17	-18.00	0.9390	9.65	97.8
	5.96	350	19.93	17.76	0.8911	9.16	92.8
HTQP16-06	6.19	350	-19.64	-17.10	0.8709	8.95	90.7
	6.42	350	19.57	16.87	0.8622	8.86	89.8
	6.64	350	-18.65	-18.67	1.0011	10.29	104.3
	6.88	350	20.37	18.45	0.9056	9.31	94.3
HTQP16-07	7.11	350	-20.19	-18.00	0.8915	9.16	92.9
HTQP16-08	8.04	350	20.15	17.50	0.8683	8.93	90.4
	8.50	350	-20.41	-18.84	0.9231	9.49	96.1
	8.96	350	19.60	17.64	0.9000	9.25	93.7
	9.43	350	-19.58	-18.45	0.9421	9.68	98.1
	9.89	350	19.57	18.02	0.9208	9.47	95.9
	10.35	350	-19.63	-18.51	0.9431	9.69	98.2
	10.82	350	19.40	18.91	0.9743	10.01	101.5
HTQP16-09	11.28	350	-19.98	-18.94	0.9479	9.74	98.7
	11.74	350	19.61	18.61	0.9490	9.76	98.8
HTQP16-10	12.20	350	-19.81	-19.14	0.9659	9.93	100.6
	12.67	350	19.94	18.09	0.9070	9.32	94.5
HTQP16-11	13.13	350	-20.02	-19.20	0.9581	9.85	99.8
	13.59	350	19.29	18.09	0.9376	9.64	97.7
HTQP16-12	14.06	350	-19.79	-18.74	0.9470	9.74	98.6
	14.52	350	19.23	17.73	0.9218	9.48	96.0
	14.98	350	-19.87	-18.84	0.9482	9.75	98.7
HTQP16-13	15.45	350	19.63	16.80	0.8559	8.80	89.2
	15.91	350	-19.69	-18.55	0.9419	9.68	98.1
	16.37	350	19.48	17.79	0.9130	9.39	95.1
	16.83	350	-20.00	-17.89	0.8945	9.20	93.2
	17.30	350	19.15	17.76	0.9274	9.53	96.6
	17.76	350	-20.00	-17.31	0.8657	8.90	90.2
HTQP16-14	18.22	350	19.00	18.13	0.9540	9.81	99.4
	18.69	350	-19.96	-17.88	0.8956	9.21	93.3
HTQP16-15	19.09	350	19.24	17.12	0.8896	9.15	92.7

HTQP17*

File #	Time (days)	Temp. (°C)	ΔPp (bars)	q x 10^{-6} (cm^3/s)	q/ΔPp x 10^{-6}	k x 10^{-19} (m^2)	k (nDa)
HTQP17-01	-0.83	25	-19.61	-15.69	0.8003	5.459	553.1
	-0.65	25	19.57	11.70	0.5979	4.078	413.2
	-0.41	25	-19.85	-15.30	0.7708	5.257	532.6
	-0.17	25	19.65	13.76	0.7003	4.776	483.9
HTQP17-02	0.02	450	-19.91	-66.06	3.3177	3.264	330.7
	0.10	450	18.99	52.75	2.7779	2.733	276.9

* Experiment terminated because of jacket leak.

HTQP18

File #	Time (days)	Temp. (°C)	ΔPp (bars)	q x 10^{-6} (cm^3/s)	q/ΔPp x 10^{-6}	k x 10^{-19} (m^2)	k (nDa)
HTQP18-01	-0.25	25	-19.92	-13.16	0.6606	4.506	456.5
	-0.10	25	19.67	13.87	0.7049	4.808	487.2
HTQP18-02	0.02	450	-19.61	-80.54	4.1071	4.040	409.3
	0.07	450	19.59	60.16	3.0710	3.021	306.1
	0.30	450	-19.62	-51.77	2.6386	2.596	263.0
	0.54	450	19.59	49.74	2.5391	2.498	253.1
	0.77	450	-19.62	-47.97	2.4450	2.405	243.7
HTQP18-02'	1.00	450	19.48	47.51	2.4389	2.399	243.1
	1.23	450	-19.61	-46.79	2.3860	2.347	237.8
	1.46	450	19.46	46.79	2.4044	2.365	239.6
	1.70	450	-19.45	-45.90	2.3598	2.321	235.2
	1.92	450	19.62	45.22	2.3046	2.267	229.7
HTQP18-03	2.16	450	-19.62	-45.26	2.3066	2.269	229.9
	2.39	450	19.59	44.07	2.2496	2.213	224.2
	2.63	450	-19.62	-43.71	2.2278	2.191	222.0
	2.86	450	19.59	43.34	2.2121	2.176	220.5
	3.09	450	-19.63	-43.30	2.2060	2.170	219.9
	3.32	450	19.45	41.60	2.1388	2.104	213.2
	3.55	450	-19.53	-41.71	2.1357	2.101	212.9
	3.78	450	19.60	41.40	2.1120	2.078	210.5
	4.01	450	-19.74	-41.86	2.1206	2.086	211.4
	4.25	450	19.45	40.00	2.0566	2.023	205.0
	4.48	450	-19.48	-40.31	2.0695	2.036	206.3
	4.71	450	19.61	39.44	2.0110	1.978	200.4
	4.94	450	-19.65	-40.06	2.0390	2.006	203.2
HTQP18-04	5.17	450	19.45	39.88	2.0502	2.017	204.3
	5.41	450	-19.81	-39.33	1.9854	1.953	197.8
	5.64	450	19.61	37.99	1.9375	1.906	193.1
	5.87	450	-19.64	-38.37	1.9536	1.922	194.7
HTQP18-05	6.10	450	19.43	37.47	1.9285	1.897	192.2
	6.33	450	-19.66	-38.30	1.9483	1.916	194.2
	6.56	450	19.67	37.16	1.8890	1.858	188.3

File #	Time (days)	Temp. (°C)	ΔPp (bars)	q x 10^{-6} (cm^3/s)	q/ΔPp x 10^{-6}	k x 10^{-19} (m^2)	k (nDa)
	6.80	450	-19.37	-37.02	1.9115	1.880	190.5
HTQP18-06	7.03	450	19.47	35.98	1.8478	1.818	184.2
	7.26	450	-19.49	-36.89	1.8928	1.862	188.6
	7.49	450	19.48	35.94	1.8452	1.815	183.9
	7.72	450	-19.49	-36.01	1.8476	1.817	184.1
	7.95	450	19.49	34.86	1.7887	1.760	178.3
HTQP18-07	8.19	450	-19.86	-34.73	1.7488	1.720	174.3
	8.42	450	19.28	34.21	1.7742	1.745	176.8
	8.65	450	-19.66	-34.80	1.7699	1.741	176.4
	8.88	450	19.61	33.94	1.7310	1.703	172.5
HTQP18-08	9.11	450	-19.74	-34.06	1.7256	1.697	172.0
	9.34	450	19.45	32.84	1.6886	1.661	168.3
	9.81	450	-19.51	-33.42	1.7130	1.685	170.7
	10.27	450	19.35	32.47	1.6781	1.651	167.2
	10.73	450	-19.66	-32.21	1.6383	1.612	163.3
	11.20	450	19.21	30.85	1.6060	1.580	160.1
	11.67	450	-19.66	-32.00	1.6277	1.601	162.2
	12.13	450	19.36	30.54	1.5773	1.552	157.2
	12.59	450	-19.77	-30.86	1.5612	1.536	155.6
	13.06	450	19.13	29.48	1.5408	1.516	153.6
	13.52	450	-19.91	-30.24	1.5190	1.494	151.4
	13.99	450	19.29	28.51	1.4778	1.454	147.3
	14.45	450	-20.00	-29.55	1.4777	1.454	147.3
	14.91	450	19.36	28.24	1.4589	1.435	145.4
	15.38	450	-19.82	-28.87	1.4564	1.433	145.2
	15.88	450	19.53	27.42	1.4042	1.381	140.0
	16.30	450	-19.86	-27.65	1.3924	1.370	138.8
	16.76	450	19.36	26.67	1.3776	1.355	137.3
	17.24	450	-19.95	-27.31	1.3691	1.347	136.5
	17.70	450	19.42	25.56	1.3160	1.295	131.2
	18.16	450	-20.17	-26.57	1.3174	1.296	131.3
	18.63	450	19.19	24.89	1.2970	1.276	129.3
	19.09	450	-20.16	-25.72	1.2758	1.255	127.2
	19.55	450	19.36	24.24	1.2521	1.232	124.8
HTQP18-09	20.02	450	-20.10	-24.80	1.2340	1.214	123.0

HTQP19

File #	Time (days)	Temp. (°C)	ΔPp (bars)	q x 10^{-6} (cm^3/s)	q/ΔPp x 10^{-6}	k x 10^{-19} (m^2)	k (nDa)
HTQP19-01	-0.66	25	19.61	10.59	0.5400	3.683	373.2
	-0.41	25	-19.92	-9.75	0.4895	3.339	338.3
	-0.18	25	19.64	9.84	0.5012	3.419	346.4
HTQP19-02	0.02	400	-19.59	-46.00	2.3481	2.341	237.2
	0.14	400	19.61	33.54	1.7103	1.705	172.8

File #	Time (days)	Temp. (°C)	ΔPp (bars)	q x 10^{-6} (cm^3/s)	q/ΔPp x 10^{-6}	k x 10^{-19} (m^2)	k (nDa)
	0.37	400	-19.27	-30.19	1.5667	1.562	158.3
	0.61	400	19.74	28.83	1.4607	1.456	147.6
	0.84	400	-19.31	-27.44	1.4209	1.417	143.5
	1.08	400	19.62	27.10	1.3811	1.377	139.5
	1.31	400	-19.54	-27.10	1.3867	1.383	140.1
	1.54	400	19.78	26.92	1.3610	1.357	137.5
	1.77	400	-19.39	-26.61	1.3721	1.368	138.6
	2.01	400	19.65	26.47	1.3473	1.343	136.1
	2.24	400	-19.61	-26.72	1.3627	1.359	137.7
	2.47	400	19.78	26.54	1.3418	1.338	135.5
	2.70	400	-19.39	-26.22	1.3522	1.348	136.6
	2.93	400	19.99	26.59	1.3300	1.326	134.3
HTQP19-03	3.16	400	-19.49	-26.28	1.3483	1.344	136.2
	3.39	400	19.63	25.69	1.3086	1.305	132.2
	3.63	400	-19.49	-26.00	1.3340	1.330	134.8
	3.86	400	19.92	26.61	1.3356	1.332	134.9
HTQP19-04	4.09	400	-19.63	-26.21	1.3353	1.331	134.9
	4.32	400	19.62	25.85	1.3176	1.314	133.1
	4.55	400	-19.67	-26.00	1.3218	1.318	133.5
	4.78	400	19.64	26.34	1.3413	1.337	135.5
HTQP19-05	5.02	400	-19.45	-26.47	1.3612	1.357	137.5
	5.25	400	19.61	25.66	1.3083	1.304	132.2
	5.48	400	-19.85	-26.31	1.3255	1.321	133.9
	5.71	400	19.66	26.00	1.3225	1.319	133.6
	5.94	400	-19.53	-26.00	1.3313	1.327	134.5
HTQP19-06	6.17	400	19.45	25.62	1.3174	1.313	133.1
	6.40	400	-19.48	-26.44	1.3574	1.353	137.1
	6.64	400	19.49	26.00	1.3334	1.330	134.8
	6.87	400	-19.33	-25.36	1.3120	1.308	132.5
HTQP19-07	7.10	400	19.44	25.75	1.3248	1.321	133.8
	7.33	400	-19.80	-26.28	1.3272	1.323	134.1
	7.56	400	19.59	25.85	1.3196	1.316	133.3
	7.79	400	-19.65	-26.21	1.3340	1.330	134.8
	8.02	400	19.44	26.19	1.3474	1.343	136.1
	8.26	400	-19.81	-26.41	1.3331	1.329	134.7
	8.49	400	19.73	26.30	1.3329	1.329	134.6
	8.72	400	-19.39	-26.31	1.3569	1.353	137.1
	8.95	400	19.60	26.61	1.3574	1.353	137.1
	9.18	400	-19.78	-26.93	1.3616	1.358	137.6
	9.41	400	19.66	26.77	1.3616	1.358	137.5
	9.64	400	-19.60	-26.70	1.3624	1.358	137.6
	9.88	400	19.76	27.03	1.3680	1.364	138.2

HTQP20

File #	Time (days)	Temp. (°C)	ΔPp (bars)	q x 10^{-6} (cm^3/s)	q/ΔPp x 10^{-6}	k x 10^{-20} (m^2)	k (nDa)
HTQP20-01	-0.52	25	-20.15	-3.60	0.1787	12.19	120.3
	-0.22	25	-20.15	-2.94	0.1457	9.94	100.7
HTQP20-02	0.06	400	19.76	39.15	1.9815	19.76	200.2
	0.30	400	-19.46	-32.84	1.6878	16.83	170.5
	0.54	400	19.74	30.66	1.5533	15.49	156.9
	0.77	400	-19.30	-28.60	1.4821	14.78	149.7
HTQP20-03	1.00	400	19.99	28.83	1.4424	14.38	145.7
	1.24	400	-19.46	-28.15	1.4463	14.42	146.1
	1.47	400	19.78	28.18	1.4246	14.20	143.9
	1.70	400	-19.16	-27.60	1.4406	14.36	145.5
	1.94	400	20.03	27.62	1.3790	13.75	139.3
HTQP20-04	2.17	400	-19.32	-27.13	1.4042	14.00	141.9
	2.40	400	20.01	27.23	1.3607	13.57	137.5
	2.63	400	-19.11	-26.88	1.4066	14.02	142.1
	2.86	400	20.11	27.69	1.3768	13.73	139.1
	3.09	400	-19.47	-27.40	1.4076	14.03	142.2
	3.32	400	19.87	27.01	1.3594	13.55	137.3
	3.56	400	-19.26	-26.57	1.3797	13.76	139.4
	3.79	400	20.04	27.59	1.3767	13.73	139.1
	4.02	400	-19.45	-26.97	1.3864	13.82	140.1
	4.26	400	19.86	26.76	1.3472	13.43	136.1
	4.49	400	-19.28	-26.87	1.3935	13.89	140.8
	4.72	400	20.14	27.46	1.3633	13.59	137.7
	4.96	400	-19.49	-26.97	1.3836	13.79	139.8
HTQP20-05	5.18	400	19.84	26.21	1.3212	13.17	133.5
	5.40	400	-19.47	-27.49	1.4119	14.08	142.6
	5.63	400	20.34	26.99	1.3267	13.23	134.0
	5.86	400	-19.30	-26.47	1.3717	13.68	138.6

HTQP21

File #	Time (days)	Temp. (°C)	ΔPp (bars)	q x 10^{-6} (cm^3/s)	q/ΔPp x 10^{-6}	k x 10^{-20} (m^2)	k (nDa)
HTQP21-01	-0.46	25	19.79	3.18	0.1609	10.98	111.2
	-0.14	25	-20.02	-2.10	0.1047	7.14	72.4
HTQP21-02	0.03	400	-19.47	-27.26	1.4001	13.96	141.4
	0.19	400	20.07	20.35	1.0138	10.11	102.4
	0.43	400	-19.65	-17.89	0.9104	9.08	92.0
	0.67	400	19.64	17.02	0.8665	8.64	87.5
	0.90	400	-19.67	-15.66	0.7962	7.94	80.4
HTQP21-03	1.13	400	19.60	16.30	0.8318	8.29	84.0
	1.36	400	-19.75	-16.57	0.8388	8.36	84.7
	1.60	400	19.60	15.40	0.7857	7.83	79.4

File #	Time (days)	Temp. (°C)	ΔPp (bars)	q x 10^{-6} (cm^3/s)	q/ΔPp x 10^{-6}	k x 10^{-20} (m^2)	k (nDa)
	1.83	400	-19.80	-15.14	0.7645	7.62	77.2
	2.07	400	19.60	14.84	0.7569	7.55	76.5
	2.30	400	-19.95	-14.84	0.7437	7.41	75.1
	2.53	400	19.60	14.91	0.7610	7.59	76.9
	2.77	400	-19.95	-14.43	0.7233	7.21	73.1
	3.00	400	19.60	14.42	0.7356	7.33	74.3
	3.23	400	-19.90	-14.43	0.7251	7.23	73.2
	3.46	400	19.60	14.61	0.7456	7.43	75.3
	3.70	400	-19.90	-13.97	0.7021	7.00	70.9
	3.93	400	19.60	14.61	0.7456	7.43	75.3
HTQP21-04	4.16	400	-19.87	-13.96	0.7023	7.00	70.9
	4.51	400	19.28	13.76	0.7138	7.12	72.1
	4.98	400	-19.47	-13.65	0.7012	6.99	70.8
HTQP21-05	5.44	400	20.19	13.11	0.6491	6.47	65.6
	5.91	400	-19.93	-12.80	0.6425	6.41	64.9
HTQP21-06	6.38	400	19.42	12.90	0.6641	6.62	67.1
	6.84	400	-20.60	-12.60	0.6118	6.10	61.8
HTQP21-07	7.30	400	19.59	12.41	0.6332	6.31	64.0
	7.77	400	-20.60	-12.58	0.6107	6.09	61.7
HTQP21-08	8.24	400	19.41	12.20	0.6286	6.27	63.5
	8.70	400	-19.98	-12.84	0.6428	6.41	64.9
	9.16	400	19.62	12.31	0.6275	6.26	63.4
	9.63	400	-19.65	-12.56	0.6390	6.37	64.5
	10.10	400	20.10	11.74	0.5842	5.82	59.0
	10.56	400	-19.62	-12.18	0.6206	6.19	62.7
	11.02	400	21.19	12.61	0.5950	5.93	60.1
	11.48	400	-19.85	-12.00	0.6045	6.03	61.1
HTQP21-09	11.95	400	19.40	11.36	0.5857	5.84	59.2
	12.41	400	-19.59	-12.00	0.6126	6.11	61.9
	12.87	400	19.56	11.73	0.5997	5.98	60.6
HTQP21-10	13.33	400	-20.72	-12.19	0.5883	5.86	59.4
	13.79	400	19.74	11.73	0.5942	5.92	60.0
HTQP21-11	14.26	400	-20.68	-11.51	0.5564	5.55	56.2
	14.73	400	20.70	11.23	0.5426	5.41	54.8
HTQP21-12	15.20	400	-21.01	-10.88	0.5178	5.16	52.3
	15.66	400	19.40	10.96	0.5648	5.63	57.1
	16.12	400	-19.76	-11.14	0.5638	5.62	57.0
	16.58	400	19.83	11.00	0.5549	5.53	56.1
	17.05	400	-19.79	-10.97	0.5543	5.53	56.0
	17.51	400	19.77	10.66	0.5391	5.37	54.5
HTQP21-13	17.97	400	-20.07	-10.56	0.5263	5.25	53.2
	18.44	400	19.59	9.95	0.5078	5.06	51.3
	18.90	400	-20.64	-10.14	0.4912	4.90	49.6
HTQP21-14	19.37	400	19.16	9.92	0.5178	5.16	52.3
	19.83	400	-20.52	-9.59	0.4675	4.66	47.2
HTQP21-15	20.30	400	19.02	9.44	0.4961	4.95	50.1
	20.76	400	-20.08	-9.54	0.4752	4.74	48.0
HTQP21-16	21.23	400	19.59	9.08	0.4636	4.62	46.8
	21.68	400	-19.97	-10.00	0.5008	4.99	50.6
HTQP21-17	22.15	400	19.15	9.03	0.4715	4.70	47.6
	22.60	400	-20.15	-9.72	0.4824	4.81	48.7

File #	Time (days)	Temp. (°C)	ΔPp (bars)	q x 10^{-6} (cm^3/s)	q/ΔPp x 10^{-6}	k x 10^{-20} (m^2)	k (nDa)
	23.07	400	19.52	9.19	0.4676	4.66	47.2
	23.53	400	-20.09	-9.55	0.4756	4.74	48.0
	23.99	400	19.65	9.33	0.4749	4.73	48.0
	24.45	400	-19.97	-9.58	0.4797	4.78	48.5
	24.92	400	19.58	9.49	0.4846	4.83	49.0
	25.38	400	-19.99	-9.42	0.4714	4.70	47.6
	25.84	400	19.61	9.61	0.4899	4.88	49.5
	26.31	400	-19.97	-9.42	0.4719	4.70	47.7
	26.77	400	19.04	9.16	0.4812	4.80	48.6
	27.23	400	-20.72	-9.45	0.4561	4.55	46.1
	27.70	400	20.27	8.77	0.4326	4.31	43.7
HTQP21-18	28.17	400	-19.68	-9.14	0.4642	4.63	46.9
	28.64	400	20.86	8.52	0.4084	4.07	41.3
HTQP21-18'	29.15	400	-19.84	-8.78	0.4426	4.41	44.7
	29.65	400	19.81	8.78	0.4430	4.42	44.8
	30.11	400	-19.84	-8.49	0.4281	4.27	43.2
	30.58	400	19.61	8.62	0.4398	4.38	44.4
	31.06	400	-19.96	-7.73	0.3874	3.86	39.1
	31.50	400	19.62	8.56	0.4361	4.35	44.0
	31.90	400	-19.97	-7.73	0.3872	3.86	39.1

of nanodarcies (1 nda = 9.87 x 10^{-22} m^2), for easier comparison with much of the older literature on permeability.

The original intent was to initiate investigations on a pure quartz system, because of its mineralogical and chemical simplicity and because solution-transfer processes involving silica are commonly invoked as a major cause of permeability change (for example, Morrow and others, 1985; Udell and Lofy, 1989; Lowell and others, 1993). An ultra-fine quartz powder was to be used in sliding experiments representing motion along a fault. Because quartzite, which is strong, also has very low permeability (for example, Morrow and others, 1985), novaculite was considered for use as the quartz-rich end pieces. The first three experiments tested the novaculite and quartz powders, with or without an applied differential stress. The results of these initial experiments are summarized below.

HTQP01. This experiment was conducted to evaluate the performance of novaculite at elevated temperatures and under an axial load. The sample was held at room temperature at 100 MPa confining pressure and 20 MPa pore pressure for about 65 hours, to determine how the novaculite would hold up under pressure. The pressures were then raised to 150 MPa confining pressure and 100 MPa pore pressure. At room temperature, flow rate was measured at a differential pore pressure of 1.0 MPa; upon heating, however, this pore-pressure difference could not be attained. For the heated samples, therefore, the differential pore pressure at a constant flow rate was measured.

The sample was heated first to 200°C and subsequently to 400°C; permeability was measured immediately after each temperature increase (Fig. 4). A differential stress of 120 MPa was then applied to the sample (File numbers HTQP01-04 to HTQP01-07 in Table 2). At that time, the novaculite began to creep (Table 2), although the shortening did not noticeably affect permeability in this case. The sample suffered a permanent change in shape during the experiment, the length decreasing by 0.051 mm and the diameter increasing by 0.025 mm.

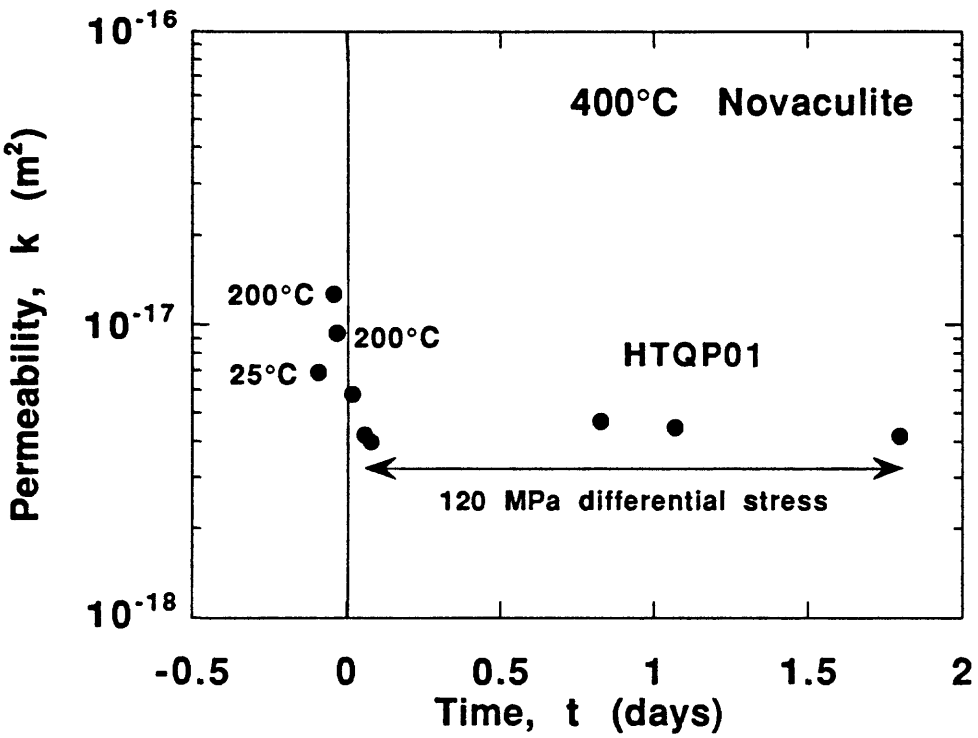

Figure 4. Permeability of intact novaculite sample HTQP01 at 25°C, 200°C, and 400°C. All of the 400°C measurements except for the first were conducted with an imposed differential stress of 120 MPa.

HTQP02. This experiment tested the behavior of the quartz powder without an applied differential stress (Fig. 5), to provide a baseline for comparison with intended later experiments involving sliding on a sawcut or fracture surface. The gouge layer shortened by about 15% as the confining pressure was applied. Upon heating, the sample began to creep (Table 2, Fig. 6) at an initially rapid rate, but within a few hours it settled into a slower, steady rate of creep. The final sample length was 1.96 mm less than the initial length. If the shortening was concentrated in the gouge layer, its length was reduced by about one-fourth. Based on the results of experiment HTQP01, however, the novaculite may also have shortened to some extent.

The permeability of this gouge-bearing sample at 400°C was relatively high (Fig. 5) and, at first, a strong function of the flow direction (Table 2). By the end of the experiment, the permeability had decreased to 20-25% of the initial heated values, and the variation with flow direction had decreased substantially. Much of the permeability decrease may be attributable to compaction/creep at 400°C.

HTQP03. This second experiment using the fine-grained quartz gouge substituted granite end pieces for the novaculite of the previous experiment. The change was made to better test the ability of rock to become sealed in the presence of a reactive gouge. The high permeability and tendency to creep of novaculite, which were identified in the earlier experiments, were not conducive to monitor potentially modest permeability changes resulting from mineral reactions. The stronger, lower-permeability granite was deemed to be a better candidate for such investigations.

Because the sample was slow to saturate at room temperature, the confining pressure was temporarily lowered to 110 MPa to force water through the sample more quickly. Confining pressure was restored to 150 MPa prior to the measurement of room-temperature permeability. Upon heating, the gouge layer began to compact, as in previous experiments (Table 2, Fig. 7). It was considered that, as a result of the compaction, water would escape

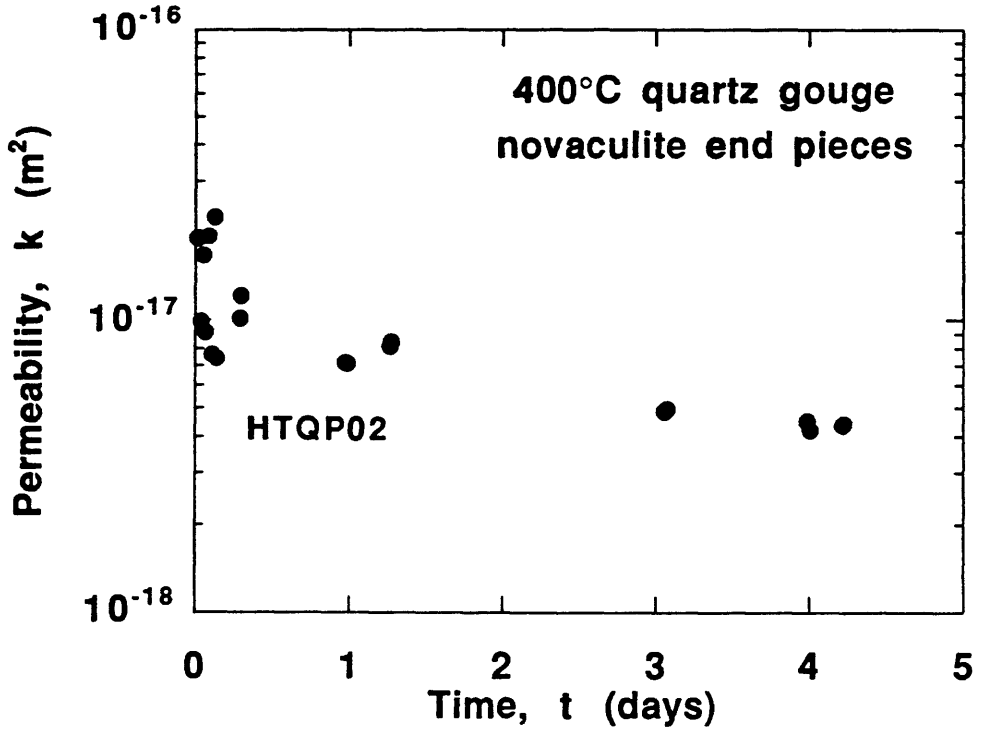

Figure 5. Permeability at 400°C of sandwich sample HTQP02, consisting of a layer of fine-grained quartz gouge between 0.795 cm-long cylinders of novaculite.

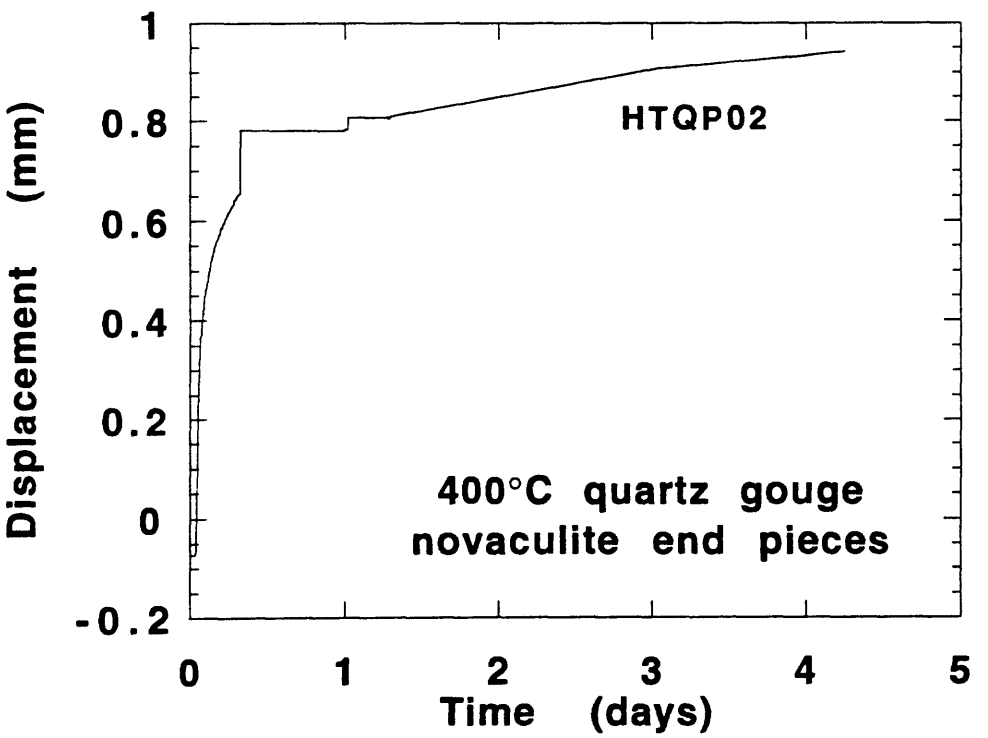

Figure 6. Change in sample length, measured as ram displacement, following heating of sample HTQP02. A positive ram displacement corresponds to sample shortening. (It is the relative change in displacement that is important in this and subsequent displacement plots, not the absolute values.)

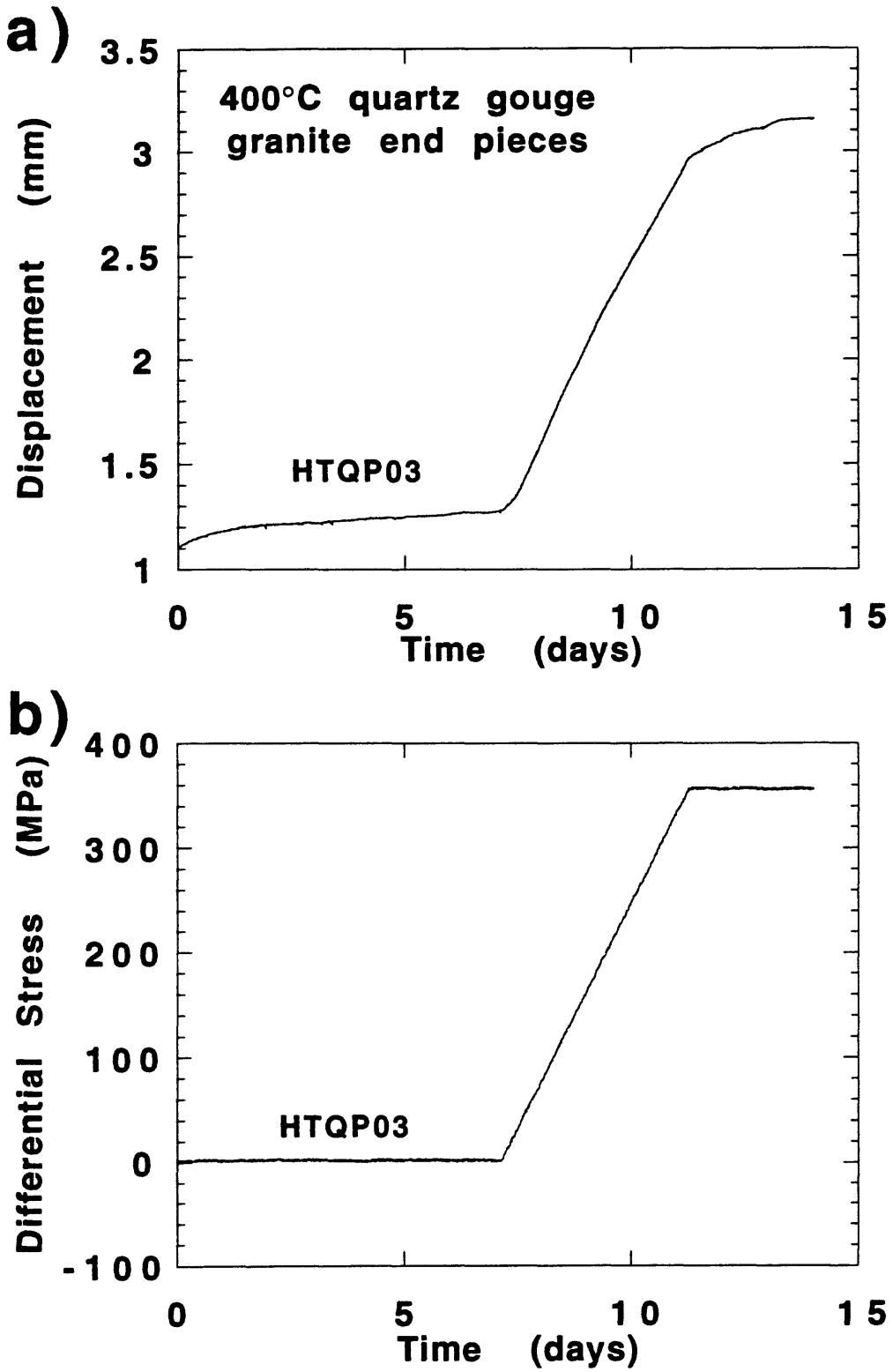

Figure 7. a). Change in sample length during experiment HTQP03. b). Differential stress applied during the same experiment. The majority of the axial shortening occurred during the time of increasing differential stress.

from the gouge into the rock, leading to the possibility of a counterflow of water during a permeability measurement. In order to identify and remove any effects of compaction upon flow rate, permeability was measured at pore-pressure drops of 0 MPa, ±1.0 MPa, and ±2.0 MPa.

The permeability of granite/gouge sample HTQP03 at 400°C (Fig. 8) was more than 2 orders of magnitude below that of the novaculite/gouge sample HTQP02 (Fig. 5). Experiment HTQP03 was run for one week at 400°C and 0 differential stress. The measurements of permeability at different pore-pressure drops and flow directions on any given day covered a wide range of values (Fig. 8a), and the average daily permeability also varied erratically with time (Fig. 8b). After 7 days, a differential stress was applied, at a slow rate of increase, to a set point of 355 MPa (Fig. 7b). The sample compacted considerably during the application of the stress (Fig. 7a), and the initial measurement of k at 76.5 MPa differential stress was somewhat lower than the unstressed measurements. However, the permeability measurements taken at 355 MPa differential stress were larger than for the unstressed state (Fig. 8). Thin-section examinations reveal the cause of this increase: HTQP03 bulges outwards at the site of the gouge layer, whereas HTQP02, which was not stressed, has collapsed inwards (Fig. 9a). Sample HTQP03 has a concentration of microcracks at the gouge-granite interfaces (Fig. 9b) that probably formed as the gouge flowed outwards under the differential stress. The crack density, measured as the number of crack intersections along lines perpendicular to the cylinder axis, increases 3- to 4-fold from each end of the sample to the rock-gouge interface. The formation of the tensile cracks led to the measured permeability increase.

Granite Experiments (HTQP04 - HTQP21).

Following the initial experiments on novaculite and quartz gouge, we switched to a wholly granitic system, despite its more complex mineralogy. The group of investigations reported here considers the effects of temperature and sample configuration on permeability, without an applied differential stress. The high-temperature results for the granite samples are presented in Moore and others (1994), and the effect of rock-water interactions on

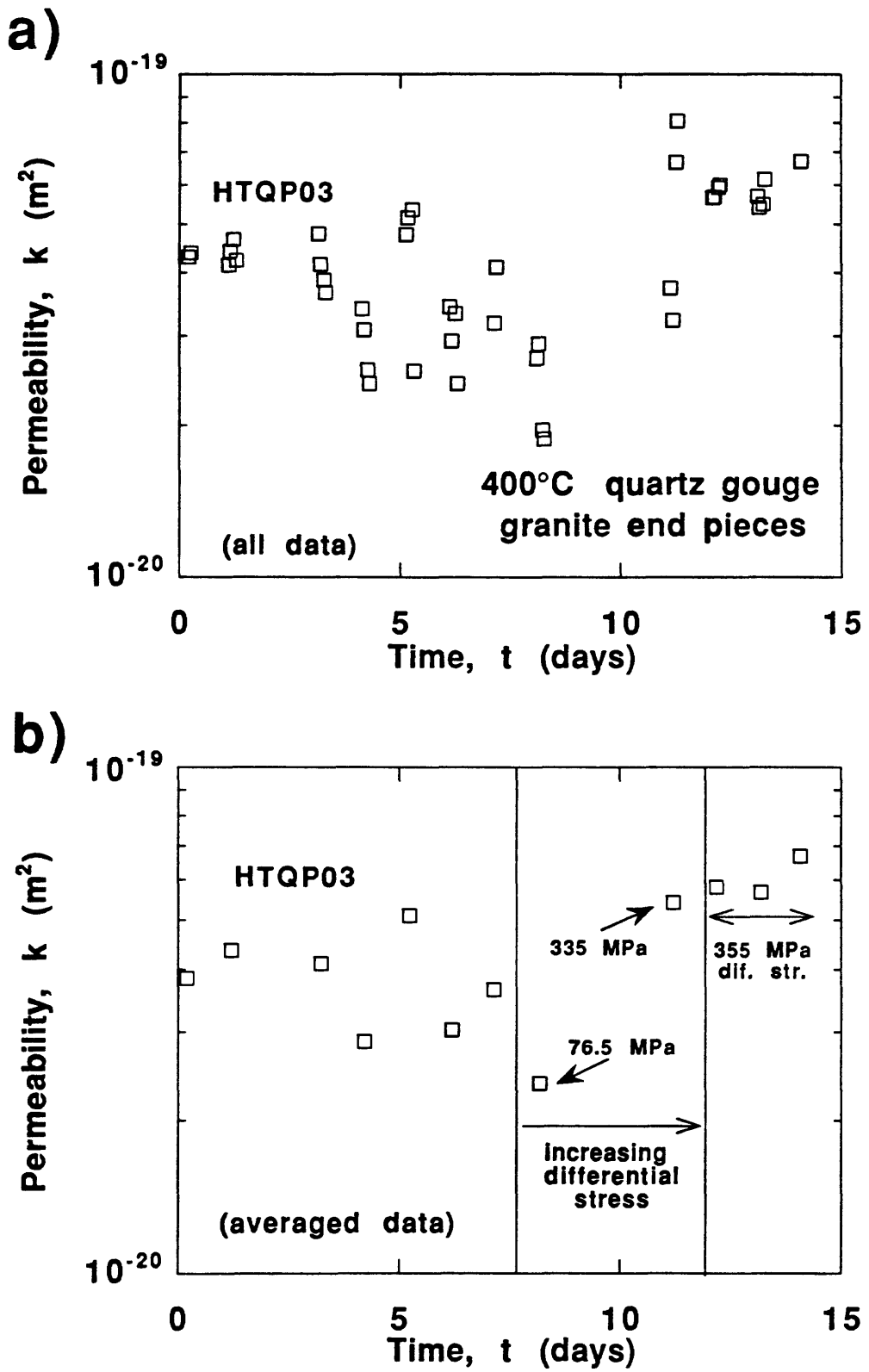

Figure 8. Permeability of sandwich sample HTQP03 -- quartz gouge and granite end pieces -- over time at 400°C. Permeability was measured each day at ±1.0 MPa and ±2.0 MPa differential pore pressure. a). Plot of all data collected. b). Plot of the average daily permeability. After 7 days, a differential stress was applied at a rate of increase of 0.005625 MPa/s, to a maximum load of 355 MPa.

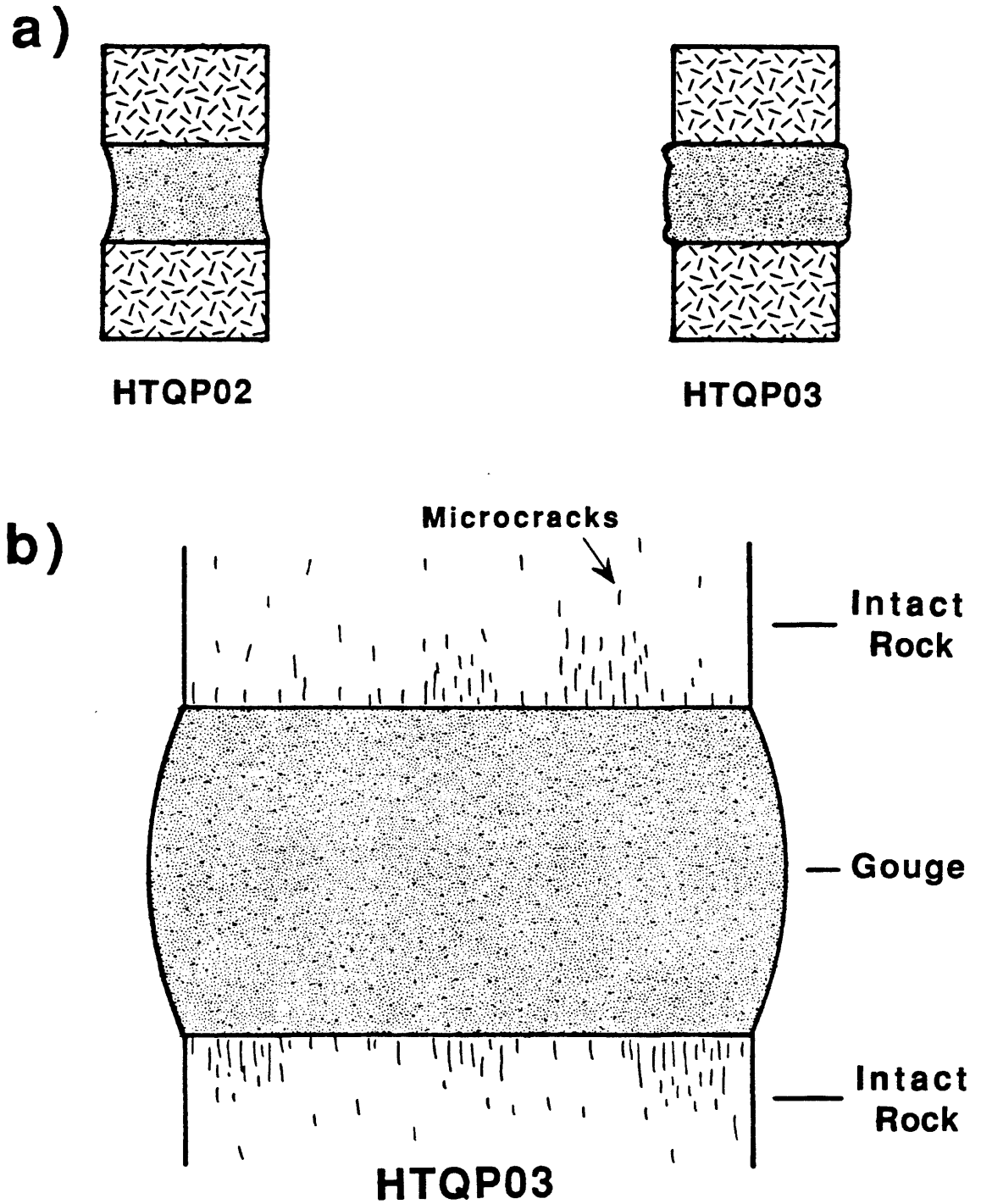

Figure 9. a). Contrasting changes in shape of gouge-bearing samples HTQP02 and HTQP03. Sample HTQP02 was not subjected to an axial load, and the gouge caved in under the effective pressure. HTQP03 was subjected to a differential stress, at which time the gouge apparently began to flow outwards. b). Sketch of part of sample HTQP03, showing microcracks formed in the granite adjacent to the gouge layer, as a result of outward flow of the gouge under the applied axial load. The crack densities of the granite cylinders decrease with increasing distance from the gouge-rock boundary.

permeability will be discussed in a subsequent paper (Moore and others, in preparation). The following sections include aspects of the experiments not dealt with in detail in those papers, such as room-temperature permeability and the possible effects of the copper jackets on the results.

Room-temperature k. The reported room-temperature permeability of intact Westerly granite at 50 MPa effective pressure is in the range 2×10^{-21} m^2 to 1×10^{-19} m^2 (Brace and others, 1968; Morrow and others, 1986). However, the measured room-temperature permeability values of many of the intact granite samples in this study were considerably higher (Fig. 10). The first measurement of experiment HTQP12 was especially high (Table 2), and k was subsequently lowered by repeatedly removing the pore pressure and raising confining pressure. This response demonstrated that the non-annealed copper jackets used in experiments HTQP01 to HTQP12 (Table 3) were too stiff to form a proper seal around the sample, at least at room temperature. The pressure cycling of experiment HTQP12 improved the seal by pressing the jacket more closely to the granite sample. To help alleviate this problem, the copper jackets used in subsequent experiments were annealed (Table 3). The samples housed in annealed jackets yielded more reasonable values of room-temperature k, although most of these values are at the upper limit of reported room-temperature permeabilities (Fig. 10). In addition, problems occurred with annealed jackets that were subsequently plated with gold. Apparently, the plating process caused the copper to become work hardened, thereby increasing jacket stiffness.

To further improve the jacket seal, the experimental start-up procedures were modified for the final experiment, HTQP21, as follows: 1) apply confining pressure (dry); 2) anneal the sample assembly at 650°C for 30 minutes; 3) return the sample to room temperature and apply fluid pressure; 4) measure permeability at room temperature; and 5) heat the sample to the run temperature. This procedure yielded the second-lowest measurement of room-temperature k and also eliminated some problems encountered in duplicating the high-

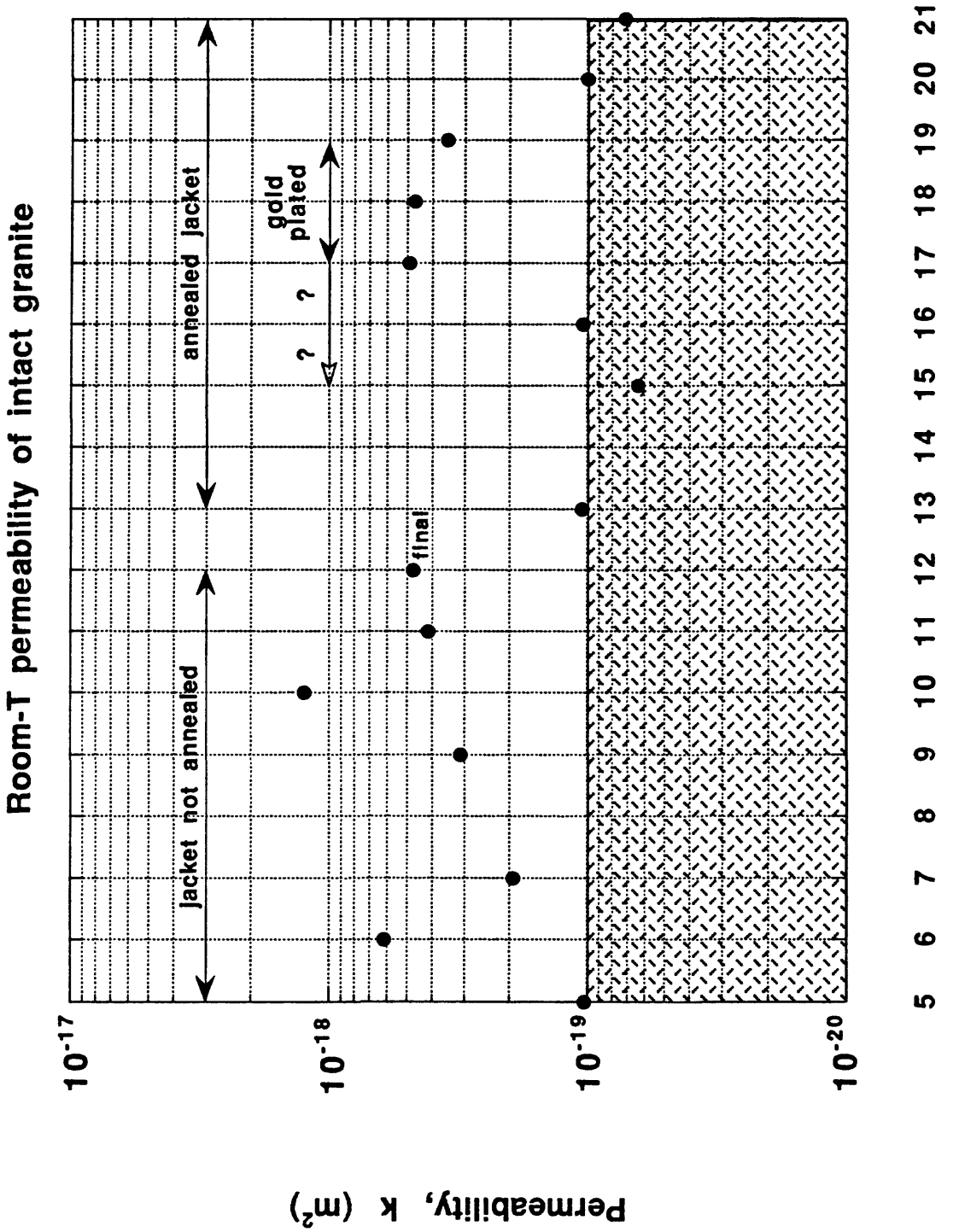

Figure 10. Measured room-temperature permeability of intact granite samples. The plotted numbers are mostly the average of all room-temperature measurements (Table 2), but for HTQP12 the final number is plotted. Experiments HTQP05-HTQP12 used non-annealed copper jackets (Table 3), which resulted in variable and often high values of k. Subsequent samples housed in annealed copper jackets (Table 3) yielded permeabilities more consistent with values reported by Brace and others (1968) and Morrow and others (1986) (indicated by the shading), although samples in jackets that were both annealed and gold-plated (Table 3) had high room-temperature k values.

Table 3. Characteristics of Copper Jackets

Experiment #	Cu-Jacket Type
HTQP01	not annealed
HTQP02	not annealed
HTQP03	not annealed
HTQP04	not annealed
HTQP05	not annealed
HTQP06	not annealed
HTQP07	not annealed
HTQP08	not annealed
HTQP09	not annealed
HTQP10	not annealed
HTQP11	not annealed
HTQP12	not annealed
HTQP13	annealed
HTQP14	annealed
HTQP15	annealed, w/wo qold plating*
HTQP16	annealed, w/wo gold plating*
HTQP17	annealed, gold-plated
HTQP18	annealed, gold-plated
HTQP19	annealed, gold-plated
HTQP20	annealed
HTQP21	annealed**

* The experimental log does not indicate whether or not these two samples were gold plated. However, the room-temperature values of k obtained for the two samples are more consistent with the use of non-plated, annealed copper jackets (Fig. 8; Table 2). In addition, copper deposits occur in cracks on the sides of both samples, but no traces of gold were found.

** The jacket was annealed a second time, with the sample inside and under confining pressure.

temperature data. As a result, this modification will be followed in future experiments. That the annealing did not cause obvious thermal cracking of the granite (see below) may be owing to the lack of an applied fluid pressure.

High-temperature k. Permeability was expected to increase upon initial heating as a result of thermal cracking (Heard and Page, 1982; Fredrich and Wong, 1986). For the samples in annealed copper jackets, the measured permeability did increase with heating (Table 2), and the amount of increase was roughly proportional to temperature. The first high-temperature k measurements of the other samples were generally lower than the room-temperature values, however, because improved jacket sealing upon heating outweighed the effects of thermal cracking. The initial measurements of k are relatively well correlated with temperature (Fig. 11a), irrespective of the jacket type used. The two experiments at 300°C provide a direct comparison of the annealed (HTQP13) and non-annealed (HTQP11) jackets (Fig. 12). After the first measurement, which is somewhat higher for the sample in the non-annealed jacket, the results are essentially identical. Similarly, the spread of the data after 10 days at temperatures above 300°C (Fig. 11b) is generally less pronounced than for the initial values. Together, these results indicate that the jacket does not affect the high-temperature permeability measurements (possible exceptions are HTQP19 and HTQP20, described below).

High-temperature permeability decreased over time in all of the granite experiments. The rate of decrease for most of the intact samples (Figs. 12-16) was rapid in the first day or two following heating but subsequently dropped to a uniform rate that in most cases continued until the end of the experiment. However, both of the intact-rock experiments at 500°C (Fig. 16) were characterized by a rapid decrease in k after 5 to 6 days. The final permeability measurement of HTQP06 was roughly 3 orders of magnitude below the initial heated value, and over the last 3 days of the experiment flow through the sample had in effect ceased. The other 500°C experiment, HTQP05, differed somewhat in that permeability partly recovered at a later time. Changes over time in the lengths of samples HTQP05 and HTQP06 are plotted in Figure

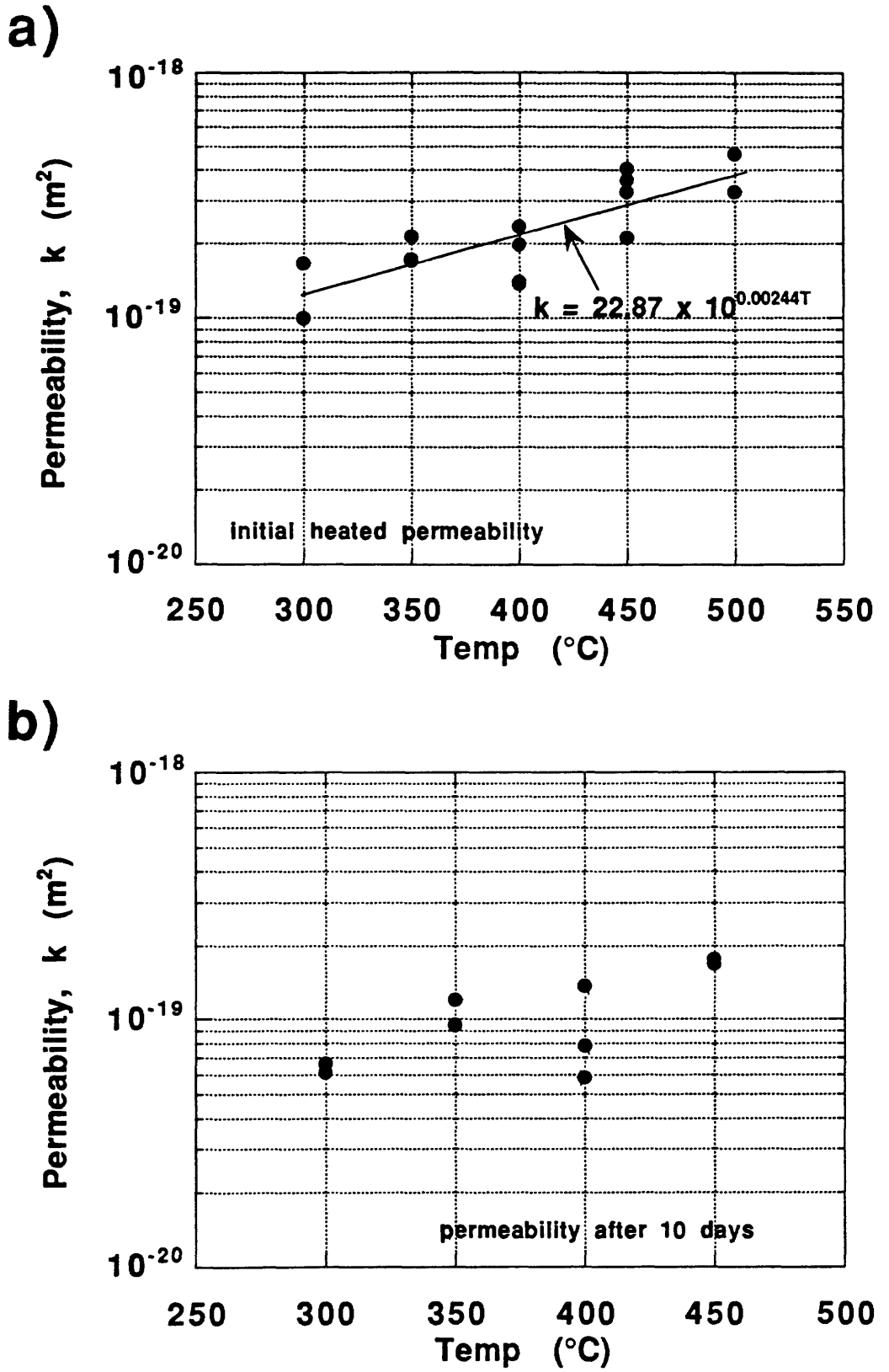

Figure 11. Permeability of intact granite plotted relative to temperature. a) Initial heated permeability values. b) Permeability after about 10 days, excluding the 500°C values. An exponential equation was fit to the data in a); the units of T and k correspond to the axes.

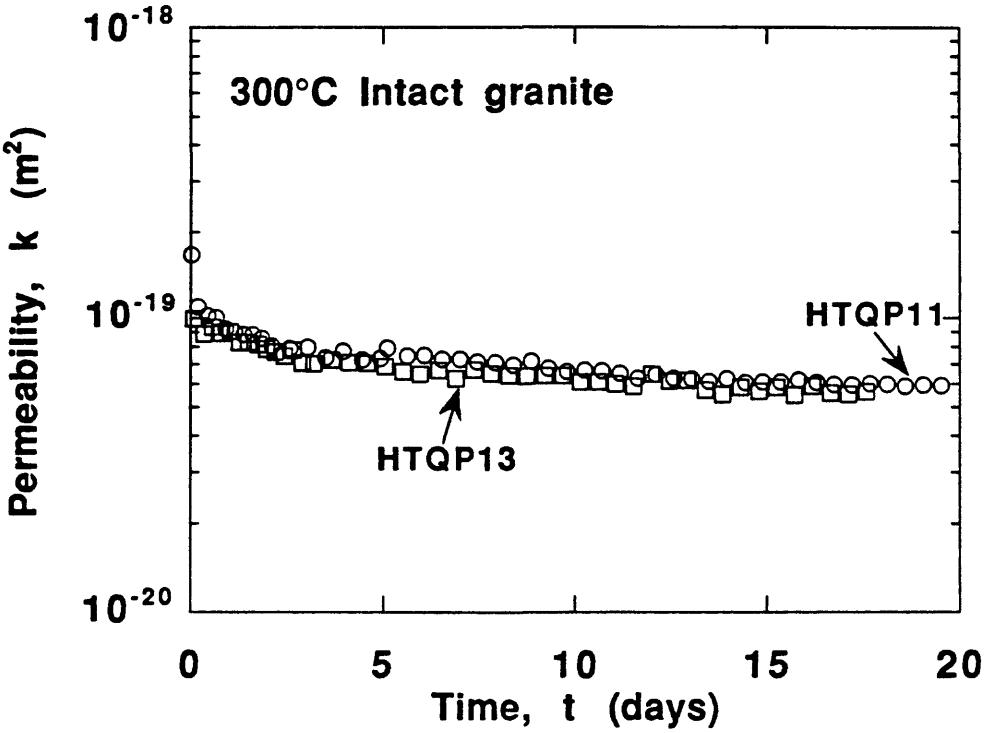

Figure 12. Permeability of 300°C intact granite samples. Experiment HTQP11 (circles) used non-annealed copper jackets and experiment HTQP13 (squares) used annealed copper jackets. Room-temperature permeability of the 2 samples differed, but the high-temperature plots are nearly coincident.

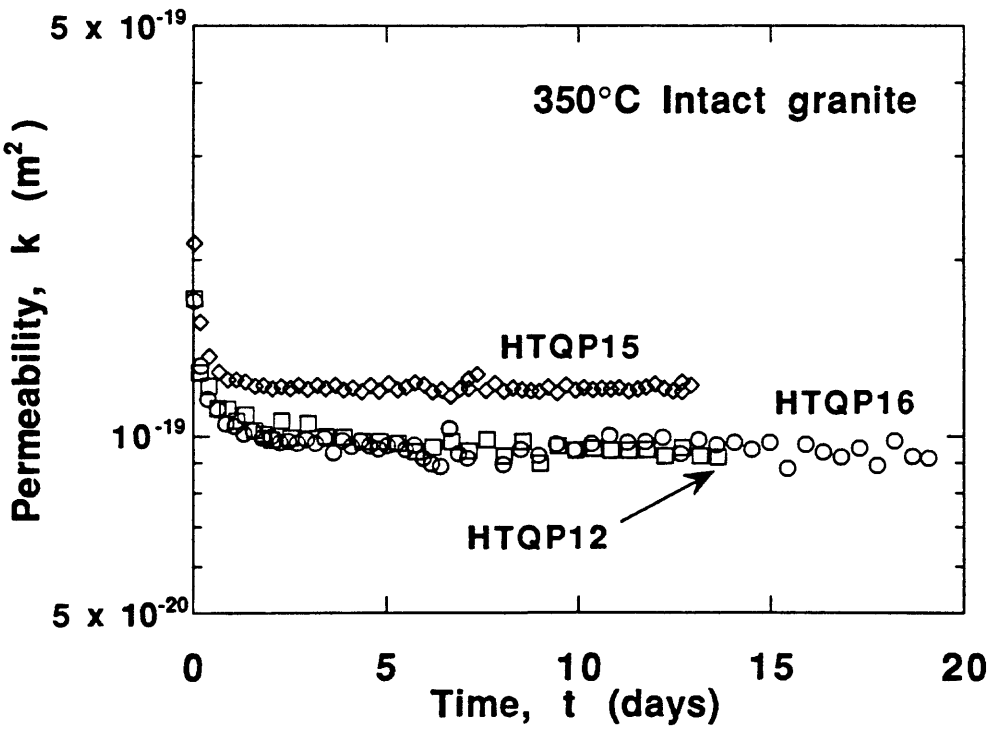

Figure 13. Changes in permeability of intact granite samples at 350°C. After the first 1-2 days, the rate of permeability decrease in all three experiments slowed considerably, to lower rates than observed at 300°C. (HtQP12 - squares; HTQP15 - diamonds; HTQP16 - circles).

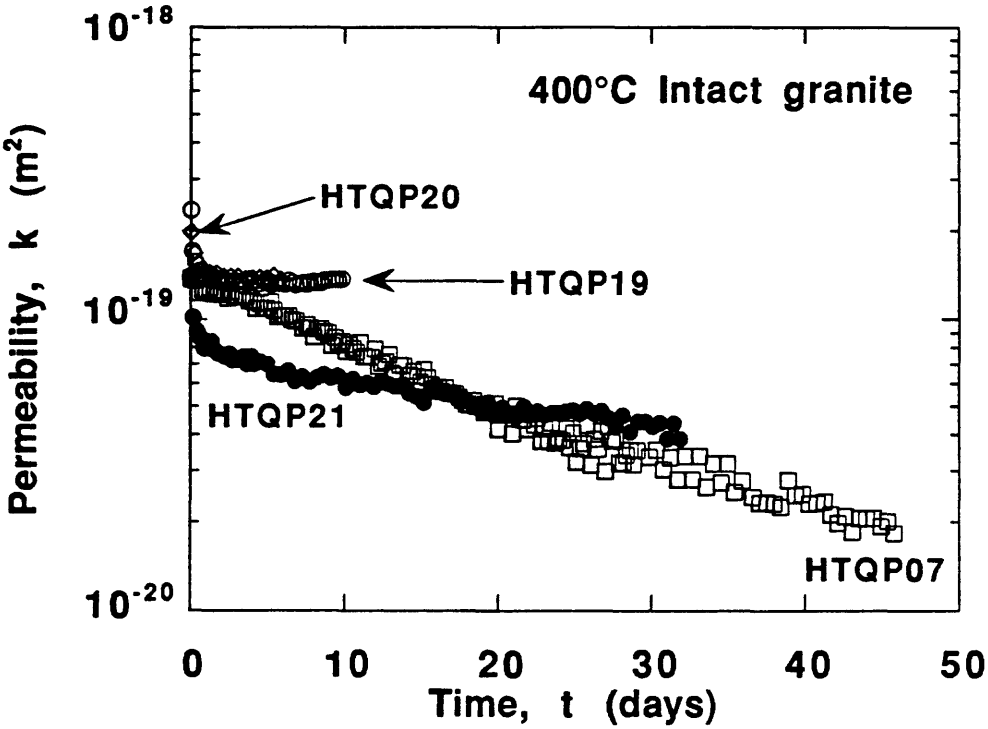

Figure 14. Permeability of 400°C intact granite samples. The flat trends of HTQP19 and HTQP20 may reflect problems with the seal between the copper jacket and the sample. (HTQP07 - squares; HTQP19 - open circles; HTQP20 - diamonds; HTQP21 - filled circles).

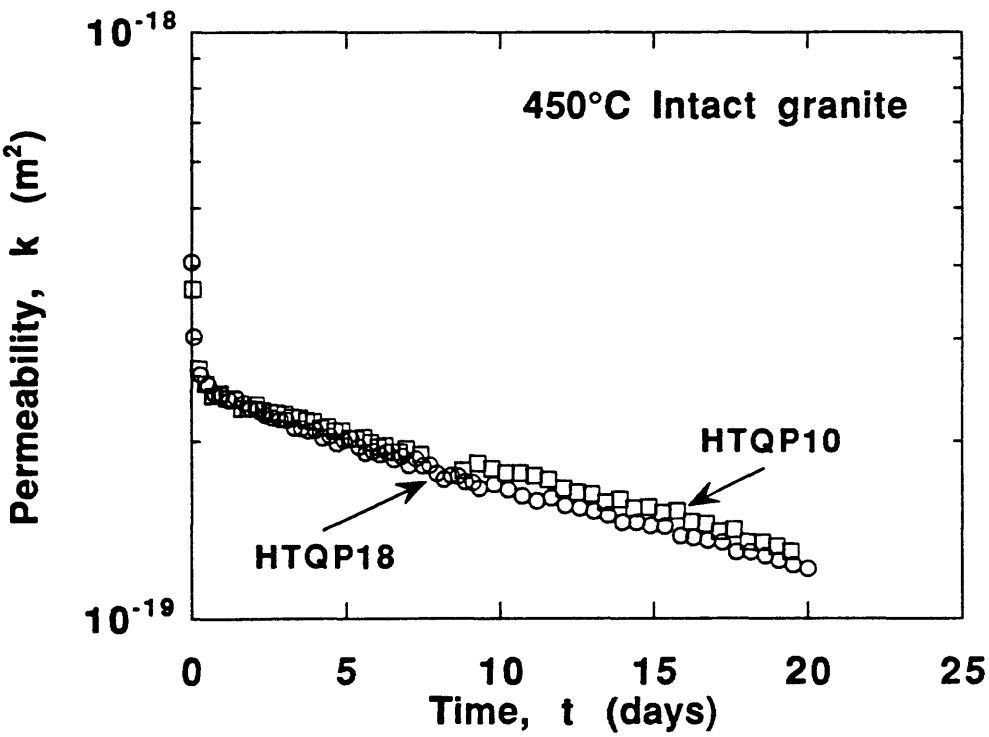

Figure 15. Permeability changes in intact granite at 450°C. The data from the 2 experiments are nearly coincident. (HTQP10 - squares; HTQP18 - circles).

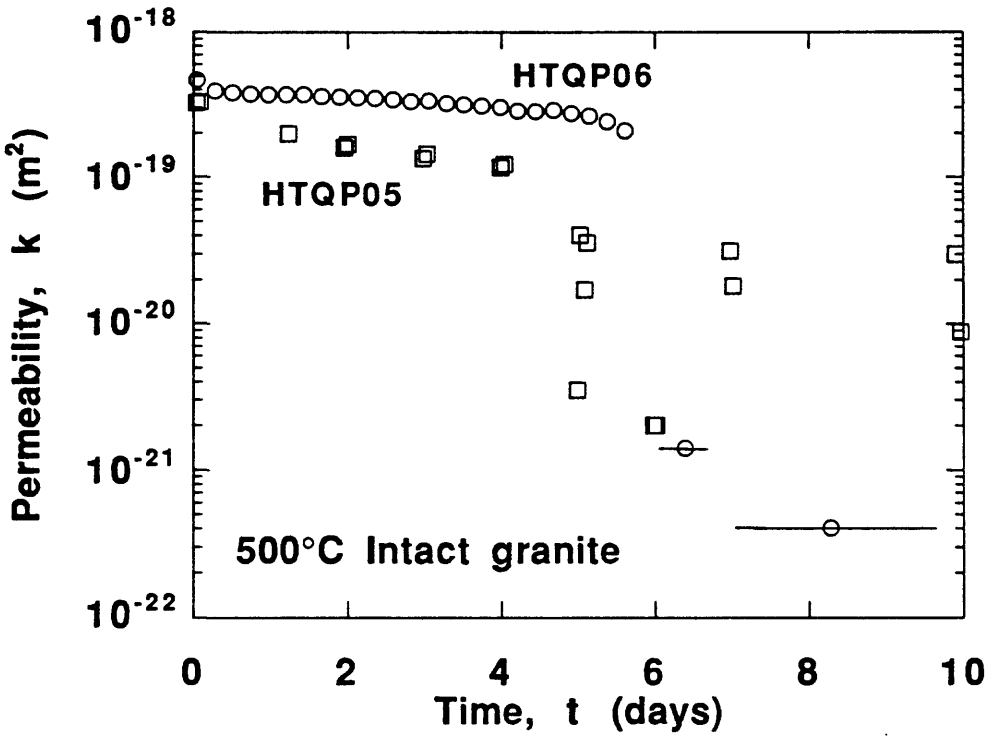

Figure 16. Permeability of intact granite at 500°C. After 5-6 days in both experiments, the rate of permeability reduction abruptly changed, decreasing by 2-3 orders of magnitude in less than one day. In HTQP06, flow essentially ceased over the last 3 days of the experiment. HTQP05 - squares; HTQP06 - circles).

17. The measured displacement during HTQP05 fluctuates irregularly over a small range, whereas that of HTQP06 is unchanging except in association with two transient, 40-45° drops in temperature (associated with adjustments to the experimental apparatus). In neither experiment does the onset of rapid permeability decrease correlate with a change in displacement.

Overall, the rate of uniform permeability reduction in the intact granite samples increased with increasing temperature in the examined range, but with some reversals. For example, the data from the two experiments at 300°C (Fig. 12) have steeper slopes than the nearly flat trends of the three experiments at 350°C (Fig. 13). The repeated experiments at 400°C (Fig. 14) yielded conflicting rates, with HTQP19 and HTQP20 unable to duplicate the permeability reductions of HTQP07. The results of HTQP19 and HTQP20 were considered to reflect jacket-sealing problems, perhaps a crease or fold in the copper. These problems led to the previously described modification of set-up procedures for experiment HTQP21. Although they followed initially different trends, the permeabilities of HTQP21 and HTQP07 were similar after about day 14. The rate of change over the first few days of experiment HTQP21 also is more consistent with other experiments than that of HTQP07.

Both the room-temperature and the first heated permeability measurements of 400°C sandwich sample HTQP08 were especially high (Table 2), because the sample was inadvertently subjected to a large, transient differential stress during set-up procedures. The subsequent high-temperature behavior of the two sandwich samples (Fig. 18) nevertheless is similar and differs from that of the intact-rock samples. Over the first several days, permeability decreased much more rapidly in the two gouge-bearing samples than in the 400°C (Fig. 14) and 500°C (Fig. 16) intact samples. The rate of permeability change in the sandwich samples nevertheless decreased continuously with time, and the final rates of permeability decrease of 400°C intact samples HTQP07 and HTQP21 and sandwich sample HTQP08 are similar. The rate of permeability decrease of 500°C sandwich sample HTQP04 had probably not stabilized when

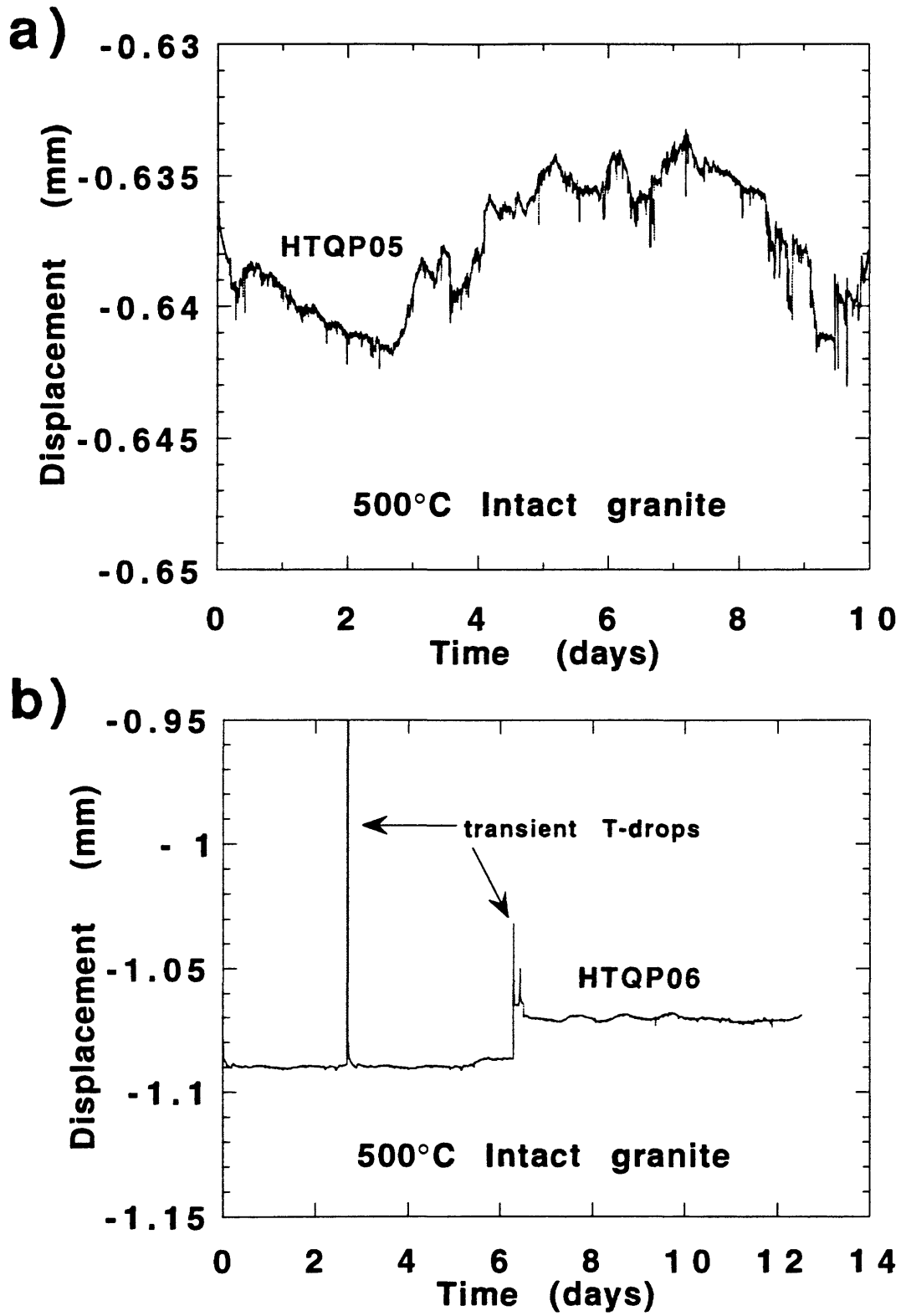

Figure 17. Changes in sample length, measured as ram displacement, following heating to 500°C during experiments a). HTQP05; and b). HTQP06. Minor, irregular fluctuations occurred during HTQP05. Sample HTQP06 had almost no change in displacement, except as a result of two short-term temperature drops. The second transient led to an offset of the axial displacement values.

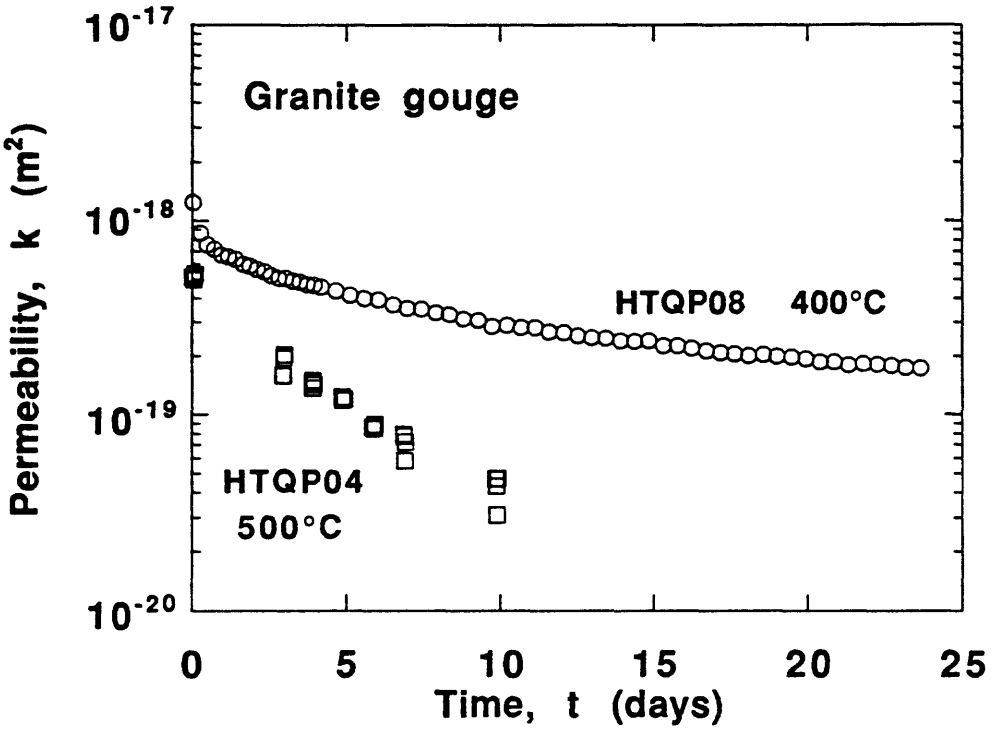

Figure 18. Changes in permeability of granite sandwich samples at 400° and 500°C. Calculation of k for experiment HTQP08 (circles) uses the final sample length of 2.1209 cm; cylinder lengths for HTQP04 (squares) are listed in Table 2. The rate of permeability decrease for each experiment is greater than that of the equivalent intact sample.

the experiment was terminated, and the final value of k is above the level at which the permeability of the 500°C intact samples began to decrease rapidly. The two gouge layers compacted throughout the two experiments, with the major decreases occurring during the first day (Fig. 19). Subsequent, steady-state creep occurred at a slightly higher rate at 500°C.

Flow through fractured sample HTQP14 was initially rapid, and for the first few days only a small pore-pressure gradient could be maintained across the sample at the maximum flow rate of the pump (Table 2), yielding fairly constant values of λ (Fig. 20). Subsequently, though, the differential pore pressure first increased to the 2.0 MPa setpoint, and then the flow rates measured over that pressure drop began to decrease rapidly. Within a week after the initiation of change, λ had decreased nearly 3 orders of magnitude, such that the rate of fluid flow was at the level of 400°C intact samples HTQP07 and HTQP21. In Table 2, the measurements at low flow rates are also calculated in terms of k; these values are consistent with permeabilities obtained at the same times during experiments HTQP07 and HTQP21.

At the end of each experiment, the samples were returned to room temperature over a roughly 30-minute span. Upon cooling, one or more room-temperature permeability measurements were made on 5 samples (HTQP05, HTQP06, HTQP10, HTQP11, and HTQP13; Table 2). These final, room-temperature values were nearly as high as the initial heated permeabilities of each sample, probably because of cracking of the fluid-charged samples accompanying the rapid temperature change.

Causes of Permeability Change

The fractured sample provides the clearest evidence of the processes leading to the permeability reductions, because changes to the freshly broken crystal surfaces are readily detected. During experiment HTQP14, the fracture became sealed to the extent that it had to be forcibly wedged apart. Scanning electron microscope (SEM) examination of the separated

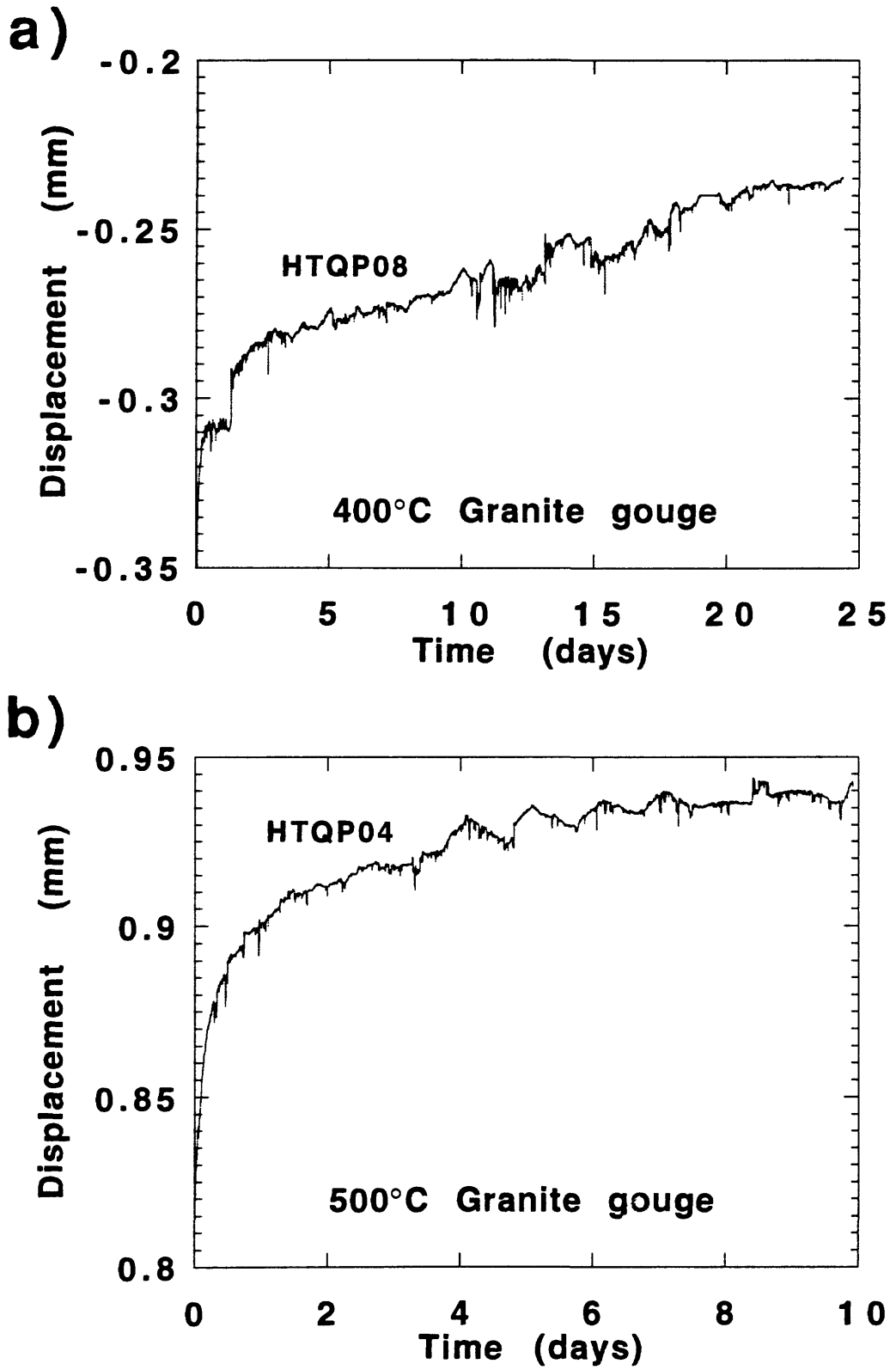

Figure 19. Changes in sample length following heating during experiments a). HTQP08 (400°C); and b). HTQP04 (500°C). Both samples showed a rapid initial shortening and subsequently slower change, caused by compaction of the gouge. The amount of compaction at the two temperatures is about the same.

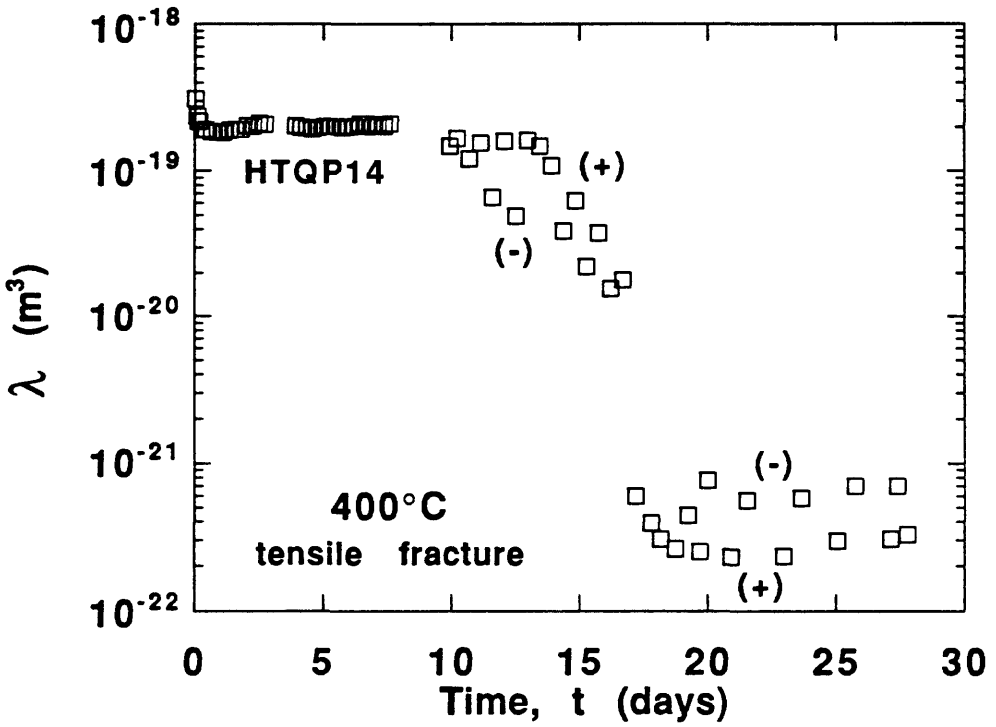

Figure 20. Changes in λ with time for flow at 400°C through a granite cylinder containing an axial tensile fracture. By the end of the experiment, flow rate was reduced by 3 orders of magnitude, to the level of intact-rock sample HTQP07 for the same time.

fracture surfaces reveals widespread evidence of mineral dissolution and precipitation. The feldspar and especially the quartz surfaces all along the fracture have been rounded by dissolution, but at least some quartz (Fig. 21a) and many K-feldspar (Fig. 21b) crystals also were deposited at other positions along the fracture. These combined features suggest the operation of solution-transfer processes, which redistribute the minerals in the rock such that asperities are chemically removed while pores and fractures are filled (Knipe, 1992; Cox and others, 1986). The plagioclase ($Ab_{80}An_{20}$) that dissolved participated in metamorphic reactions. The sodic component of the plagioclase precipitated as albite, whereas the calcic component reacted with biotite to form bladed crystals (Fig. 21c) containing Si-Ca-Fe-Al-Mg, that may be an actinolitic amphibole. The potassium released from the biotite may have contributed to the numerous K-feldspar deposits on the fracture surface. Sprays of a fibrous Ca-Si mineral are also common (Fig. 21d).

It is more difficult to verify that a given crack texture or crack-filling mineral in the intact cylinders formed during the permeability experiments. One possible example consists of rounded, widened cracks in quartz that resemble the dissolution features of quartz in the fractured sample. This texture was not found in a thin section of the starting material. Lumpy Ca-Si minerals, which fill cracks in several samples, may correspond to the acicular sprays that formed on the fracture surface. Such Ca-Si deposits also have not been found in the starting material. Small amounts of the possible actinolitic amplibole were identified in intact samples heated to at least 400°C. Minerals such as chlorite, epidote, and quartz (Fig. 22a) fill some cracks, but they can also be found in the starting material. These latter deposits, therefore, could have existed prior to the experiments.

Albite ($Ab_{89}An_9Or_2$) rims some of the plagioclase crystals in the Westerly starting material (Moore and others, 1987); even so, some albite crystallization can be linked to the permeability experiments at all temperatures tested. High-temperature water housed in the mesh of the screens adjacent to the granite cylinders (Fig. 2) reacted with exposed feldspars.

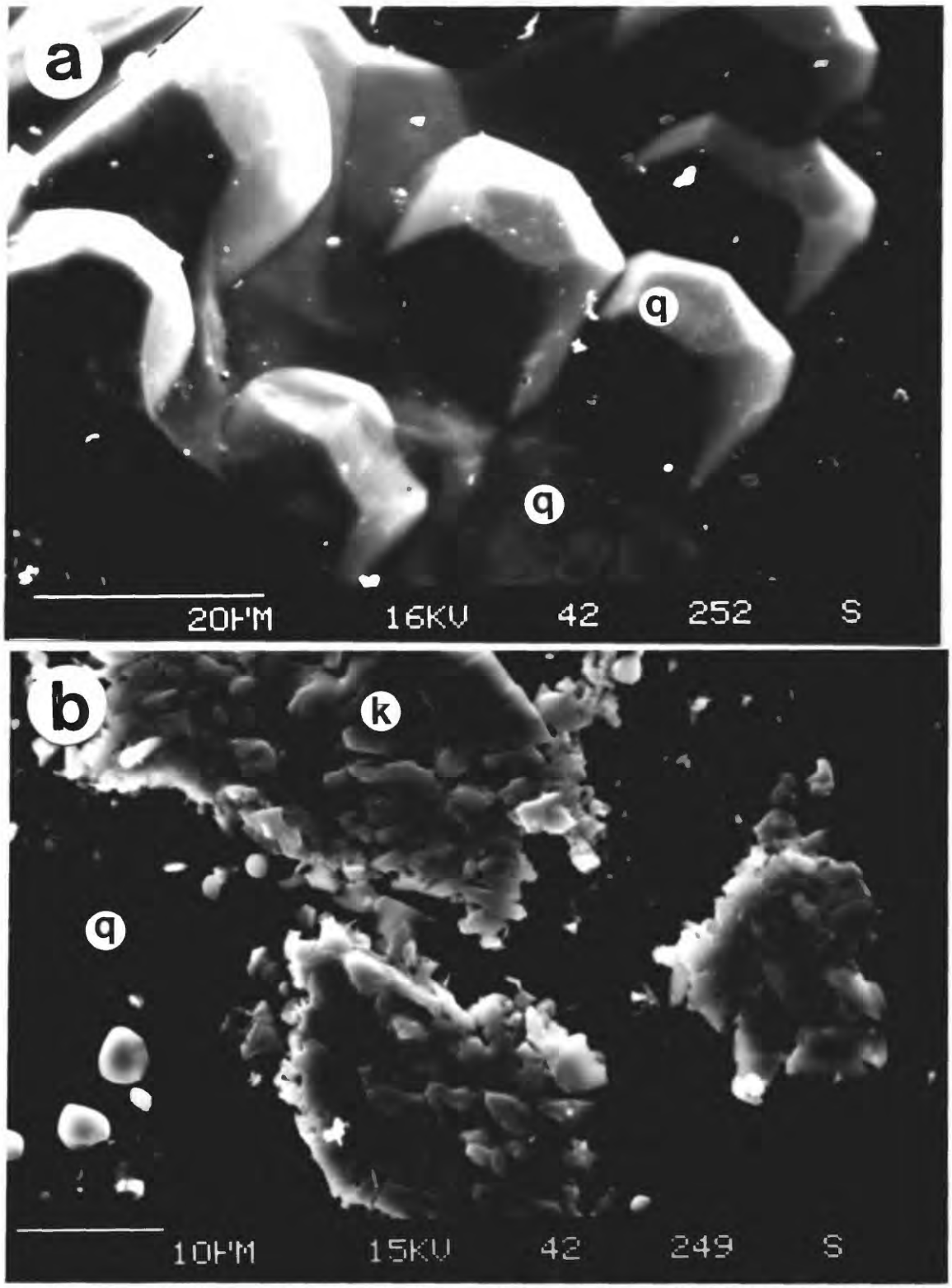

Figure 21. Minerals deposited on the fracture surfaces of sample HTQP14. a). Euhedral quartz (Q) crystals projecting from a quartz base. b). Clots of K-feldspar (K) crystals deposited on quartz. Crystals near the edges of the masses have euhedral outlines. Albite and K-feldspar deposits on the fracture surface typically have a similar appearance, and element spectra are required to distinguish between the two minerals.

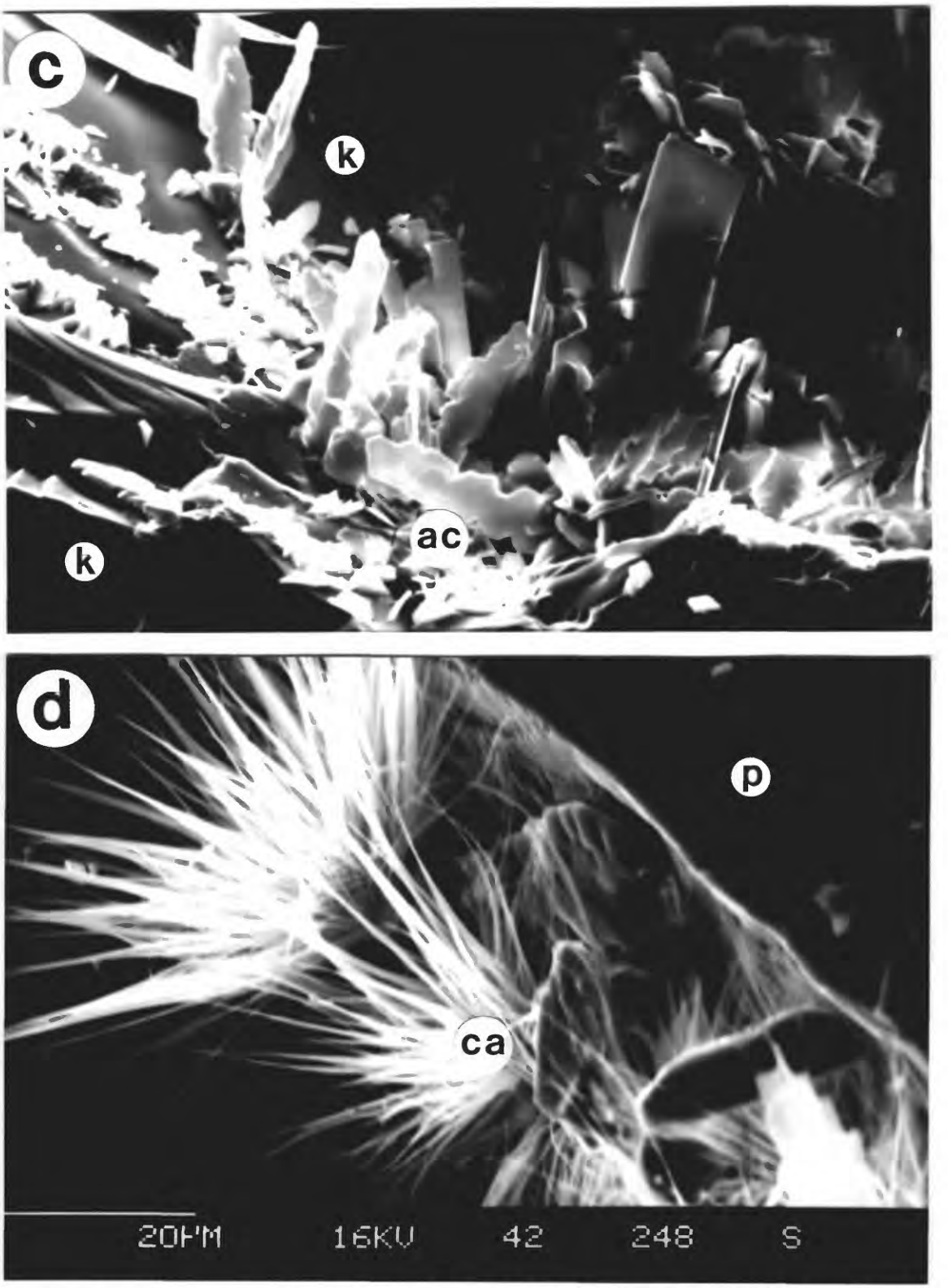

Figure 21, continued. c). Bladelike, Si-Ca-Fe-Al-Mg-bearing crystals (Ac), that may be actinolitic amphibole, grow out from a K-feldspar crystal into a small cavity. d). Fragile-looking sprays of an unidentified Ca-Si-bearing mineral (Ca), growing on plagioclase.

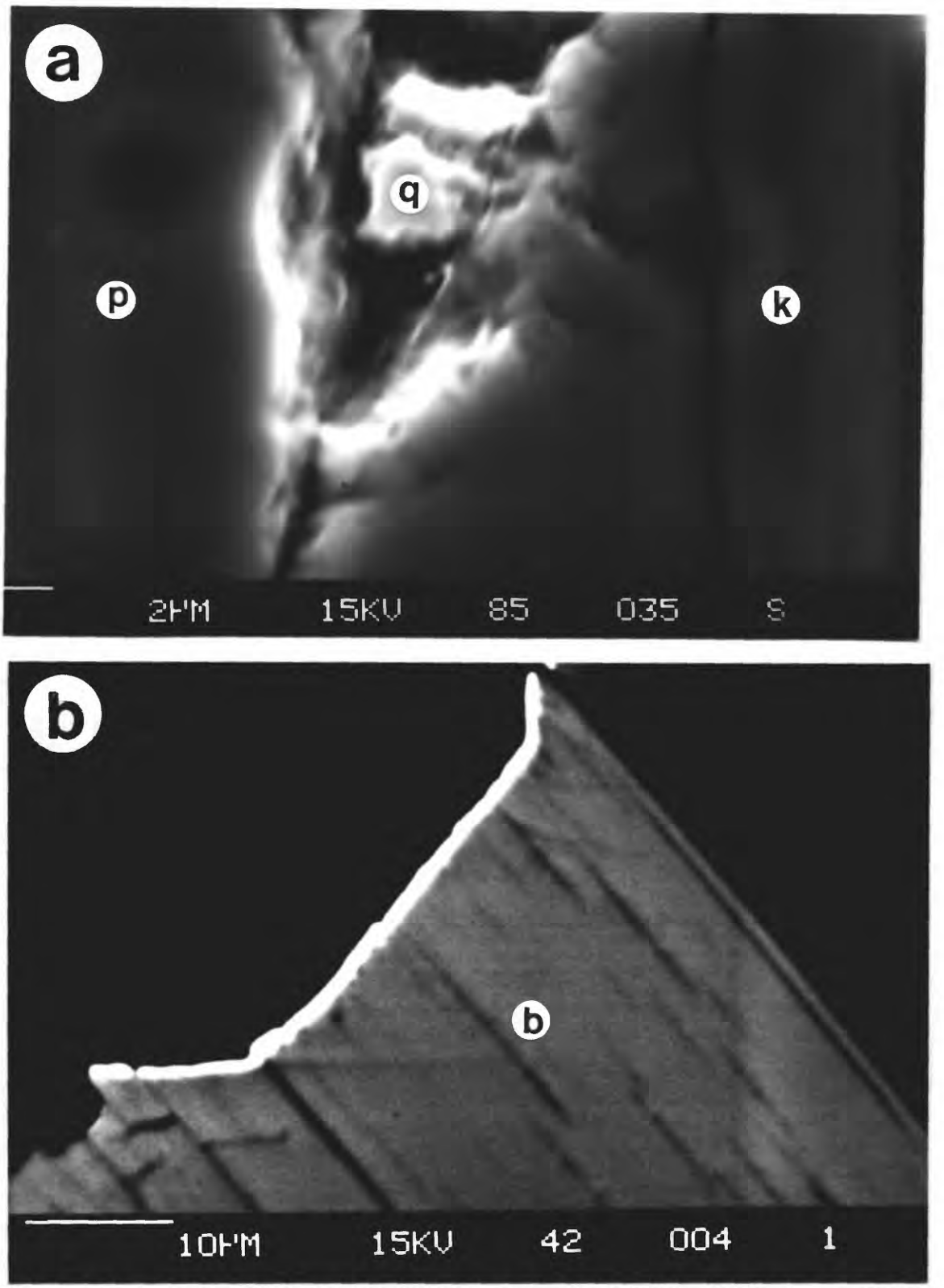

Figure 22. Mineral deposits of intact samples. a). Quartz (Q) deposit filling a crack between plagioclase (P) and K-feldspar (K) crystals. (Sample HTQP10, 450°C). b). Coating of Ca-Ce-La silicate (bright mineral) on a biotite (B) crystal at the bottom edge of sample HTQP16 (350°C). The coating covers the ends of cleavage cracks in the biotite.

Both plagioclase and K-feldspar crystals were albitized ($Ab_{96}An_1Or_3$), and some crystals have a fringe of new albite growth extending out into the mesh. Westerly granite also contains an accessory mineral, probably allanite, that is rich in the rare-earth elements cerium (Ce) and lanthanum (La). These crystals were attacked by hydrothermal fluids at some time in the history of the granite, and Ce-La-bearing calcium silicates were deposited in cracks around the altered crystals. At least some of these crystals were also affected by the hydrothermal fluids of the permeability experiments. An allanite crystal near one end of sample HTQP16 has been partly dissolved, and a thin layer of Ca-Ce-La silicate now forms a coating on the cylinder surface along the screen (Fig. 22b). This coating extends across some crack terminations.

Enhanced dissolution of some of the gouge materials may explain the changing rate of permeability decrease for the gouge-bearing samples (Fig. 15). Grinding minerals such as quartz to a fine powder creates surface layers of disordered or amorphous material with higher solubilities than the undamaged crystals (Morey and others, 1962; Beckwith and Reeve, 1969). Dissolution of these materials will temporarily raise solution concentrations above equilibrium values. In addition, as reviewed by Iler (1979), the equilibrium solubility of convex grains of quartz increases markedly with decreasing radius below 5 nm. The smallest grains will therefore dissolve preferentially, and the excess silica in solution will be redeposited as overgrowths that may be identifiable under cathodoluminescence. Such studies are planned for the gouge-bearing samples, to aid in testing this hypothesis. The disordered and ultra-fine materials may have been removed from the samples in the first several days of the gouge experiments, leading to the higher initial rates of permeability decrease. Thereafter, the rates of change declined towards the levels for the intact rocks.

During the SEM examinations, small, lumpy masses of copper minerals were found lining cracks along the sides of the cylinders, near the copper jackets. The deposits are principally a copper- and sulfur-bearing mineral, with minor amounts of native copper. Sources of sulfur in Westerly granite include accessory sulfide minerals such as pyrite, along

with sulfate ion in the existing pore fluids in the rock (Moore and others, 1983). With one exception, all of the copper-bearing deposits are confined to the outer 50-1000 μm of the cylinder, and the distance traveled by the copper during a given experiment is directly correlated with temperature and run duration. The greatest migration of about 1 mm was observed in the two 500°C samples (HTQP05 and HTQP06) and in the sample that was heated to 400°C for 6 weeks (HTQP07). At the other extreme, copper deposits were found at most 50 to 100 μm from the sides of the cylinders heated to 300° or 350°C. The exception mentioned above is the 500°C gouge-bearing sample (HTQP04), in which copper moved for some distance along the gouge-granite boundaries. In all cases, the copper-sulfur-bearing mineral migrated farther into the cylinder than did the native copper.

The scattered occurrence and general restriction of the copper deposits to the very outer edges of the cylinders suggest that these deposits should not have a significant effect on permeability. Nevertheless, because the copper is mobile in experiments using deionized water as the pore fluid, experiments planned to test saline brines or acidic groundwaters should not be attempted with copper exposed to the pore fluids. An attempt was made to plate some of the copper jackets with gold (Table 3), because gold should not react with any of the proposed pore fluids. Unfortunately, as described previously, the first attempt at plating caused the annealed copper jackets to stiffen. More seriously, the layer of gold did not adhere to the copper during the high-temperature tests. A more durable plating technique that also does not adversely affect the malleability of the copper needs to be found before experiments using potentially corrosive fluids can be attempted.

Comparison to Other Studies

The rapidly changing early rates of permeability decrease of the intact granite samples are similar to but less pronounced than those of granite samples that were tested in a large

temperature or pressure gradient (Summers and others, 1978; Morrow and others, 1981; Moore and others, 1983). The rapid initial decreases in all of these experiments may reflect a combination of thermal and fluid equilibration processes. Fractured sample HTQP14 differed from the 2 fractured samples examined by Morrow and others (1981) in that flow rates through HTQP14 remained uniformly high for several days. Once the permeability of HTQP14 began to decrease, the measured change was substantially greater than for the samples tested at maximum temperatures of 200° and 280°C by Morrow and others (1981).

The changes in permeability over time observed in this and previous studies have all been attributed to mineral dissolution and/or deposition. The experiments of different types nevertheless have some distinguishing features with respect to these processes. In the samples subjected to a large temperature or pressure gradient, minerals apparently dissolved on the high temperature/pressure side and were redeposited on the low temperature/pressure side. In this study, solution-transfer processes and metamorphic reactions redistributed minerals along cracks under nearly uniform pressure-temperature conditions. No evidence has yet been found that either the modest temperature gradients or the pore-pressure drops across the samples led to any preferred mineral reactions. Some reactions were concentrated at the ends of our cylinders, however, because of interaction with the fluid reservoirs in the screens.

Morrow and others (1981) noted that, on a fracture surface, low-temperature mineral deposits tended to form on a like substrate -- for example, silica deposits were found on quartz crystals and Ca-silicates grew on plagioclase. Fractured sample HTQP14 did not show such marked selectivity, although certain associations were common, for example the growth of actinolitic amphibole on the biotite that it was replacing. In contrast, K-feldspar deposits were found on quartz, plagioclase, and K-feldspar crystals, euhedral quartz crystals grew on plagioclase as well as quartz, and Ca-Si deposits formed on most of the minerals in Westerly granite.

The modest long-term increase in the permeability of quartz monzonite at elevated temperatures, found by Potter (1978), is a function of his one-way flow system. Distilled water moved continuously in one direction across the samples and was not recycled. This water was out of equilibrium with the heated samples, and it dissolved minerals such as quartz along its path. The material in solution then exited the sample with the water. Continued flow eventually increased the widths of some cracks. Our two-way, closed pore-fluid system minimized the effects of such leaching. Finally, the lack of significant permeability decreases of the novaculite samples is comparable to the permeability studies on tuffs (Morrow and others, 1984; Moore and others, 1986). Both the tuffs and the novaculite have high initial porosities and permeabilities that were not significantly affected by mineral reactions in the time span of the experiments.

Implications for Fault Zones

To quantify the rates of permeability change, an exponential equation of the form:

$$k = c\,(10^{-rt}) \qquad (5)$$

was fit by least-square methods to the uniform part of each intact granite experiment. c and r are constants, with units of $10^{-21}m^2$ and $days^{-1}$, respectively; k is in units of $10^{-21}m^2$ and t is in units of days. For consistency, the data from the first 2.0 days of each experiment were excluded from the calculations. The rapidly decreasing permeability values at the ends of the two 500°C intact granite experiments were also omitted. Calculated values of the exponent r are listed in Table 4 and plotted relative to the temperature of each experiment in Figure 23. The figure illustrates the rate reversals for the intact samples that were described previously.

Table 4. Permeability Reduction Rates of Intact Granite Samples

Temperature (°C)	Experiment Number	r in $k = c(10^{-rt})$	days to reduce k by x10
300	HTQP11	0.00810	123
300	HTQP13	0.00830	120
350	HTQP12	0.00341	293
350	HTQP15	0.00012	8445
350	HTQP16	0.00079	1258
400	HTQP07	0.01908	52
400	HTQP21	0.00842	119
450	HTQP10	0.01349	74
450	HTQP18	0.01450	69
500*	HTQP05	0.06525	15
500*	HTQP06	0.04125	24

* Equations for 500°C experiments were fit to k data taken from 2 to 4 days (HTQP05) and 2 to 5 days (HTQP06). The other equations were fit to all k data taken after the first 2 days of the experiments.

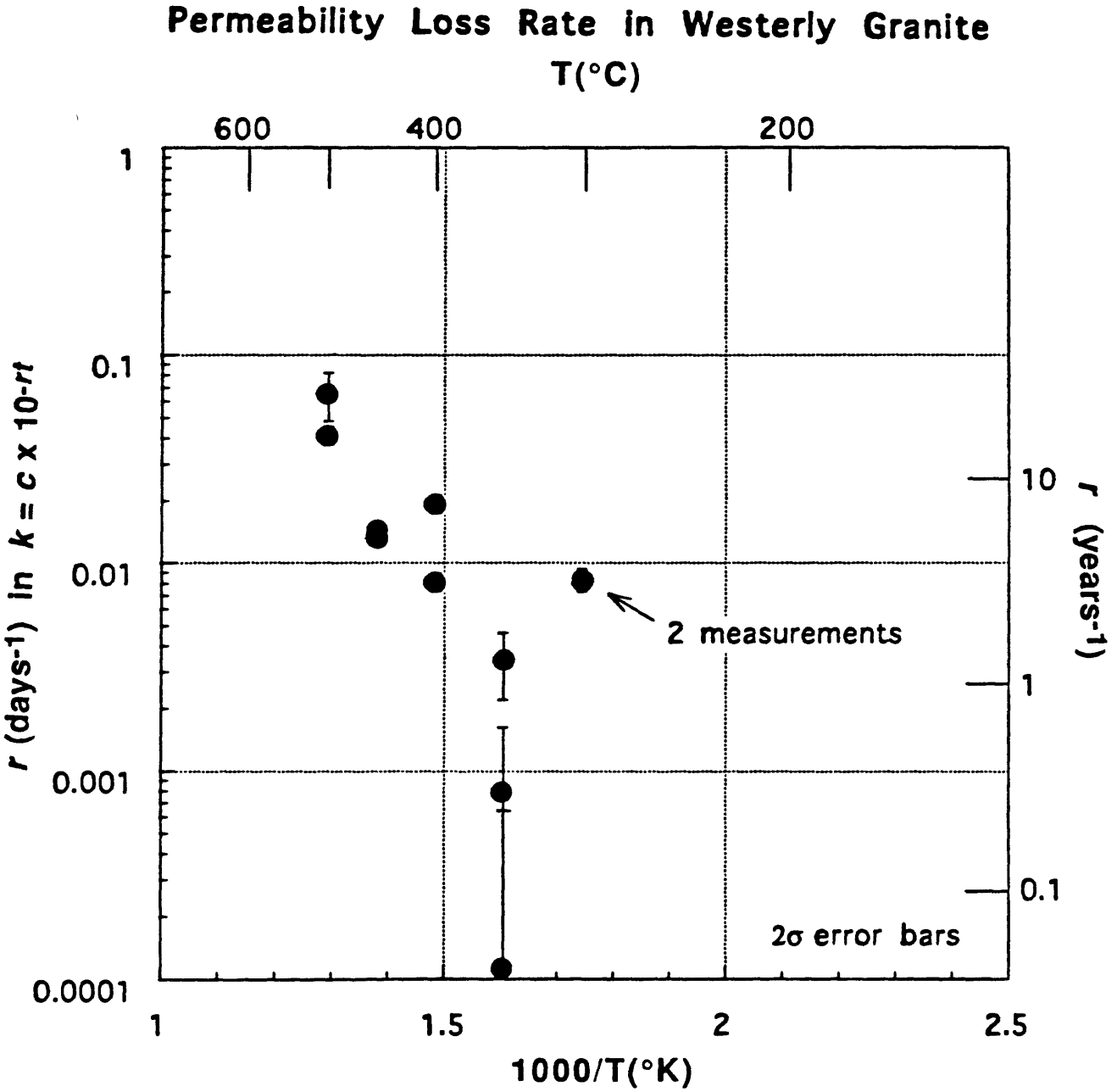

Figure 23. Plots of the coefficient r of exponential equations of the form $k = c(10^{-rt})$, fit to intact-granite permeability data (≥2.0 days), versus temperature and the inverse of temperature. The right-hand vertical axis gives the yearly decrease in permeability, in powers of 10. Error bars, 2σ.

The very low slopes of the data from the 350°C experiments lead to the large relative error estimates for those determinations of r.

If the steady exponential decay of permeability can be extrapolated to much longer times, permeability at 400° to 500°C could be reduced by several orders of magnitude in one year (Table 4, Figure 23). These higher-temperature results suggest that a well connected crack network may be impossible to maintain for any appreciable length of time in deeply buried granitic rock. The brittle-ductile transition occurs at about 350°C; accordingly, temperatures of interest for the seismogenic zone of the San Andreas fault in Figure 23 and Table 4 are at 350°C and below. Permeability is predicted to decrease by roughly 3 orders of magnitude within a single year at 300°C, but the yearly decrease at 350°C would be at most about 1 order of magnitude and possibly substantially less. Similar variability in sealing rates at elevated temperatures was described by Scholz and others (in review).

The formation of impermeable mineral seals has been invoked at various depths in and around faults. To play an effective role in the earthquake cycle, a seal must be created in less time than the earthquake recurrence interval of a given fault or fault segment, because the seal will probably be destroyed by the fracturing and crushing that accompany an earthquake. Our high-temperature results support the fault-valve model for the development of mesothermal ore deposits (Sibson and others, 1988; Sibson, 1990), in which seals are formed at the base of the seismogenic zone of high-angle thrust faults. Our lower temperature data provide less conclusive support for models requiring seals at shallower depths in fault zones such as the San Andreas (for example, Byerlee, 1993; Blanpied and others, 1992; Sleep and Blanpied, 1992), where earthquake recurrence times of 50 to 300 years have been proposed (Sieh and others, 1989). The permeability reduction rates of the 300°C intact experiments support the possibility that such seals can develop within the time constraints, but the data at 350°C suggest considerably slower sealing rates. In addition, mineral reactions different from those observed in this study may be expected to occur at temperatures below 300°C. For instance,

amphiboles would not be stable at lower temperatures, whereas zeolites and clay minerals might crystallize. Such different mineral reactions might occur at very different rates from those identified in this study. Because of these uncertainties, we must extend our experiments to lower temperatures to obtain an accurate picture of sealing rates at shallow depths in fault zones.

Summary and Conclusions

(1) The permeability of Arkansas novaculite at 400°C is high and does not change significantly in experiments up to 4 days in length. The rock deforms by creep when a differential stress is applied at elevated temperatures.

(2) The copper jackets housing the rock samples can affect the room-temperature measurements of permeability and, in a few cases, those at elevated temperatures as well. Non-annealed copper is relatively stiff at room temperature, and it does not always provide a tight seal around the sample. Annealed copper jackets, if not modified by processes such as gold plating, improve the measurements of room-temperature permeability. The best results to date were obtained when the jacketed sample was heated to 650°C for 30 minutes under an applied confining pressure but no fluid pressure. Some copper migrates along cracks a short distance into the samples (up to 1mm, depending on temperature and time), but the limited penetration and scattered occurrence of the copper deposits suggest that they have no significant effect on permeability.

(3) The permeability of Westerly granite in the temperature range 300° to 500°C decreases with time during experiments in which the same small volume of water is continually pushed back and forth through the sample. The permeability reductions are caused by a combination of solution transfer processes and metamorphic reactions. The rate of

permeability reduction increases irregularly with increasing temperature, perhaps reflecting changing mineral reactions.

(4) Intact granite cylinders tested at 500°C showed a rapid drop in permeability after 5 to 6 days, to the extent that flow through one rock cylinder essentially ceased. The cause of this precipitous decrease has not yet been determined, although crack healing is a likely possibility.

(5) The results of these experiments are consistent with previous permeability studies on granite and other rock types at elevated temperatures. The rates of permeability change in this study commonly are lower -- especially over the first few days -- and probably more realistic than for samples tested under large gradients of temperature and pressure.

(6) The higher-temperature permeability results are consistent with models invoking the rapid development of impermeable barriers at the base of the seismogenic zone. The lower-temperature results yield varying estimates of mineral sealing rates, although they generally support the hypothesis that such seals can develop in faults in less time than the recurrence interval for moderate to large earthquakes. Because of this uncertainty in sealing rates, combined with the probability that different mineral reactions will predominate at lower temperatures, long-term experiments at temperatures below 300°C should be conducted to obtain an accurate picture of seal development at shallow depths in fault zones.

(7) The permeabilities of samples containing a layer of granite gouge decreased at more rapid rates over the first 10-14 days than they did for equivalent intact samples. With time, however, the rates of change of intact and gouge-bearing samples became more similar. Preferential dissolution and redeposition of a finite amount of extremely fine-grained gouge may cause the rapid initial decreases in permeability. When the fines are removed, the sample behaves more like an intact sample. The presence of gouge may therefore enhance the initial rates of permeability reduction in a fault zone.

(8) A granite sample containing a throughgoing tensile fracture initially had a uniformly high flow rate at 400°C. After about 10 days of little or no change, the resistance to flow increased abruptly, and the parameter λ was reduced by 3 orders of magnitude in a 7-day period. The flow rate then settled down at a level similar to that of an intact sample at 400°C. During the experiment the originally clean fracture surfaces became covered with mineral deposits, that sealed the fracture surfaces to the extent that the two halves of the cylinder could not be separated by hand. These results suggest that the fractured country rock surrounding a fault may also be subject to rapid sealing after an earthquake.

Acknowledgment

We thank C. G. Stone of the Arkansas Geological Commission for kindly supplying the novaculite samples used in these experiments.

References

Aruna, M., 1976. *The effects of temperature and pressure on the absolute permeability of sandstones.* Ph. D. dissertation, Stanford University, Stanford, California, 310 pp.

Balagna, J. P., and Charles, R. W., 1975. Permeability of a monzo-granite at elevated temperature. *EOS, Transactions American Geophysical Union* **56**: 913.

Beckwith, R. S., and Reeve, R., 1969. Dissolution and deposition of monosilicic acid in suspensions of ground quartz. *Geochimica et Cosmochimica Acta* **33**: 745-750.

Blanpied, M. L., Lockner, D. A., and Byerlee, J. D., 1992. An earthquake mechanism based on rapid sealing of faults. *Nature* **358**: 574-576.

Brace, W. F., Walsh, J. B., and Frangos, W. T., 1968. Permeability of granite under high pressure. *Journal of Geophysical Research* **73**: 2225-2236.

Burnham, C. W., Holloway, J. R., and Davis, N. F., 1969. *Thermodynamic Properties of Water to 1,000°C and 10,000 Bars.* Geological Society of America Special Paper **132**, 90 pp.

Byerlee, J., 1993. Model for episodic flow of high-pressure water in fault zones before earthquakes. *Geology* **21**: 303-306.

Byerlee, J. D., and Lockner, D. A., 1994. The earthquake instability on faults containing water in seal-bound compartments. *EOS, Transactions American Geophysical Union* **75**(44): 425-426.

Chester, F. M., Evans, J. P., and Biegel, R. L., 1993. Internal structure and weakening mechanisms of the San Andreas fault. *Journal of Geophysical Research* **98**: 771-786.

Cox, S. F., Etheridge, M. A., and Wall, V. J., 1986. The role of fluids in syntectonic mass transport, and the localization of metamorphic vein-type ore deposits. *Ore Geology* **2**: 65-86.

Fredrich, J. T., and Wong, T.-f., 1986. Micromechanics of thermally induced cracking in three crustal rocks. *Journal of Geophysical Research* **91**: 12743-12764.

Gale, J. E., 1975. *A numerical field and laboratory study of flow in rocks with deformable fractures.* Ph. D. Thesis, University of California, Berkeley, 255 pp.

Heard, H. C., and Page, L., 1982. Elastic moduli, thermal expansion, and inferred permeability of two granites to 350°C and 55 megapascals. *Journal of Geophysical Research* **87**: 9340-9348.

Iler, R. K., 1979. *The Chemistry of Silica.* Wiley, New York, 866 pp.

Keller, W. D., Viele, G. W., and Johnson, C. H., 1977. Texture of Arkansas novaculite indicates thermally induced metamorphism. *Journal of Sedimentary Petrology* **47**: 834-843.

Knipe, R. J., 1992. Faulting processes and fault seal. In: R. M. Larsen, H. Brekke, B. T. Larsen, and E. Talleraas (eds.), *Structural and Tectonic Modelling and its Application to Petroleum Geology.* Elsevier, Amsterdam, pp. 325-342.

Lowell, R. P., Van Cappellen, P., and Germanovich, L. N., 1993. Silica precipitation in fractures and the evolution of permeability in hydrothermal upflow zones. *Science* **260**: 192-194.

Moore, D. E., 1993. *Microcrack populations associated with a propagating shear fracture in granite.* U. S. Geological Survey Open-File Report **93-245**, 88 pp.

Moore, D. E., Lockner, D. A., and Byerlee, J. D., 1994. Reduction of permeability in granite at elevated temperatures. *Science* **265**: 1558-1561.

Moore, D. E., Morrow, C. A., and Byerlee, J. D., 1983. Chemical reactions accompanying fluid flow through granite held in a temperature gradient. *Geochimica et Cosmochimica Acta* **47**: 445-453.

Moore, D. E., Morrow, C. A., and Byerlee, J. D., 1986. High-temperature permeability and groundwater chemistry of some Nevada Test Site tuffs. *Journal of Geophysical Research* **91**: 2163-2171.

Moore, D. E., Morrow, C. A., and Byerlee, J., 1987. *Fluid-rock interaction and fracture development in 'crystalline' rock types.* U. S. Geological Survey Open-File Report **87-279**, 53 pp.

Morey, G. W., Fournier, R. O., and Rowe, J. J., 1962. The solubility of quartz in water in the temperature interval from 25° to 300°C. *Geochimica et Cosmochimica Acta* **26**: 1029-1043.

Morrow, C. A., Bo-Chong, Z., and Byerlee, J. D., 1986. Effective pressure law for permeability of Westerly granite under cyclic loading. *Journal of Geophysical Research* **91**: 3870-3876.

Morrow, C., Lockner, D., Moore, D., and Byerlee, J., 1981. Permeability of granite in a temperature gradient. *Journal of Geophysical Research* **86**: 3002-3008.

Morrow, C. A., Moore, D. E., and Byerlee, J. D., 1984. Permeability and pore-fluid chemistry of the Topopah Spring Member of the Paintbrush tuff, Nevada Test Site, in a temperature gradient - Application to nuclear waste storage. *Materials Research Society Symposium Proceedings* **26**: 883-890.

Morrow, C. A., Moore, D. E., and Byerlee, J. D., 1985. Permeability changes in crystalline rocks due to temperature: Effects of mineral assemblage. *Materials Research Society Symposium Proceedings* **44**: 467-474.

Potter, J. M., 1978. *Experimental permeability studies at elevated temperature and pressure of granitic rocks.* Ms. Thesis, University of New Mexico, Albuquerque, 101 pp.

Scholz, C. H., Léger, A., and Karner, S. L., in review. Experimental diagenesis: Exploratory results. Submitted to *Geology*.

Sibson, R. H., 1981. Fluid flow accompanying faulting: Field evidence and models. In: D. W. Simpson and P. G. Richards (eds.), *Earthquake Prediction: An International Review.* Maurice Ewing Series, vol. 4. American Geophysical Union, Washington, D. C., pp. 593-603.

Sibson, R. H., 1990. Conditions for fault-valve behavior. In: R. J. Knipe and E. H. Rutter (eds.), *Deformation Mechanisms, Rheology, and Tectonics.* Geological Society of London Special Publication **54**: 15-28.

Sibson, R. H., Robert, F., and Poulsen, K. H., 1988. High-angle reverse faults, fluid-pressure cycling, and mesothermal gold-quartz deposits. *Geology* **16**: 551-555.

Sieh, K., Stuiver, M., and Brillinger, D., 1989. A more precise chronology of earthquakes produced by the San Andreas fault in southern California. *Journal of Geophysical Research* **94**: 603-623.

Sleep, N. H., and Blanpied, M. L., 1992. Creep, compaction and the weak rheology of major faults. *Nature* **359**: 687-692.

Summers, R., Winkler, K., and Byerlee, J., 1978. Permeability changes during the flow of water through Westerly granite at temperatures of 100°-400°C. *Journal of Geophysical Research* **83**: 339-344.

Tödheide, K., 1972. Water at high temperatures and pressures. In: F. Franks (ed.), *Water - A Comprehensive Treatise. Vol. 1. The Physics and Physical Chemistry of Water.* Plenum Press, New York, pp. 463-514.

Udell, K. S., and Lofy, J. D., 1989. Permeability reduction of unconsolidated media caused by stress-induced silica dissolution. *SPE Formation Evaluation* **4**: 56-62.